International specialized medium for agricultural mechanization in developing countries

ISSN 0084-5841

AMA

AGRICULTURAL MECHANIZATION IN ASIA, AFRICA AND LATIN AMERICA

VOL.55, NO.1, WINTER 2024

Special Edition:

Massage for the 6th CIGR International Conference 2024

FARM MACHINERY INDUSTRIAL RESEARCH CORP.


Changes from technology
to HUMANOLOGY to live with nature
TAISHO
We make the most of customers' viewpoint and best quality of products.
Enhancing the spirit of cooperation and executive talent, we contribute
to the development of agriculture.
BLEND BROADCASTER
BLEND SOWER
Properly blend fertilizers with
different specific gravity
● Suitable for
organic soil
preparation !
BLEND SOWER
BLD-340
FERTILIZER SPREADER
GRAND SOWER
RS SERIES RD SERIES
Broadcast various type of fertilizer
(powder, granules, fine granules, chicken manure, organic pellets, etc.)
properly without waste
RD-1714
GRAND SOWER


SUGANO
LISTEN TO THE SOILS
Tsuchi-tsukuri
There is no English word corresponds to 'Tsuchi-tsukuri',
which is not only a traditional but also modern practice to maintain and improve soil productivity in Japan.
'Tsuchi-tsukuri' describes as 'producing soil' in Kanji character.
Actual practice of 'Tsuchi-tsukuri' is composed of periodical deep plowing, incorporating well matured manure (both green and animal) into not only top soil but also subsoil.
'Producing' explicitly means caring, conserving, growing soil by farmers.
We consider a feasibility of achieving sustainable agriculture through preventing soil and land degradation with this unique concept of 'Tsuchi-tsukuri' at soil by soil.
SUGANO FARM MACHINERY MFG. CO., LTD.
Head Office : 300, Tenjindai, Mano, Miho-mura, Inashiki-gun, Ibaraki-pref, 300-0405, Japan https://www.sugano-net.co.jp

International specialized medium for agricultural mechanization in developing countries

ISSN 0084-5841

AMA

AGRICULTURAL MECHANIZATION IN ASIA, AFRICA AND LATIN AMERICA

VOL.55, No.1, WINTER 2024

Edited by

YOSHISUKE KISHIDA

Published quarterly by

Farm Machinery Industrial Research Corp.

in cooperation with

The Shin-Norinsha Co., Ltd.

and

The International Farm Mechanization Research Service

TOKYO

EDITORIAL STAFF
(Tel.+81-(0)3-3291-3674)
Yoshisuke Kishida, Chief Editor
Peeyush Soni, Executive Editor
Shinjiro Tetsuka, Managing Editor

ADVERTISING
(Tel.+81-(0)3-3291-3674)
Yuki Komori, Director (Head Office)
Advertising Rate: 300 thousand yen per page

CIRCULATION
(Tel.+81-(0)3-3291-3674)
(Fax.+81-(0)3-3291-5717)
Editorial, Advertising and Circulation Headquarters
1-2-5, Kanda Jimbo-cho, Chiyoda-ku, Tokyo 101-0051, Japan
URL: https://www.agriculturalmechanization.com/
E-Mail: ama@shin-norin.co.jp

Printed in Japan

This is the 199th issue since its maiden issue in the Spring of 1971

EDITORIAL

Recently, Kubota, Japan's top agricultural machinery manufacturer, unveiled a prototype hydrogen fuel cell tractor; a tractor is equivalent to about 60 horsepower. While battery tractors require recharging when they run out of electricity, the hydrogen fuel cell tractors require the supply of new hydrogen. The required time for the latter is significantly shorter than the time required to recharge the batteries

Carbon dioxide is a growing problem in the world today, and various efforts are underway around the world to prevent further increases in carbon dioxide concentrations. One such effort is the use of electric power and batteries instead of internal combustion engines. Electric cars have already been developed and mass-produced.in many countries. Recently, however, sales of electric vehicles have been sluggish in the U.S., Europe, and other regions. Instead of fully electric vehicles, sales of hybrid vehicles, which combine electric power and engines, are growing.

Power plants are also making various efforts to reduce carbon dioxide emissions, such as the use of ammonia. As I mentioned earlier, I am not too concerned about the increase in the concentration of carbon dioxide. A study of the temperature history of our earth over several million years shows a repetition of glacial and interglacial periods. This must be due to the cycles of solar activity. There are periods when the radiation of energy from solar activity decreases and periods when it increases. Therefore, the carbon dioxide emitted by human use is not thought to be a major cause of global warming.

Currently, the population of the earth has exceeded 8 billion and is still growing. Farmland, which supports food production for human life, is decreasing in area per capita every year. Under such circumstances, land productivity must be increased. The way to increase land productivity is to increase carbon dioxide concentration and temperature, as can be seen in greenhouse agriculture.

There are many Japanese horticultural farmers who have installed carbon dioxide gas generators in their facilities. Increasing carbon dioxide concentration is good for agricultural production from a macro perspective.

Agricultural machinery must be operated efficiently. For this purpose, agricultural information technology is necessary. Measurement technology is essential to determine what work to do, how to do it, and when to do it. Energy issues are also inseparable from information technology. New agriculture requires information technology to accurately grasp the conditions of the soil and plants, and also it requires appropriate tasks at appropriate time by new agricultural mechanization.

New robotization of agricultural machinery is about to begin due to the decrease in the agricultural labor force. New mechanization is needed to meet the needs of the times.

Yoshisuke Kishida
Chief Editor
March, 2024

CONTENTS

AGRICULTURAL MECHANIZATION IN ASIA, AFRICA AND LATIN AMERICA

Vol.55, No.1, Winter 2024

Message for the 6th CIGR International Conference 2024

MESSAGE for the 6th CIGR INTERNATIONAL CONFERENCE 2024

Seishi Ninomiya

President CIGR, Professor Emeritus, the University of Tokyo

As CIGR President, I am delighted to host the CIGR International Conference in May 2024 on Jeju Island, Korea, which is blessed with rich nature and a pleasant climate.. I would like to express my heartfelt gratitude to the many participants from numerous countries and my sincere appreciation to the local organizing committee members and sponsors in Korea who have worked tirelessly to prepare for this conference.

This conference is not just an event but a crucial gathering of scientists, researchers, technicians, and government officials from all over the world. We are convening to address the pressing challenges of food systems, such as global food security, provision of safe and quality food, environmental protection, food loss, water use, rapid decline in farm population, and stable management of farm households. The urgency to focus on research and development of agricultural engineering technologies for a sustainable and secure food supply has never been greater. The active exchange of cutting-edge knowledge and innovative solutions at this conference will undoubtedly pave the way for significant advances in this field.

CIGR's long-standing role over 90 years in fostering collaboration and recognizing outstanding contributions within the agricultural engineering community is truly commendable. We believe that the CIGR 2024 conference will further solidify this tradition, foster meaningful connections, and propel us toward a future of safe and abundant food for all.

Finally, I would like to express my sincere gratitude to AMA (Agricultural Mechanization in Asia, Africa, and Latin America), published by Shin-norin Co., for its continued support of research and development in agricultural engineering worldwide.

We eagerly await a successful conference filled with insightful discussions, groundbreaking research, and lasting cooperation. Your participation will greatly contribute to the success of this event.

Fedro S. Zazueta
CIGR Secretary General

To all participants of the 6th CIGR International Congress and friends of CIGR,

CIGR has reached the milestone of 90 years of service to its constituents and stakeholders. The "Congrès International du Génie Rural" was founded in 1930 in Liège, Belgium, by a small group of farsighted European agricultural engineering scientists from Belgium, France, Germany, The Netherlands, Spain, Switzerland, and the UK. With time, CIGR increased its membership and by 2008 it had become an organization with worldwide representation. During this time, the name of the organization was changed to "CIGR: International Commission of Agricultural and Biosystems Engineering".

Since its origins CIGR has focused on addressing problems and improving agriculture, biosystems and the environment through sound, science-based engineering practice. CIGR's organization and evolution are reflected in its technical sections, which in turn are organized to address current and future issues in agriculture, biosystems and the environment. In its beginning years, CIGR addressed four areas: Land reclamation; Farm buildings; Mechanization; and Scientific Collaboration.

Today, the technical organization of CIGR reflects contemporary problems along seven areas: Land and Water; Structures and Environment; Plant Production; Energy in Agriculture; System Management; Bioprocesses; and Information Technology. In addition, there are 14 workgroups comprised of top researchers and industry representatives addressing specific issues related to the field. Part of CIGR's mission is to provide an environment were scientific and technical exchanges can take place.

The prime mechanism to achieve this goal are CIGR's International Conferences and Congresses. I would like to congratulate and encourage all attendees to engage in deep discussion and constructive criticism of the issues facing our profession in the 21th century, the science that will enable us to solve them, and the best ways to implement improvements and solutions. Sincerely,

Fedro S. Zazueta
CIGR Secretary General March 20, 2024

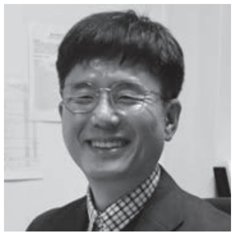

Hyuck-Joo Kim

President, Korean Society of Agricultural Machinery; Professor, Sunchon National University

Esteemed scholars from Japan and all attendees of the 6th International Conference of CIGR, welcome to Jeju, South Korea. It is my honor to greet you, and I extend a special welcome to Mr. Yoshisuke Kishida, who has dedicated over half a century to advancing the agricultural machinery industry in Japan, East Asia, and globally.

As the president of the Korean Society for Agricultural Machinery, it is a privilege to host this distinguished gathering. The CIGR International Conference is a big event for enhancing our network and collaboration among agricultural engineers worldwide. This year's theme, "Digital Agriculture," highlights the urgency of sharing the latest research and technological advancements in agricultural engineering. Amidst the climate crisis, our collective effort towards sustainable agriculture and food security is more crucial than ever.

The conference will feature keynote speeches from experts in various fields and sessions designed to foster the exchange of research, experiences, and innovative approaches. We will focus particularly on addressing global challenges such as climate change, ecosystem conservation, and smart agricultural technologies.

Finally, I hope your experience in Jeju, an island renowned for its beautiful nature and rich culture, will leave you with enjoyable memories. May this conference contribute significantly to international cooperation and friendship in the field of agricultural engineering.

Thank you

With my warm Regards,

HJ Kim

Yong-Joo Kim

Dean of Office of Research-affairs and Director of Foundation of Research and Business, CEO of CNU Technology Holdings, and Professor of Dept. of Biosystems Machinery Engineering of Chungnam National University in Republic of Korea

It is with great pleasure that I send my most sincere, profound, and heartfelt thanks to Mr. Yoshisuke Kishida and his reputed journal AMA for his tremendous and continuous contribution during the last 6 decades in sciences and research for agricultural mechanization in Asia, Africa, and Latin America regions. It is my great honourable moment as a co-editor that AMA offered a special issue on the occasion of the 6th CIGR International Conference 2024, to be held in Jeju, Korea. When I received a new copy of AMA magazine, I was extremely happy not only for the technical information from renowned researchers worldwide but also impressive improvement of the magazine having advanced technology in developing countries. Whenever I meet Mr. Kishida with exciting mechanization thinking. I was pleased to arrange a similar at Chungnam National University, Korea last August 18, 2023, and invited him as a speaker. We also attend the meetings of the "Club of Bologna" in Italy and Germany during EIMA and Agritechnica in the previous years. The dedication of Mr. Kishida to agricultural mechanization in developing countries is also impressive and inspiring for young researchers globally. I also celebrated and congratulated him on the occasion of the 90th anniversary of Shin-norinsha Co., Ltd. on 25th October 2023, and presented a token of appreciation on that milestone. Let us congratulate Mr. Kishida and his team for their dedication and sacrifice for agricultural mechanization. I wish every success and fortune for AMA in the future as well as this new special issue on the occasion of the 6th CIGR International Conference 2024.

Noboru Noguchi

President of Japanese Association of International Commission of Agricultural and Biosystems Engineering

On behalf of the Japanese Association of International Commission of Agricultural and Biosystems Engineering (JAICABE), I am pleasure to send a message of congratulations on 6th CIGR International Conference 2024. I am now working as the president of the JAICAB, and we also promoting international exchanges worldwide.

Looking at the world, it is estimated that the world population will reach 9.8 billion in 2050, and that the demand for food will increase by 60% of the current level, which will cause an imbalance between the supply and demand of food in the world, resulting in food shortages in the future. Furthermore, the labor shortage in agriculture is facing is common to both developed and emerging countries. The number of agricultural workers is decreasing, especially the shortage of skilled human resources is in high demand internationally.

The theme of this CIGR International Conference is “Digital Agriculture” is one of the most important technologies we need to address for resolving current global food problems. I do hope all the participants will take this opportunity to communicate and exchange their opinions and make successful conference.

Takehiko Hoshi

President, Japanese Society of Agricultural Informatics

On behalf of the Japanese Society of Agricultural Informatics (JSAI), I extend warm congratulations to you for hosting the 6th CIGR International Conference 2024 in scenic Jeju Island, Korea.

As indicated by the United Nations Population Fund, the global population is projected to reach 8.045 billion by mid-2023 and will continue to grow. Agronomy and agricultural engineering are expected to play a bigger role in ensuring a stable food supply for human consumption.

Additionally, due to global warming, agricultural weather disasters such as droughts and floods are becoming more severe, Consequently, controlling the release of substances and energy are challenges that will have a significant impact on the global environment in the future. We believe that efforts to address this challenge using agricultural systems and data science will become increasingly important.

In certain countries such as Japan, where the population is declining and aging, sustaining agricultural systems for food production is becoming increasingly difficult. In these countries, the impetus for research and development in the digitization of production knowledge as well as the development and introduction of automated machinery is gaining importance. Expectations for agricultural informatics to serve as a foundation for these efforts are growing.

We hope that researchers, engineers, government officials, and others involved in agricultural engineering from around the world will actively engage in lively discussions and make proposals for the future. The goal is to find scientific and technological solutions to such issues. We envision that the conference will yield fruitful discussions and lead to a brighter future for humanity.

Michihisa Iida

President, Japanese Society of Agricultural Machinery and Food Engineers, Professor, PhD. Graduate School of Agriculture, Kyoto University, Japan

Congratulations on holding the 6th CIGR international conference in Jeju, Korea.

I sincerely hope that the first conference will be held successfully after the restrictions on participation due to the COVID-19. We look forward to fruitful discussions and exchanges among scientists, researchers, and engineers from around the world regarding the theme of this conference, “Digital Agriculture (Feed the Future)” .

Dana Osborne
President, 2023-2024

Darrin J. Drollinger
Executive Director

American Society of Agricultural and Biological Engineers

Greetings to participants and friends of the 6th CIGR International Conference.

We at ASABE congratulate you on the 6th CIGR World Conference in Jeju, Korea, as CIGR continues to promote dialogue and sharing of information for the benefit of enhancing sustainable use of natural resources. In this age of adverse global climate change and accompanying impacts, the role of agricultural and biological engineers, and those in related fields, take on even more importance.

The challenges faced by our world make it imperative that we achieve great strides in circularity of the use of resources to provide food, water, energy, fiber, and a safe environment needed to thrive. We are encouraged by this conference to improve our knowledge, encourage technological innovation, apply our research judiciously, and collaborate effectively for the good of all the world' s population.

Such a great gathering of conference participants is an accomplishment. We extend our best wishes for a satisfying and successful event. We acknowledge with appreciation the contributions of the organizers, promoters, and presenters to advance "Digital Agriculture (Feed the Future)."

Best regards,

Design and Development of Onion De-topping Machine

by
A. Carolin Rathinakumari
Principal Scientist
ICAR-Indian Institute of Horticultural Research,
Bengaluru, INDIA
CAROLINA.KUMARI@icar.gov.in

G. Senthil Kumaran
Principal Scientist
ICAR-Indian Institute of Horticultural Research,
Bengaluru, INDIA

B. Chittappa
M.Tech Student
ICAR-Indian Institute of Horticultural Research,
Bengaluru, INDIA

Abstract

Onion (*Allium cepa*, L.) is one of the important commercially cultivated vegetable crops grown throughout India. De-topping is one of the post harvest operations in cultivation of onion crop. It is the removal of onion tops from the harvested cured onion bulbs and this is carried out in the field. It is tedious, laborious and time consuming operation. Onion de-topping requires huge labour to an extent of 12.5 man-hrs/t. Mechanization of onion de-topping will reduce cost of cultivation and drudgery. Keeping these points in view, a power operated onion de-topper was designed and developed at ICAR-Indian Institute of Horticultural Research, Bengaluru. It consisted of a feeding conveyor for feeding cured onion crop, de-topping rollers for shearing the tops, collection chutes for the de-topped onion bulbs and leaves, main frame and power transmission system. The onion de-topper was operated by a 1440 rpm three phase, 2 hp electrical motor with necessary speed reduction gear box. The performance parameters of onion de-topper were found to be de-topping efficiency of 95.22 ± 1.42%, effectiveness of de-topping of 97.80, percent damage of 2.30 ± 0.29%, percent non de-topped onions of 2.56 ± 0.25% and capacity of 372.88 ± 7.22 kg/h. Cost of operation of onion de-topping was Rs. 296.60/tonne against manual de-topping of Rs. 468.75 /tonne.

Keywords: Onion, mechanization of onion, de-topping, onion de-topper.

Introduction

Onion (*Allium cepa*, L.) is one of the important commercially cultivated vegetable crops grown by all category of farmers and also consumed worldwide. Onion is not only for domestic market consumption but is also as highest foreign exchange earner among the fruits and vegetables. World's onion production is 93.2 million tonnes, led by China, India, Egypt, United States, Iran, Turkey and Russia contributing 26% and 21% by China and India, respectively[1]. India exports onions to Bangladesh, Malaysia, Sri Lanka, United Arab Emirates and Nepal.

India produces of 215.64 lakh MT (2016-17) of onion under the area of 12.70 lakh ha[2]. India has exported 1,949,482.67 MT of fresh onion worth of Rs. 285,782.13 lakhs (2018-19)[3]. Area under onion cultivation and onion production have increased to an extent of 49.70% and 39.53% during 2006-07 to 2016-17. Maharashtra ranks first in onion production (5,786.40 thousand tons) followed by Madhya Pradesh (2,403.14 thousand tons.), Karnataka (1,995.62 thousand tons), Rajasthan (1,250.64 thousand tons.) and Gujarat (1,034.49 thousand tons.)[4].

One of the on farm post harvest operations involved in cultivation of onions is de-topping. Onions are harvested when 50% tops begins to collapse on the ground but before the foliage dries down completely. After digging, the onions are field cured for 3-5 days, cut the necks for separation of onions from the tops, graded, shed cured and stored. Separation of onion bulbs from tops is called de-topping, women labourers are engaged for this operation and individual onions are de-topped by sickle thus makes it highly drudgery (**Fig. 1**). Hence onion de-topping is highly labour intensive operations which requires to an extent of 12.5 woman-hrs/t.

Grishkumar et al. (2015) developed a power operated onion de-topper. The machine consisted of main frame, conveying unit, cutting unit, safety guard and power transmission unit. The conveying unit was a set of spiral rollers and the cutting unit consisted of plain cutters (two numbers) and one serrated cutter. The plain cutters and the serrated cutter counter rotated. The average de-topping efficiency was observed as 86.59 percent with 315.03 kg/h output capacity. The power requirement was found to be 0.5 kW The cost of operation was Rs. 18.84 per quintal[5]. Mozaffary and Kazmeinkhah (2014) designed, constructed and evaluated a onion topping mechanism. Three types of onion topping mechanisms viz., flail, rotary and roller topper were designed and tested at three rotational speeds of 1500, 1700 and 2000 rpm. Performance parameters such as acceptable top percentage, not acceptable top percentage, not topped percentage and damaged bulbs percentage were determined and analyzed. It was reported that the flail topper was the most suitable mechanism for onion topping with the results of 87.7% acceptable top at 2000 rpm in stage one and 83.9% acceptable top at 1500 rpm in second stage[6].

Rani and Srivastava (2012) designed and developed an onion de-topper which consisted of a chute type feeding unit, a belt conveyor, an oscillating conveyor, rotating fingers, a rotating cutter, main frame and power transmission system. The belt conveyor had a speed of 0.53 m/sec. The oscillating conveyor had a frame, round rods and a crank mechanism to facilitate downward orientation of onion leaves. The cutter provided at the downward side of the oscillating conveyor could cut the onion leaves. The onion de-topper had a capacity of 300 kg/h with the de-topping efficiency of 79%[7]. Duane Kido (2006) invented an orientation system for vegetables which consisted of rotating rollers that pull the vegetables into an inverted position with leaves top down and advancement of the vegetable along the length of the rollers so as to deliver the vegetable to a cutting system[8]. Chen (1994) developed a de- stemming machine for oranges. The de-stemmer included a roller-cutter assembly and an oscillating conveyor. The roller-cutter assembly consisted of a pair of 250 mm long cylindrical cutting units, each made of a set of eleven 150 mm diameter parallel disks, 6.4 mm thick and 23.2 mm apart, which rotated at about 70 rpm between each pair of the disks was a high speed rotating blade that rotated at a tip speed of 45.5 m/sec. The blade was 16 mm thick and 144 mm in diameter. The oranges were get through a simulating hopper, which are then spun, oscillated and conveyed forward by the oscillating conveyor, and conveyed forward along the cutting cylinders. The high-speed blades cut any stem that entered the space between the rotating disks to a length of less than 3 mm. The machine worked best at a speed of 60 to 75 rpm and conveyor frequency range of 110 to 120 rpm de-stemming about 80 to 90 percent of the oranges[9].

The objective of this study was to design and develop an efficient power operated onion de-topper to ensure timeliness in operation, reduce the input cost and drudgery involved in the operation.

Material and Methods

2.1 Prototype Onion De-topper

The onion crop parameters in terms of onion bulb size and thickness of onion top were studied to design the onion de-topper. From the review of literature it was inferred that the onion crop has to be oriented having the onion top down for de-topping. It was also understood that efficiency of de-topping should be increased by developing a suitable efficient de-topping mechanism considering the production level of onion in India. Accordingly, the present onion de-topping machine was designed and developed. The design and operational parameters were also optimized to achieve highest de-topping efficiency and capacity. The onion de-topper consisted of (i) conveyor for feeding onion crop, (ii) de-topping unit, (iii) collection chutes for the de-topped onion bulbs and tops, (iv) main frame and v) power transmission system (**Fig. 2**).

Fig. 1 Manual onion de-topping in the field

2.1.1 Feeding Conveyor

The feeding conveyor was a belt conveyor for uniform feeding of the onion crop to the onion de-topping unit. This conveyor consisted of i) two rollers, ii) endless belt, iii) main frame, iv) enclosure and v) power transmissions (**Fig. 3**). The rollers were fabricated out of 100 mm dia. M.S pipe and had a length of 400 mm. The endless belt is a canvas belt having 1000 × 400 × 2 mm (L × W × T). This belt was fitted to the rollers. This conveyor belt set was further mounted on a suitable frame with necessary bearings and fasteners. The frame had a dimension of 900 × 500 mm (L × W) and fabricated out of 40 × 4 mm M.S 'L' Section. All the four sides of the conveyor belt was provided with enclosures except at the delivery side of the conveyor. The enclosure was fabricated out of 1.8 mm thickness M.S. Sheet and was provided to a height of 250 mm.

2.1.2 De-topping Unit

The de-topping unit is the critical component of the de-topping machine which should detop the onion tops efficiently without damaging the onion bulbs. Hence the performance of the onion de-topping completely depended on the design of the de-topping component of the de-topping machine. The de-topping unit consisted of (i) set of de-topping rollers, (ii) main frame and (iii) power transmission system (**Fig. 2**). The de-topping unit is a set of rollers comprising one helical roller and the other one a plain roller. The helix angle was designed to de-top the onion bulbs leaving the top less than 25 mm (Chauhan et al., 1995[10]).

Fig. 2 Drawing of power operated onion de-topping machine

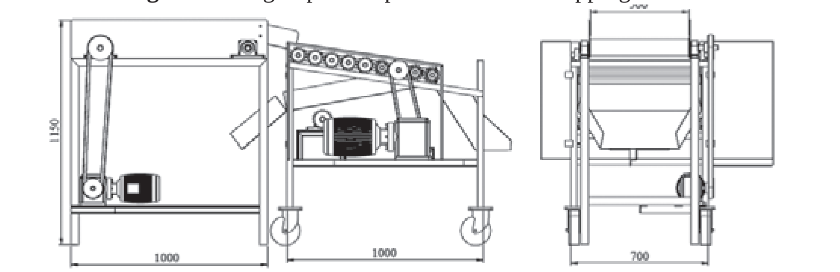

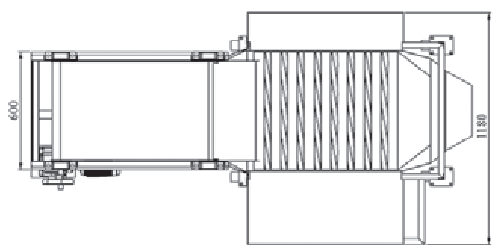

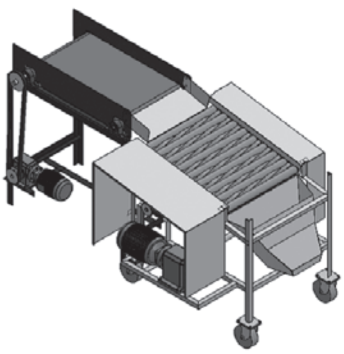

1) Conveyor for feeding onion crop, 2) De-topping unit, 3) Collection chutes for the de-topped onion bulbs and tops, 4) Main frame and 5) Power transmission system

Fig. 3 Drawing of Feeding Conveyor of the power operated onion de-topping machine

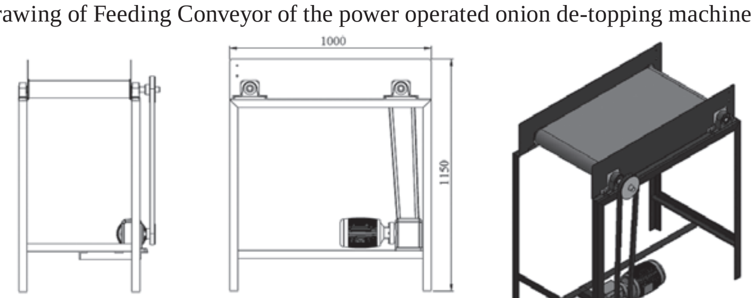

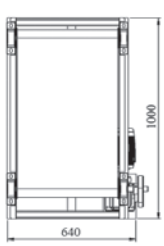

1) Rollers, 2) Endless belt, 3) Main frame, 4) Enclosure and 5) Power transmissions

Detopping tools with three helix angles viz. 75°, 80° and 85° were designed, fabricated and performance was evaluated. Each helical roller was fabricated out of M.S. shaft having 20 mm and 735 mm length. The details of the helical rollers are shown in **Figs. 4(a-c)**. The plain roller was a G.I. Pipe having 600 mm length, 50 mm diameter and 3 mm thickness. Eight such set of rollers were fabricated and mounted on a main frame. A gap of 2 mm was provided between the rollers. Experiment was conducted to study the effect of three different helix angles of detopping tool on performance parameters of onion detopping in term of (i) detopping efficiency, (ii) percent damage, (iii) effectiveness of detopping and (iv) detopping capacity. Freshly harvested and cured onion crop was procured from farmer's field of Village of Kadur (Dt.). The design of experiment was Completely Randomised Design with ten replications and the sample size was 5 kg. The observations recorded were (i) weight of detopped onions, (ii) weight of undetopped onions, (iii) weight of damaged onions and (iv) time taken to reach the delivery chute. The results was statistically analysed using statistical tool[11]. The optimized detopping tool design was used in the detopping unit.

A frame was fabricated out of M.S angles section of 40 × 40 × 5 mm having 1000 mm length and 700 mm width. This frame was mounted at an angle of 9 degree slope with reference to the ground. The rollers were fitted on this frame with suitable bearings and fasteners. The rollers were driven by sprocket and chain system and were counter rotated. The rollers were enclosed at both the sides (lengthwise) and this enclosures were fabricated out of 1 mm thickness M.S. Sheet.

2.1.3 Collection Chutes for the De-topped Onion Bulbs and Tops

Collection chute was fabricated out off M.S sheet of 1 mm thickness having trapezoidal shape for directing the de-topped onion bulbs into the crates. The collection chute had a dimension of 530 mm width at the upper end, 150 mm at the lower end, 680 mm length and 200 mm height. This was fitted to the main frame at angle of 740 in order to have the free fall of the de-topped onion bulbs. A tray to collect the detopped onion leaves was fabricated was fitted below the rollers (**Fig. 2**).

2.1.4 Main Frame

The main frame of the machine was fabricated out of M.S. angle section of 40 × 40 × 5 mm. Four numbers of swivel type caster wheels of 150 mm diameter and 50 mm width were provided for easy mobility of the machine. The feeding conveyor, de-topping unit, collection chute for de-topped onion bulbs, collection tray for onion tops, power transmission systems, and electric motor were fitted to the main frame. The frame was well braced to mount and support other parts of the machine (**Fig. 2**).

2.1.5 Power Transmission System

A three phase, 1440 rpm, 2 hp electric motor was mounted on the main frame with necessary supports and gearbox of 1:5 reduction was fitted to the motor. A power train system was fabricated as shown in **Fig. 2** to transmit power (i) to plain rollers with chain and sprocket system to rotate the rollers in clockwise direction, (ii) to helical rollers with chain and sprocket system to rotate the rollers in anti-clockwise direction, (iii) feeding conveyor.

2.2 Evaluation of Performance of Onion Set Planter

The performance of the power operated prototype onion de-topper was evaluated at Agricultural Engineering Workshop of ICAR-Indian Institute of Horticultural Research, Bengaluru. One hundred kilogram of cured onion were procured from the farmers field and performance of the power operated onion de-topper was evaluated. Moisture content of the onion bulb and onion tops were 84.11 ± 0.88 % and 17.18 ± 1.82 %, respectively. Twenty replications having sample of each 5 kg cured onion crop were weighed, counted and kept in separate trays. Each sample was fed manually through the feeding conveyor. The observations recorded were (i) weight of onions de-topped, (ii) weight of onion neck length of de-topped onion bulbs, (iii) weight of damaged onions, (iv) weight of non de-topped onion crop collected in the onion bulb collection tray and (v) time taken to de-top the onion crop. From data the performance parameters (i) de-topping efficiency, (ii) effectiveness of de-topping, (iii) percent damage and (iv) capacity were determined by using the following formulae.

2.2.1 De-topping Efficiency

De-topping efficiency was determined by using the following formula.

De-topping efficiency, % = (No. of detopped onion collected at the de-topped onion bulbs collection chute per unit time) / (Total no. of onions fed) × 100 [1]

2.2.2 Effectiveness of De-topping

Effectiveness of de-topping unit was determined by using the following formula. This was required to study how effectively the de-topping unit could de-top the onion bulb with required length of onion leaves (Chauhan et al. (1995) and Singhal (2000)).

Effectiveness of de-topping = (No. of de-topped onions with leaf length ≤ 25 mm) / (Total no. of de-topped onions) × 100 [2]

2.2.3 Percent Damage

It was estimated by separating the damaged de-topped onion bulbs from the sample collected at the outlet. It was calculated by using the following formula.

Percent damage, % = (No. of damaged onion bulbs collected at the de-topped onion bulbs collection chute per unit time) / (Total no. of onions fed) × 100 [3]

2.2.4 Percent Non De-topped Onion Crop

Few onion crops passed the de-topping unit without getting de-topped. This percent escapes was calculated as follows:

Percent non de-topped onions, %

Fig. 4 Helical roller

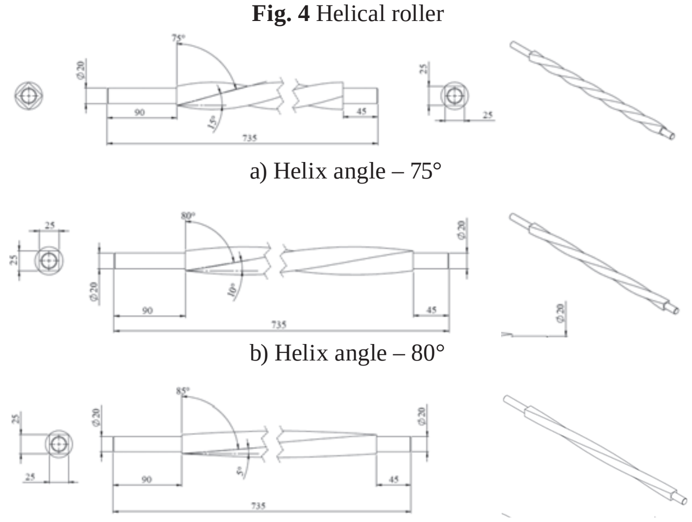

a) Helix angle – 75°

b) Helix angle – 80°

c) Helix angle – 85°

= (No. of non de-topped onion crop collected in the de-topped onion bulbs collection chute per unit time) / (Total no. of onions fed) × 100 [4]

2.2.5 Capacity

The de-topping capacity was calculated by weighing the de-topped onion bulbs collected per unit time in the de-topped onion bulbs collection chute of the machine.

De-topping capacity, kg/h = (Weight of onion bulbs collected in the collection chute, kg) / (Time Taken, h) × 100 [5]

2.3 Cost Economics

The fixed and variable costs for operating onion detopping machine per hour was calculated as per the procedure described by IS:9164-1979[11]. From the capacity of the machine, the cost of operation per hectare was calculated. This cost was compared with cost incurred by conventional detopping practice and the cost saved was worked out.

Results and Discussion

3.1 Power Operated Onion De-topper

The developed power operated onion consisted of (i) Feeding conveyor - to feed the cured onion crop to the de-topping unit, (ii) De-topping unit - to shear the onion tops and separate the leaves and onion bulbs, (iii) Collection chutes for de-topped onion bulbs and tops and iv) power transmission systems (**Fig. 5**). The feeding conveyor had a speed of 5.65 m/min. The feeding conveyor ensured positive and uniform conveying and feeding of cured onion crop to the de-topping unit. The enclosures provided for the feeding conveyor prevented the spilling of cured onion crop while loading the feeding conveyor. This ensured the estimated capacity of the de-topping machine. This enclosure also would act as a safeguard to the worker.

3.2 Experiment to Optimize the Detopping Tool Design

As the helix angle would have effect on the performance of the detopping of onion crop, experiment was carried out as explained Section 2.1. The results are presented in **Figs. 6(a-d)**. When the helix angle increased from 75° to 85° with an increment of 5°, it was observed that the detopping efficiency, effectiveness of detopping and detopping capacity increased from 93.59 % to 95.69%, 97.11% to 98.15%, 329.20 kg/h to 370.60 kg/h, respectively. Whereas, percent damage decreased from 6.62% to 2.56%. However, it was observed that different helix angles did not have effect on detopping efficiency and effectiveness of detopping (**Table 1**). As all the designs basically has helical cutting edge, the design could successfully secure the onion bulbs (which are spherical in shape) and shear the leaves near to the neck of onion bulbs.

Further, it was observed that different helix angles had highly significant effect on percent damage and capacity. Highest detopping capacity of 370.60 kg/h was recorded at 85° helix angle, followed by 340.70 kg/h at 80° and 329.20 kg/h at 75° helix angle. Similarly, highest damage of 6.62% was recorded at 75° helix angle followed by 4.83% at 80° and 2.56% at 75° helix angle. This might be due to the reason that, at lesser helix angle the detopping tool has a shape nearer to roller. The pitch of notch increased with an increment of 2 pitches for the above mentioned helix angles. Hence, the detopped onions were held for slightly extended duration even after completion of detopping function. With the increase in helix angles, the cutting edge could only shear the onion leaves and further does not hold them. Thus, the cutting edge having higher angle w.r.t roller axis, could quickly and efficiently shear the leaves, further contributed to achieve higher detopping efficiency of 95.69% and detopping capacity of 370.60 kg/h.

Fig. 5 Power operated onion de-topping machine

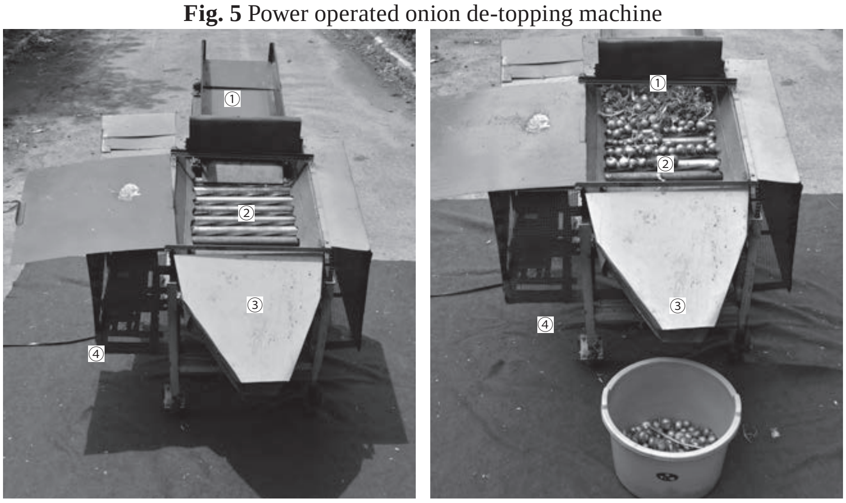

(1) Feeding conveyor, (2) De-topping unit, (3) Collection chutes for de-opped onion bulbs and tops and (4) power transmission systems

3.2 Performance Evaluation of the Power Operated Onion De-topper

The developed de-topping unit with the standarised detopping tool was mounted on the main frame. Each set rollers were mounted with a clearance of 2 mm as the thickness of onion top ranged from 7.14 ± 0.48 mm to 10.65 ± 0.62 mm. The cured onion crop was fed by the feeding conveyor to the de-topping unit. Due to counter rotating of the plain and helical rollers, the onion tops were pulled in between the rollers and made an orientation of tops down position. The sharp edges of the helical rollers further de-tops the onion tops and the onion tops dropped down. Due to plurality of the rollers, the rollers conveyed the de-topped onion bulbs further for delivery. The plurality of rollers also ensured higher chances for de-topping the onion tops before the onion crop reached the delivery. The clearance provided was found suitable for onion tops having moisture content range from 17.18 % (Chittappa, 2016)[12] to 32.60 % (Grishkumar, 2012)[5]. Though the thickness of the onion top varied from 7.14 ± 0.48 mm to 10.65 ± 0.62 mm depending on the moisture content, this de-topping mechanism was able to de-top the onion tops effectively.

The de-topped onion tops were collected by the collection tray provided below the onion de-topping unit and de-topped onion bulbs were collected in crates which were guided by collection chute (**Fig. 5**). The machine was operated by a three phase, 2 hp, electrical motor with reduction gear box (1:5 ratio). As three power transmission systems were required viz., i) for plain rollers to rotate clock wise direction, ii) for helical rollers to rotate anti-clockwise direction and iii) for feeding conveyor, a common power transmission was drawn from the main power source. Further, the power transmission systems were provided for each units from the common power transmission system (**Fig. 5**). Accordingly the plain rollers rotated with a peripheral speed of 0.27 m/sec at clockwise direction, helical rollers rotated with a peripheral speed of 0.5 m/sec at anticlock wise direction and the feeding conveyor at 5.65 m/min speed.

The performance of power operated onion de-topper was evaluated and was found to be 95.20 ± 1.42% of detopping efficiency, 97.80 ± 0.00% of effectiveness of detopping, 2.30 ± 0.29% of percent damage and 372.88 ± 7.22 kg/h of capacity. The machine could save about 37% of cost of operation against the present method i.e by manual detopping.

Table 1 ANOVA for Effect of helix angle of detopping tool on Performance parameters of detopping machine

Helical Angle	Detopping efficiency	Percent damage	Effectiveness of detopping	Capacity
75°	9.73	2.75	9.91	329.20
80°	9.76	2.41	9.93	340.70
85°	9.83	1.87	9.96	370.60
CD (p = 0.01)	---	0.21	---	14.36
SeM	0.04	0.07	0.02	4.92
CV	1.36	9.73	0.48	4.49

Conclusions

A power operated onion de-topper was designed and developed at ICAR-Indian Institute of Horticultural Research, Bengaluru to de-top the tops of harvested onion crop. The major components were i) feeding conveyor - to feed the cured onion crop to the de-topping unit, ii) de-topping unit - to cut the tops of harvested onion crop; separate the tops and onion bulbs, iii) collection chutes for de-topped onion bulbs and tops and iv) power and power transmission systems. The de-topping unit consisted of a set of rollers which was a critical component comprised of helical roller and plain rollers. The machine was operated by a three phase, 2 hp, electrical geared motor. The machine had a capacity of 372.88 kg/h against the manual method of 80 kg/h/person. The performance parameters of the power operated onion de-topper were found to be detopping efficiency as 95.20 percent, percent damaged onions as 2.30% and percent non de-topped onions

Fig. 6 Effect of Helix Angle

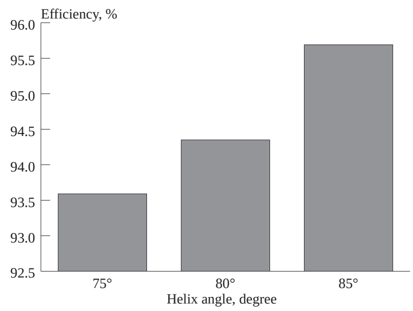

(a) Effect of helix angle on detopping efficiency of onion detopping machine

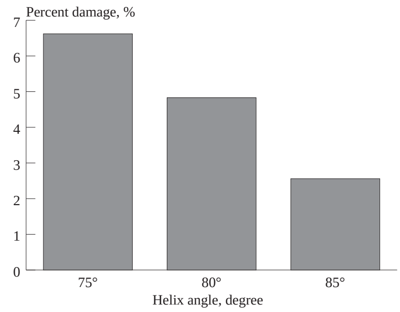

(b) Effect of helix angle on percent damage of onion detopping machine

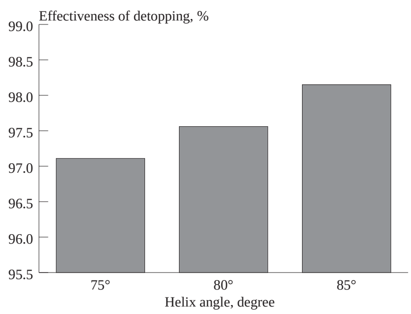

(c) Effect of helix angle on conveying efficiency of onion detopping machine

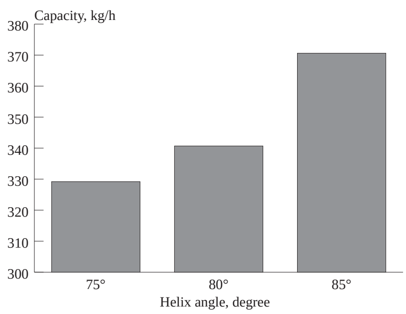

(d) Effect of helix angle on detopping capacity of detopping machine was 2.50%. The saving in the cost of onion crop de-topping by using the onion de-topper is 37 percent against the cost associated with the conventional method.

Acknowledgement

The authors express their heartfelt gratitude to The Director, ICAR-Indian Institute of Horticultural Research for providing facility and extend his support to carry out this project at ICAR-Indian Institute of Horticultural Research, Bengaluru.

REFERENCES

[1] http://www.fao.org/faostat accessed on 15.05.2019

[2] Horticultural Statistics at a Glance 2017. Horticulture Statistics Division, Department of Agriculture, Cooperation & Farmers Welfare, Ministry of Agriculture & Farmers Welfare, Government of India.

[3] http://www.dgciskol.gov.in/ accessed on 15.05.2019

[4] http://agriexchange.apeda.gov.in/indexp/genReport_combined.aspx#content

[5] Grishkumar Bhanage, V. D. Deshmukh, P. J. Thokale and S. V. Wandkar. 2016. Development of power operated onion detopper. Bioved. 27(1): 73-78.

[6] Mozaffary, M. and K. Kazmeinkhah. 2014. Design, construction and evaluation of onion harvester suitable for small farms (In Laboratorial Condition). Azarbaijan Sharghi Agricultural and Natural Resources Research Center. 42p.

[7] Rani, V. and A. P. Srivastava. 2012. Design and development of onion detopper. Agricultural Mechanization in Asia, Africa and Latin America-AMA. 43(3): 69-73.

[8] Duane Kido. 2006. Onion harvester with leaf topper. U.S. Patent Sr.No. 7007449.

[9] Chen, P. 1994. An experimental machine in De-stemming Oranges. Applied Engg in Agri., 10(6): 765-769.

[10] Chauhan, K. P. S., S. P. Singh and A. Chougule. 1995. Studies on the effect of windrow curing, neck cut and shade curing on export quality of onion bulbs during storage. National Horticultural Research and Development Foundation Newsletter, Vol.15(4): 5-7.

[11] Sheoran, O. P., D. S. Kaushik, L. S. Tonk, R. C. Hasija and R. S. Pannu. 1998. Statistical Software Package for Agricultural Research Workers. Recent Advances in information theory, Statistics & Computer Applications by D.S. Hooda & R.C. Hasija Department of Mathematics Statistics, CCS HAU, Hisar (139-143).

[12] Chittappa, B. 2016. Design and development of a onion de-topper cum grader. Unpublished M.Tech Thesis. University of Agricultural Sciences, Bengaluru.

■■

Comparative Performance of Different Paddy Threshing Methods in Odisha, India

by
Prerana P. Jena
Research Scholar
Dept. of Farm Machinery & Power,
College of Agricultural Engineering & Technology,
OUAT, Bhubaneswar - 751003, INDIA
preranajena.54@gmail.com

Aswini K. Goel
Professor
Dept. of Farm Machinery & Power,
College of Agricultural Engineering & Technology,
OUAT, Bhubaneswar - 751003, INDIA

Sangram K. Swain
Professor
Dept. of Farm Machinery & Power,
College of Agricultural Engineering & Technology,
OUAT, Bhubaneswar - 751003, INDIA

Debaraj Behera
Professor & Head
Dept. of Farm Machinery & Power,
College of Agricultural Engineering & Technology,
OUAT, Bhubaneswar - 751003, INDIA

Abstract

Four paddy threshers; namely power operated thresher-cum-winnower, power-tiller operated thresher, tractor operated thresher and tractor operated half feed thresher were evaluated with three varieties of paddy at three levels of grain moisture content. Their performances were compared with conventional methods i.e. hand beating and bullock treading. Threshers were evaluated with respect to output capacity, threshing efficiency, cleaning efficiency and grain losses. It was found that with increase in grain moisture content, the output capacity, the percentage of un-threshed grain and total grain losses increased while the percentage of grain breakage decreased for all the threshing methods used. Maximum output capacity was observed in case of tractor operated paddy thresher while it was minimum in case of conventional hand beating.

Introduction

Paddy (*Oryzasativa* L.) is an ancient and most important cereal crop cultivated in more than 110 countries in the world with a total production of 769,658 thousand tonnes (World Agricultural Statistics, 2019). India is the largest grower of paddy in terms of area with about 43.95 million hectares producing about 110.15 million tonnes of rice and approximately 166 million tones of straw (Indian Agricultural Statistics, 2015-16). In Odisha, about 70% of the population depend on agriculture. Out of the total cultivable land of 61.80 lakh hectare, paddy covers 38.80 and 3.00 lakh hectare in Kharif and Rabi season respectively. Odisha produces 115.35 lakh tonnes of paddy and about 177.46 lakh tonnes of straw (Anonymous, 2014-15).

Threshing is required to detach the grains from the bundle of panicles of any cereal crop. Threshing methods affect grain loss and damage. Paddy could either be manually or mechanically threshed (Amposah et al., 2017). The output of manual threshing is up to 30 kg of grain per man-hour depending on the variety of paddy (Appiah et al., 2011). The manual threshing method is popular due to its low cost; however quantitative and qualitative losses can be as high as 20-30% (Rickman et al., 2013). A study conducted to find the effect of machine and crop parameters revealed that when grain moisture content increased, total un-threshed grain increased and grain damaged decreased (Naik et al., 2010).Also they found that the threshing methods have significant effect on rice quality. The percentage of grain damage, un-threshed grains, germination rate and storage life depend upon threshing methods (Miah et al., 1994).

Factors like labour shortage, low quality yield, low output and huge loss of grains forced the farmers to shift towards mechanical threshing. Small and marginal farmers of the state use conventional threshing methods like hand beating and bullock treading. At present, power operated thresher-cum-winnower, power tiller operated thresher and tractor operated paddy threshers are used by progressive farmers across the state of Odisha. In both power tiller and tractor operated threshers, chopped straw are discharged which are of mostly no use. The discharged straw is generally burnt in the field itself which cause environmental pollution as well as soil degradation. The farmers who require whole straw for thatching houses and mushroom cultivation are using only hold on type power threshers operated by 1.0 hp electric motor, but these type of threshers have very low capacity ranging from 150-180 kg/h and threshed material needs further cleaning. In order to avoid burning of straw and wastage of chopped straw, recently tractor operated half feed thresher is being introduced in the state. This thresher discharges whole straw which can be used by farmers for mushroom cultivation, cattle feed, thatching of roofs etc. By using this thresher, farmers can generate additional income by selling straw bundles. The objectives of this present study is to evaluate the performance of all these threshers available in the state of Odisha with respect to their output capacity, threshing efficiency, cleaning efficiency, percentage of broken grain, blown grain and un-threshed grain with different varieties of paddy at different grain moisture content and to compare their economics of use.

Fig. 1 Threshing methods used for study

T_1: Power operated thresher-cum-winnower

T_2: Power tiller operated paddy thresher

T_3: Tractor operated paddy thresher

T_4: Tractor operated half feed thresher

T_5: Bullock treading method

T_6: Hand beating method

Material and Methods

This study was carried out in village Sanabhimdaspur and Balanga of Puri district, village Gania of Nayagarh district and village Tangibanta of Khurda district. Three varieties of paddy namely Swarna, Lalat and Hasanta were used in this study. The moisture content of paddy grain and straw were determined by standard hot air oven at 105 °C. The study was conducted at three levels of grain moisture content ranging from 13-16%. The six threshing methods used in this study were power operated thresher-cum-winnower (T_1), power-tiller operated thresher (T_2), tractor operated thresher (T_3), tractor operated half feed thresher (T_4), bullock treading (T_5)and conventional hand beating (T_6) (**Fig. 1**). The specifications of the threshers and crop parameters used in the study are presented in **Table 1** and **Table 2** respectively.

The performance of the threshers were evaluated with three paddy varieties at three levels of moisture content and parameters like output capacity, threshing efficiency, cleaning efficiency, percentage of un-threshed grains, broken grain and blown grain were measured as per relevant Indian standard test code (IS 6284:1985).The performance of these threshers were compared with conventional threshing methods. The cost economics of all these threshing methods were computed and compared.

Output Capacity

It is the mass of grain mixture received at all grain outlets when collected at rated input capacity. It is expressed in kg h^{-1}.

Output capacity = threshed grain at main grain outlet (kg) / duration of test run

Threshing Efficiency

The un-threshed grains from all outlets with respect to total grain input, expressed as percentage by mass.

Percentage of un-threshed grains = (w/W) × 100

where,

w = Quantity of un-threshed grain from all outlets per unit time

W = Total grain input per unit time.

Threshing efficiency = 100 − Percentage of un-threshed grains

Broken Grains

Broken grains include wholly or partially cracked or broken grain which is collected from all grain outlets with respect to total grain input expressed as percentage by mass.

Visible grain damage (broken grains) = (B/I) × 100

where,

B = Quantity of broken grain from all outlets per unit time.

I = Total grain input per unit time

Blown out Grain

It is the ratio of the quantity of the grain blown out to the quantity of the total grain input by weight.

Blown out grain (%) = (G/A) × 100

where,

G = Quantity of clean grain obtained at bhusa outlet per unit time

A = Total grain input.

Total Losses

Total loss is determined by adding loss due to un-threshed grain, loss due to blown grain and loss due to broken grain expressed in terms of percentage.

Total loss = un-threshed grain + broken grain + blown grain

Experimental Design

The experiment was conducted by using 3-factor CRD and each treatment was replicated thrice.

Results and Discussion

The performance of the paddy threshers under study with respect to the dependent parameters like output capacity, threshing efficiency, cleaning efficiency, percentage of un-threshed grain, percentage of blown grains and percentage of grain damage were analysed in accordance with 3-factor completely randomized design of experiment and their performances were compared with the conventional methods. The results obtained are presented in **Table 3** and the analysis of variance (ANOVA) of the above parameters is presented in **Table 4**.

Output Capacity

The output capacity varied from 136.91 to 141.12 kg/h for power operated thresher-cum-winnower (T_1),

Table 2 Crop parameters

Sl. No.	Parameters	Values		
1	Variety	Swarna	Lalat	Hasanta
2	Grain/crop ratio	0.38	0.36	0.41
3	Length of crop fed, cm	71	82	89
4	Moisture content of grain, %	13.2, 14.4, 15.7	13.6, 14.2, 15.9	13.1, 14.9, 15.5
5	Moisture content of straw, %	14.4, 15.6, 16.5	14.5, 15.6, 16.8	14.2, 16.1, 16.9

Table 1 Specification of threshers

Sl. No.	Parameters	Power operated thresher-cum-winnower	Power tiller operated thresher	Tractor operated thresher	Tractor operated half feed paddy thresher
1	Type of machine	Hold-on	Throw-in	Throw-in	Hold-on (feeding by chain conveyor)
2	Make	Brundabanjew Enterprises	Bidisha Enterprises Pvt. Ltd.	Vardhman Agencies	Jasoda Agro Works
3	Overall dimension (L × W × H) (in mm)	1660 × 825 × 1265	2120 × 1480 × 1610	4045 × 2160 × 2530	3650 × 2570 × 2530
4	Weight (kg) (including transport wheels)	75	548	1470	1,060
5	Power source	1.0 hp motor	13 hp power tiller	42 hp tractor	42 hp tractor
6	Power transmission system	Through V-belt & pulley	Through V-belt & pulley	Through V-belt & pulley	Through V-belt & pulley
7	Threshing cylinder	Wire loop	Spike tooth	Spike tooth	Wire loop
8	Crop feeding type	Manual	Manual	Manual	Manual
9	Transport wheel	Hard rubber wheel (140 × 40) mm	Pneumatic wheels (5.65 × 12.00)	Pneumatic wheel (7.00 × 19.00)	Pneumatic wheels (6.5 × 17.00)
10	Cost (INR) (2019)	26,175	100,000	160,000	180,000

Table 3 Performance of different threshers at three levels of grain moisture content

Threshing methods	Variety	Grain-crop ratio, %	Grain moisture content, %	Straw moisture content, %	Output capacity, kg/h	Losses, %				Efficiency,%	
						Un-threshed	Broken grain	Blown grain	Total losses	Threshing	Cleaning
Power operated thresher-cum winnower (T_1)	Swarna	38	13.2	14.4	136.91	1.4	0.59	0.05	2.04	98.6	97.67
			14.4	15.6	138.75	2.2	0.56	0.03	2.79	97.8	96.23
			15.7	16.5	140.44	2.9	0.52	0.03	3.45	97.1	95.34
	Lalat	36	13.6	14.5	135.32	1.88	0.62	0.06	2.56	98.12	96.95
			14.2	15.6	137.22	2.68	0.59	0.05	3.32	97.32	95.99
			15.9	16.8	139.71	3.18	0.53	0.04	3.75	96.82	95.13
	Hasanta	41	13.1	14.2	137.23	1.05	0.48	0.04	1.57	98.95	98.06
			14.9	16.1	139.43	1.84	0.41	0.03	2.28	98.16	97.11
			15.5	16.9	141.12	2.03	0.36	0.02	2.41	97.97	96.98
Power tiller operated thresher (T_2)	Swarna	38	13.2	14.4	330.6	2.77	0.74	0.85	4.36	97.23	96.23
			14.4	15.6	332.12	3.35	0.7	0.8	4.85	96.65	95.2
			15.7	16.5	335.16	6.86	0.68	0.74	8.28	93.14	94.11
	Lalat	36	13.6	14.5	329.24	3.11	0.81	0.91	4.83	96.89	96.01
			14.2	15.6	331.41	4.46	0.75	0.85	6.06	95.54	95
			15.9	16.8	334.89	6.01	0.69	0.79	7.49	93.99	94.05
	Hasanta	41	13.1	14.2	331.67	2.35	0.65	0.5	3.5	97.65	97.89
			14.9	16.1	333.48	3.05	0.59	0.45	4.09	96.95	97.12
			15.5	16.9	336.95	3.85	0.52	0.41	4.78	96.15	96.23
Tractor operated thresher (T_3)	Swarna	38	13.2	14.4	1,320.88	1.55	1.24	1.11	3.9	98.45	99.93
			14.4	15.6	1,323.92	3.74	1.21	1.08	6.03	96.26	98.89
			15.7	16.5	1,326.96	5.98	1.17	1.04	8.19	94.02	97.87
	Lalat	36	13.6	14.5	1,319.32	2.15	1.56	1.15	4.86	97.85	98.19
			14.2	15.6	1,322.41	3.26	1.34	1.11	5.71	96.74	97.32
			15.9	16.8	1,325.99	6.04	1.29	1.07	8.4	93.96	96.67
	Hasanta	41	13.1	14.2	1,321.78	1.01	1.12	1.04	3.17	98.99	99.75
			14.9	16.1	1,324.56	2.15	1.05	0.97	4.17	97.85	98.95
			15.5	16.9	1,328.11	3.76	0.97	0.89	5.62	96.24	98.15
Tractor operated half feed thresher (T_4)	Swarna	38	13.2	14.4	289.08	2.63	2.38	2.87	7.88	97.37	95.95
			14.4	15.6	291.56	4.18	2.32	2.84	9.34	95.82	94.87
			15.7	16.5	293.98	6.21	2.27	2.8	11.28	93.79	93.83
	Lalat	36	13.6	14.5	288.65	3.88	2.54	2.95	9.37	96.12	94.16
			14.2	15.6	290.23	5.64	2.43	2.9	10.97	94.36	93.25
			15.9	16.8	292.15	7.73	2.38	2.84	12.95	92.27	92.98
	Hasanta	41	13.1	14.2	290.32	2.05	2.05	2.35	6.45	97.95	96.14
			14.9	16.1	292.87	3.76	1.96	2.16	7.88	96.24	95.23
			15.5	16.9	294.45	4.9	1.89	1.95	8.74	95.1	94.45
Bullock treading (T_5) followed by winnowing by bamboo swing basket	Swarna	38	13.2	14.4	121.62	4.68	5.67	5.43	15.78	95.32	93.54
			14.4	15.6	125.73	6.86	5.54	4.97	17.37	93.14	92.67
			15.7	16.5	128.56	7.35	4.95	4.35	16.65	92.65	91.78
	Lalat	36	13.6	14.5	120.12	5.35	5.92	5.35	16.62	94.65	92.67
			14.2	15.6	124.23	7.46	5.83	5.18	18.47	92.54	91.76
			15.9	16.8	126.87	7.85	5.1	5.03	17.98	92.15	90.24
	Hasanta	41	13.1	14.2	123.65	4.05	5.07	4.96	14.08	95.95	95.12
			14.9	16.1	127.24	5.58	4.95	4.24	14.77	94.42	94.62
			15.5	16.9	130.12	6.31	4.62	3.99	14.92	93.69	93.89
Hand beating method (T_6) and winnowing by bamboo swing basket	Swarna	38	13.2	14.4	14.53	1.25	3.54	3.65	8.44	98.75	96.73
			14.4	15.6	15.68	2.01	3.03	2.98	8.02	97.99	95.54
			15.7	16.5	16.72	2.85	2.91	2.15	7.91	97.15	94.87
	Lalat	36	13.6	14.5	13.27	1.85	3.79	3.89	9.53	98.15	95.19
			14.2	15.6	14.15	2.48	3.24	3.16	8.88	97.52	94.23
			15.9	16.8	15.76	3.11	3.06	2.98	9.15	96.89	93.45
	Hasanta	41	13.1	14.2	15.92	1.01	3.02	2.95	6.98	98.99	96.29
			14.9	16.1	16.14	2.15	2.83	2.12	7.1	97.85	95.65
			15.5	16.9	17.39	2.65	2.12	1.84	6.61	97.35	94.87

330.6 to 336.95 kg/h for power tiller operated thresher (T_2), 1,320.88 to 1,328.11 kg/h for tractor operated thresher (T_3), 289.08 to 294.45 kg/h for tractor operated half feed thresher (T_4), 121.62 to 130.12 kg/h for bullock treading (T_5) and 14.53 to 17.39 kg/h for hand beating when grain moisture content varied from 13.2 to 15.7% for Swarna; 13.6 to 15.9% for Lalat and 13.1 to 15.5% for Hasanta variety respectively (**Table 3**). The output capacity was found to be maximum in case of tractor operated thresher while it was minimum in case of conventional method. Highest output capacity of tractor operated thresher is due to its higher feed rate which was possible due to its proper size of feeding chute and threshing drum size. It was observed that the output capacity increased with increase in grain moisture content for all the threshing methods for all paddy varieties but it did not vary significantly for a particular threshing method. The effect of threshing methods, variety and grain moisture content have significant effect on output capacity of all the threshing methods. The interaction of threshing methods, variety and grain moisture content on output capacity was also found to be significant for all the treatments.

Threshing Efficiency

Threshing efficiency varied from 96.82 to 98.60 % for T_1, 93.14 to 97.65% for T_2, 93.96 to 98.45 % for T_3, 92.27 to 97.95 % for T_4, 92.15 to 95.95% for T_5 and 96.89 to 98.99% for T_6 when grain moisture content varied from 13.2 to 15.7% for Swarna variety; 13.6 to 15.9% for Lalat variety and 13.1 to 15.5% for Hasanta variety respectively. Threshing efficiency of all the threshing methods decreased as the grain moisture content increased for all paddy varieties. This may be due to the fact that unthreshed grain increased with increase in moisture content and hence threshing efficiency decreased.

Table 4 Analysis of variance of dependent parameters studied

Sources of variation	Degrees of freedom	F_{cal}						
		Output Capacity	Losses				Efficiency	
			Un-threshed	Broken grain	Blown grain	Total losses	Threshing	Cleaning
Factor A	5	4,127,352.9225**	6,400.0541**	11,327.5234**	300,275.9447**	1,251,938.3262**	5,295.2387**	1,951.0052**
Factor B	2	47.4938**	2,619.9577**	357.6608**	11,987.5843**	174,140.8969**	2,146.4272**	985.0965**
Factor C	2	200.1072**	9,022.6176**	158.4336**	5,472.3968**	119,467.7830**	7,042.1584**	861.1002**
AB	10	0.4748	84.3087**	7.6373**	923.2583**	1,621.5742**	102.6949**	47.5509**
AC	10	4.8268**	212.2770**	15.7373**	1,085.0208*	14,282.2398**	229.1774**	1.3475
BC	4	0.1061	75.5454**	2.2114*	217.0520**	2,585.7067**	105.8539**	7.3564*
ABC	20	0.1660	29.6675**	2.6052**	93.1270**	1,057.0971**	32.3234**	2.7079**

Factor A: (Threshing methods), Factor B: (Variety), Factor C: (Moisture Content),

Fig. 2 Effect of grain moisture content on output capacity

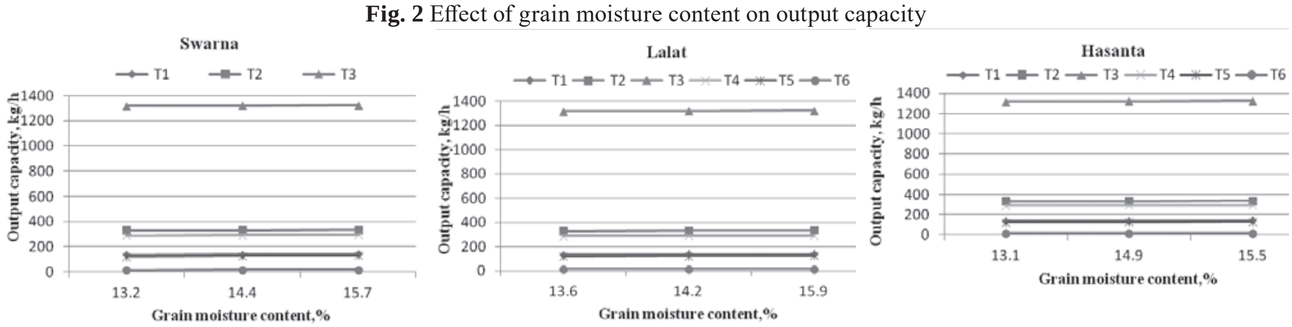

(a) (b) (c)

Fig. 3 Effect of grain moisture content on threshing efficiency

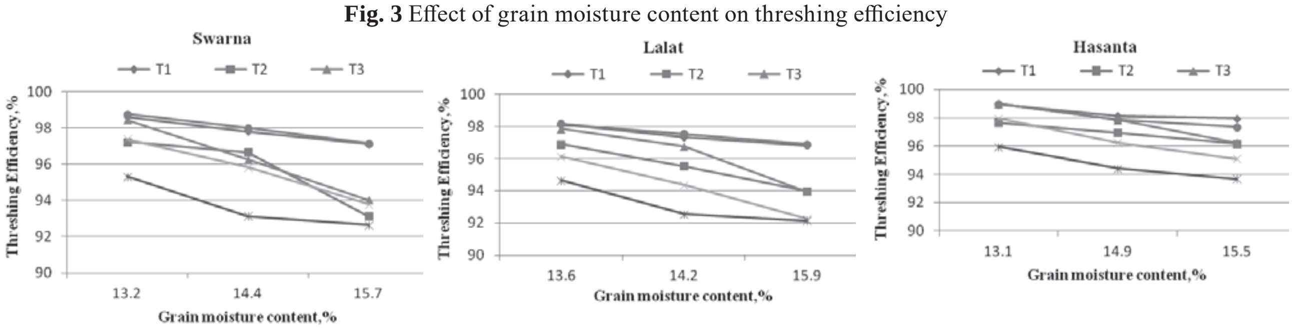

(a) (b) (c)

Percentage of un-threshed grain increased because at higher grain moisture content, grains are attached with the panicle more rigidly as compared to dry grain. This result is in agreement with Naik et al. (2010). The effect of threshing methods, variety and grain moisture content has significant effect on threshing efficiency. The interaction of threshing methods, variety and grain moisture on threshing efficiency were found to be highly significant.

Cleaning Efficiency

Cleaning efficiency varied from 95.13 to 98.06% for T_1, 94.05 to 97.89% T_2, 96.67 to 99.93% for T_3, 92.98 to 96.14% for T_4, 90.24 to 93.89% for T_5 and 93.45 to 96.73% for T6when grain moisture content varied from 13.2 to 15.7% for Swarna; 13.6 to 15.9% for Lalat and 13.1 to 15.5% for Hasanta variety respectively. It was observed that cleaning efficiency of all threshing methods decreased with increase in moisture content for all paddy varieties. It may be due to the reason that at higher moisture content, chaff and foreign particles needs higher wind velocity to be blown out. The highest cleaning efficiency of 99.93% was observed with tractor operated paddy thresher and this may be due to the provision of higher number of aspirators (3 nos.) and side blowers at main grain outlet. The effect of threshing methods, variety and moisture content on cleaning efficiency is found to be highly significant. The interaction of threshing methods and grain moisture content and the interaction of variety and moisture content on cleaning efficiency were also found to be highly insignificant.

Broken Grain

Broken grain varied from 0.36 to 0.59% for T_1, 0.52 to 0.74 for T_2, 0.97 to 1.24% for T_3, 2.38 to 1.89 to 2.27% T_4, 4.62 to 5.67 % T_5 and 2.12 to 3.79% for T_6 when grain moisture content varied from 13.2 to 15.7% for Swarna; 13.6 to 15.9% for Lalat and 13.1 to 15.5% for Hasanta variety respectively. It was observed that the percentage of broken grain for all the threshing methods decreased as the moisture content increased. This may be due to the reason that at higher grain moisture content grain can sustain higher impact force as compared to dry grain. This result is in agreement with Naiket al. (2010). The broken grain percentage was maximum in case of bullock treading where as it was least in case of power operated thresher-cum-winnower. Higher broken grain in bullock treading may be due to repeated trampling of grains by bullocks. The effect of threshing methods, variety and moisture content on broken grain were found to be highly significant whereas the interaction of variety and grain moisture content on broken grain percentage were insignificant at 5% level of significance.

Blown Grain

Percentage of blown grain varied from 0.02 to 0.06% for T_1, 0.41 to 0.91% T_2, 0.89 to 1.11% T_3, 1.95 to 2.87% T_4, 3.99 to 5.43% T_5 and 1.84 to 3.65% T_6 when grain moisture content varied from 13.2 to 15.7% for Swarna; 13.6 to 15.9% for Lalat and 13.1 to 15.5% for Hasanta variety respectively. Percentage of blown grain are maximum at lower grain moisture content for all the threshing methods and it decreased with increase in moisture content and this may be due to the reason

Fig. 4 Effect of grain moisture content on cleaning efficiency

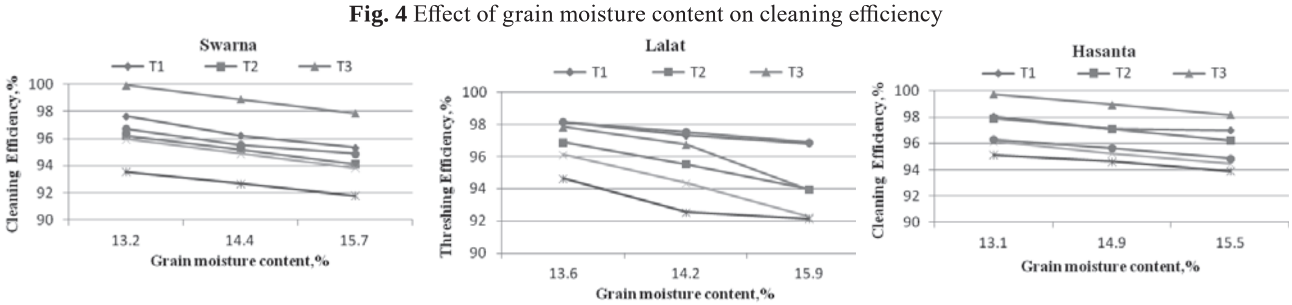

(a) (b) (c)

Fig. 5 Effect of grain moisture content on broken grain

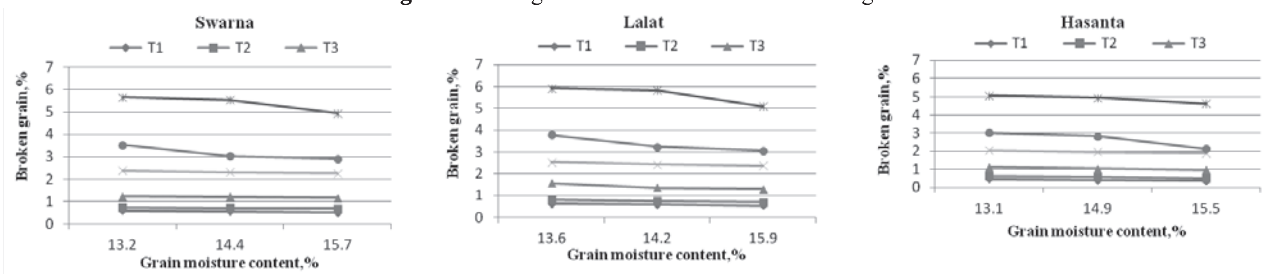

(a) (b) (c)

that at higher grain moisture, grains are heavier and at particular wind speed tends to overcome the terminal velocity. The effect of threshing methods, variety and moisture content on percentage of blown grain were found to be highly significant and the interaction of threshing method, variety and grain moisture content on blown grain percentage was also significant.

Cost of Operation

The cost of operation of threshing methods were computed as per IS test code (IS: 9164-1979). The highest cost of operation ($15.72/h) was found for T_4 due to its higher cost while minimum ($0.52/h) was with T_6 (**Table 5**). The highest threshing cost of $5.43/q was found with T_4 due to its lower output capacity as compared to its cost of operation and minimum with T_1. Although the cost of operation of T_4 is much higher as compared to other threshing methods, revenue of $0.81/q can be generated by selling straw bundles.

Conclusion

The performance of different threshers i.e. power operated thresher-cum-winnower, power-tiller operated paddy thresher, tractor operated paddy thresher and tractor operated half feed paddy thresher were evaluated with three varieties of paddy at three levels of moisture content varying from 13.1 to 15.9%. Their performances were compared with those of conventional methods like bullock treading and hand beating. The findings of the study are summarised below.

- The output capacity increased with increase in grain moisture content for all threshing methods used. Output capacity was found to be maximum (1,328.11 kg/h) in case of tractor operated thresher at 15.5% moisture content in case of Hasanta variety while it was minimum (98.15 kg/h) in case of hand beating at 13.6% moisture content in case of Lalat vareity.
- Threshing efficiency of all the threshing methods decreased as grain moisture content increased. Threshing efficiency was found to be maximum (99.75%) in case of tractor operated thresher at 13.1 % moisture content in case of Hasanta where as it was minimum (92.15%) in case of bullock treading at at 15.9% for Lalat variety.
- Cleaning efficiency was maximum (99.93%) at 13.2% moisture content in case of tractor operated thresher for Swarna variety and minimum (90.24%) in case of bullock treading followed by winnowing by bamboo swing basket at 15.9% for Lalat.
- Un-threshed grain percentage of all the threshers increased with increase in grain moisture content whereas percentage of broken grain and blown grain of threshers decreased as grain moisture content increased.
- Highest cost of threshing of $5.43/q was found for tractor operated half feed thresher while it is minimum ($0.87/q) for power operated thresher-cum winnower at all three levels of moisture content.

REFERENCES

Amponsah, S. K., A. Addo, K. Dzisi, J. Moreira and S. A. Ndindeng. 2017. Comparative evaluation of mechanised and manual threshing options for Amankwatia and AGRA rice varieties in Ghana. Journal of Agricultural Engineering. XLVIII: 664,181-189.

Anonymous. 2013-14. Odisha Agriculture Statistics, Directorate of Agriculture and Food Production, Odisha, Bhubaneswar.

Anonymous. 2014-15. Status of Agriculture in Odisha, Directorate of Agriculture and Food Production, Odisha, Bhubaneswar.

Anonymous. 2019. World Food and Agriculture Statistical Pocketbook, Food and Agriculture Organization of the United Nations.

Annonymous. 1985. Test code for power operated cereal thresher (IS: 6284:1985), Indian Standard Institutions, Manak Bhawan, New Delhi.

Annonymous.1979. Test code for power operated cereal thresher (IS: 9164-1979), Indian Standard

Table 5 Cost of operation of threshing methods

Description	T_1	T_2	T_3	T_4	T_5	T_6
Cost of operation (USD / h)	1.37	6.96	13.86	15.72	2.43	0.52
Cost of operation (USD / quintal) (at 13.2% grain moisture content of Swarna)	0.87	1.83	1.04	5.43	1.99	3.57

Fig. 6 Effect of grain moisture content on broken grain

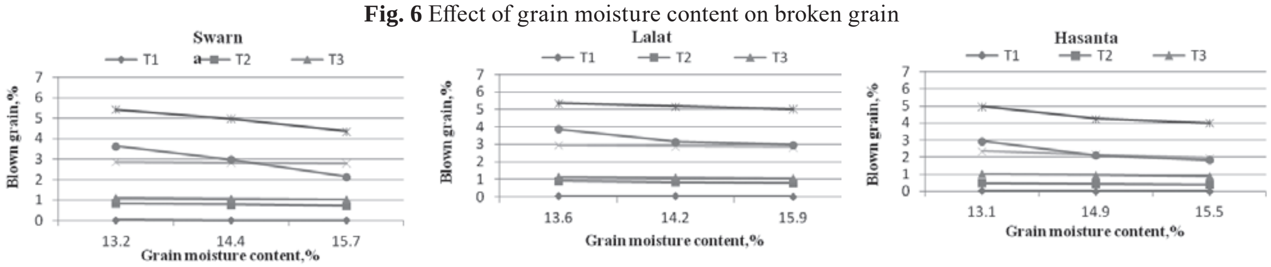

(a) (b) (c)

Institutions, Manak Bhawan, New Delhi.
Appiah, F., R. Guisse and P. K. Dartey. 2011. Post-harvest losses of rice from harvesting to milling in Ghana. J. Stored Prod. Postharvest Res. 2:64-71.
Miah, A. K., A. K. Roy, M. A. Hafiz, M. Haroon and S. S. Seddique. 1994. A comparative study on theeffect of rice threshing methods on grain quality.Agricultural Mechanization in Asia, Africa and Latin America. 25(3): 63-66.
Naik, R. K., S. Patel, A. K. Verma and A. K. Shrivastava. 2010. Effect of crop and machine parameters on performance of paddy thresher. Agricultural Engineering Today. Vol.34(I): 30-32.
Rickman, J., J. Moreira, M. Gummert and M. C. S. Woperies. 2013. Mechanising Africa's rice sector. Realising Africa's rice promise. CAB International. 332-242.

■■

(Continued from page35)

Development & Performance Evaluation of Solar Biomass Drying System for Ginger (*Zingiber officinale*)

Applied Science. Vol.6(2): 170-184.
Mondal, K. 2006. Development and storage behaviour of ginger paste and powder. Thesis, M.tech. G.B. Pant University of Agriculture and Technology, Pantnagar.
Panwar, N. L., S. C. Kaushik and S. Kothari. 2012. Renewable and Sustainable Energy Reviews, 16, 2812-2819.
Rajat, P. 2013. Studies On Development and Quality Evaluation of Ginger Powder. Unpublished Thesis. Sardar Vallabhbhai Patel University of Agriculture and Technology, Meerut, India.
Swain, S., M. Din, R. Chandrika, G. P. Sahoo and S. D. Roy. 2014. Performance Evaluation of Biomass Fired Dryer for Copra Drying: A Comparison with Traditional Drying in Subtropical Climate. J Food Process Technology Vol 5: 294. doi:10.4172/2157
Sreekumar, A., P. E. Manikantan and K. P. Vijayakumar. 2008. Performance of indirect solar cabinet dryer. J. Energy Conversion and Management Vol. 49(6): 88-1395.

■■

Development & Performance Evaluation of Solar Biomass Drying System for Ginger (*Zingiber officinale*)

by

S. R. Kalbande
Professor
Dept. of Unconventional Energy Sources and Electrical Engineering,
Dr. Panjabrao Deshmukh Agricultural University,
Akola (MH), INDIA
surendra_kalbande@gmail.com

A. J. Dhondge
Assistant Professor
Dept. of Unconventional Energy Sources and Electrical Engineering,
Dr. Panjabrao Deshmukh Agricultural University,
Akola (MH), INDIA
amol.jd1107@gmail.com

D. S. Karale
Assistant Professor
Dept. of Farm Power and Machinery,
Dr. Panjabrao Deshmukh Agricultural University,
Akola (MH), INDIA
dhiraj_karale@hotmail.com

R. D. Pawar
M.Tech. (RES) Scholar
Dept. of Unconventional Energy Sources and Electrical Engineering,
Dr. Panjabrao Deshmukh Krishi Vidyapeeth,
Akola (MH), INDIA

Abstract

Drying of agricultural commodity by use of electricity or petroleum is an expensive process in developing countries. Therefore, an appropriate technology for drying of agricultural produce has been designed and developed and its performance for the drying of ginger has been evaluated. A continuous type solar biomass drier was developed. The system is capable of generating an adequate and continuous flow of hot air of temperature between 55 and 65 °C. Splitted ginger rhizomes were successfully dried in developed system. Dried ginger obtained under continuous type solar biomass (hybrid) drying by a treatment viz., slicing was similar in quality with respect to physical appearance like color, texture etc. The quantitative analysis showed that the traditional drying i.e., open sun drying had taken 3 days to dry the slices while continuous type solar biomass drier took only 16 hours and produced better quality produce. The efficiency of the whole unit obtained was 34.54 percent.

Keywords: Drying, Hybrid, Solar-biomass drier, Ginger, *Zingiber officinale*.

Introduction

Drying of agricultural produce is an essential process used all over the world for its preservation. It helps to reduce the water activity of the produce to a level below which deterioration does not occur for a definite duration. Ginger (*Zingiber officinale*) is an important commercial crop grown for its aromatic rhizomes which are used both, as spice and medicine. It is a valuable cash crop and plays an important role in Indian Ayurvedic medicine as a folk remedy to promote cleaning of the body through perspiration, to calm nausea, and to stimulate the appetite (Rajat, 2013). Ginger contains gingerol, an oleoresin (combination of volatile oils and resin) that accounts for the characteristic aroma and therapeutic properties (Ismail et al., 2012). Components of gingerol (zingiberene, bisabolene, cam phene, geranial, linalool and borneol) possess beneficial properties for the treatment of poor digestion, heartburn, vomiting and preventing motion sickness (Mondal, 2006).

This continuous biomass based drying system integrated with a simple biomass combustor. The biomass combustor is constructed from a thin metallic sheet and it is surrounded by another metallic sheet cylinder. The gap is provided in between for easy heat transfers. Briquettes, which is the most common source of energy in rural areas of developing countries, is mainly designated to be the fuel for the burner. The biomass combustor will provide the solution for efficient utilization of available biomass. It utilizes the flue gas heat for an application like drying of fruit and vegetables with minimum pollution and product degradation. The overall efficiency of biomass utilization can be increased by using heat loss into the atmosphere. Solar radiation is one of the most promising sources of energy. Unlike fossil fuels and nuclear energy, it is an environmentally clean source of energy. By proper application of technologies, excellent thermodynamic match between the solar energy resources and many end uses can be achieved (Sreekumar et al., 2008).

Dryers may be classified as open-air or sun, fuel fired or kiln, electric and solar dryers. Open air or sun drying (OSD) is cheap but it has the major problem of slow and intermittent drying, no protection over rain, contamination, undesirable quality change and nonuniformity of dried products (Panwar et al., 2012). This paper presents a continuous type solar biomass drier integrated with a simple biomass gasifier. The system has been evaluated under summer and rainy season of Akola district region in India for drying of ginger.

Material and Methods

2.1. Description of the Solar Biomass Drier

The continuous type solar biomass drier was fabricated for drying of ginger and other such produce. The details of the drier are shown in **Fig. 1**.

The drier has two parts: (i) solar tunnel drier and (ii) biomass combustor.

(i) Solar tunnel drier. The system mainly consists of a cover of UV stabilized polyethylene sheet (200-micron thickness) mounted on a semi cylindrical pipe frame. The cross-sectional area covered by the solar tunnel drier is 24 m^2. The axis of tunnel was oriented in the East-West direction to maximize the capture of solar radiation at Akola (latitude 20°30'N) during the test period. The dryer was given sufficient height to move a man freely to load and unload the product. End frame is made of aluminium members fitted on both ends of solar tunnel dryer. The end frame structure is having provision for door (1.90 × 0.90 m). A turbo ventilator of 0.5 m diameter was fitted at the centre of the entire length of solar tunnel dryer for natural convection. The north wall provides the height of 1.37 m at entire length of dryer

(ii) Biomass combustor. The combustion chamber is cylindrical in shape having inner diameter of 0.54 m and outer diameter of 0.64 m and height of 0.32 m depending on required operating time. At the bottom of burner an adjustable door is provided for feeding the biomass and controlling airflow for combustion and an iron grate is provided for burning biomass. The exhaust gases exit through a chimney of 0.080 m diameter and a long flue pipe placed on one side of the biomass burner. Two blowers of 0.5 and 3 hp motor was used with biomass combustor for the purpose of air supply.

Fig. 1 Schematic diagram of biomass combustor

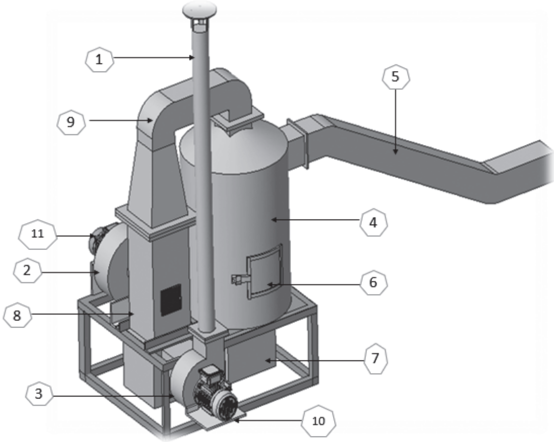

1. Chimney
2. Blower for combustion chamber
3. Blower for combustion chimney
4. Combustion chamber
5. Main air duct
6. Biomass feeding door
7. Ash collector
8. Preheating arrangement
9. Air duct to flue gas intake for preheating arrangement
10. Half Hp motor
11. 3 Hp motor

Fig. 2 Schematic diagram of biomass combustor

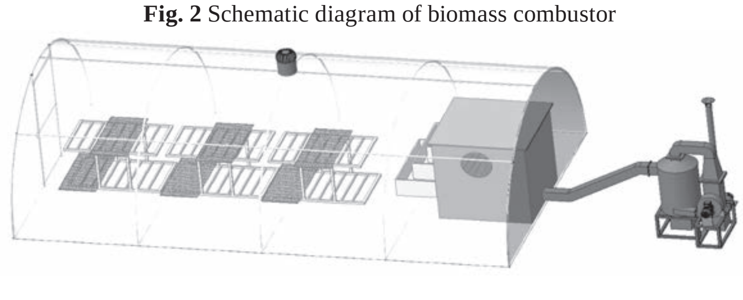

2.2. Operation of Drier

This drier is designed to make use of solar energy during day time and biomass during night time as source of heat. Drying parameters were observed at five different points i.e., centre and corners of each of the trays (Kalbande et al., 2017). The samples were weighed at different time interval during day and night. As the solar radiations falls on UV stabilized polyethylene sheet, these enter inside the drier and get absorbed by the produce, resulting in an increase of drier temperature. This process produces temperature difference between the inside and outside air. Inside the tunnel, heated air goes upward, pick up moisture from the product and comes out from the turbo ventilator provided at the top of the solar tunnel drier. During periods of low or zero solar radiation, biomass burner is used for back up heating. The combustion gases heat up the drying surface, which in turn warm the air as it moves over the outer surface. The warm air rises up into the drying chamber, evaporating and picking up moisture from the produce as it passes through the trays, and then escapes through the top vents as before. Temperature inside the tunnel drier is controlled feeding rate of the soyabean briquette in the biomass burner.

2.3. Performance Evaluation of Drier

The drier is installed at Department of Unconventional Energy Sources and Electrical Engineering, Dr. Panjabrao Deshmukh Agricultural University, Akola in India and tested during the months of May & June 2021. For the separate trials, 30 kg of fresh ginger rhizomes were obtained and visually checked for any defect. Spoiled rhizomes have been removed and good one was selected for testing. Each trial was made for 30 kg of ginger rhizomes. Batch of 15 kg ginger rhizomes was sliced in 50 to 70 mm length and 5 mm thickness.

A separate batch of 100 g rhizomes was sliced in same length and thickness and dried in open sun. In order to simplify the evaluation, solar energy was the sole source of heat for drying during the daytime and the biomass burner was used only at night. The drier was operated as a solar drier from 09.00 am to 06.00 pm. Biomass operation was restored after 06.00 pm when solar radiation was not enough for drying. The drying was stopped when product reached at constant weight.

2.4. Instrumentation and Observations

The following parameters were measured during the trials: solar radiation, mass of ginger rhizomes, temperatures, relative humidity, wind speed, airflow through the drier and biomass burnt. Temperature of product and relative humidity of air was measured by infrared thermometer and hygrometer, respectively. Solar radiation was recorded with Digital pyranometer with data logger and wind speed by hot wire anemometer with an accuracy of 0.2 m/s. The mass of the product and biomass fuel was measured with electronic balance.

Fig. 3 Variation in moisture content in CSBD, STD and OSD with respect to drying time

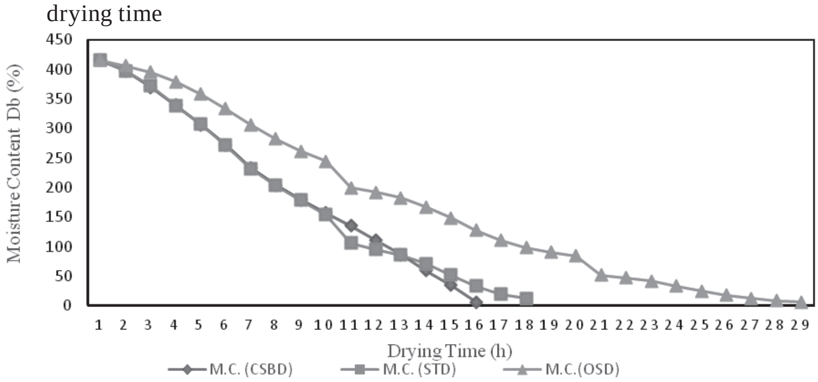

Fig. 4 Variation in temperature and solar radiation during full load test in CSBD with respect to drying time

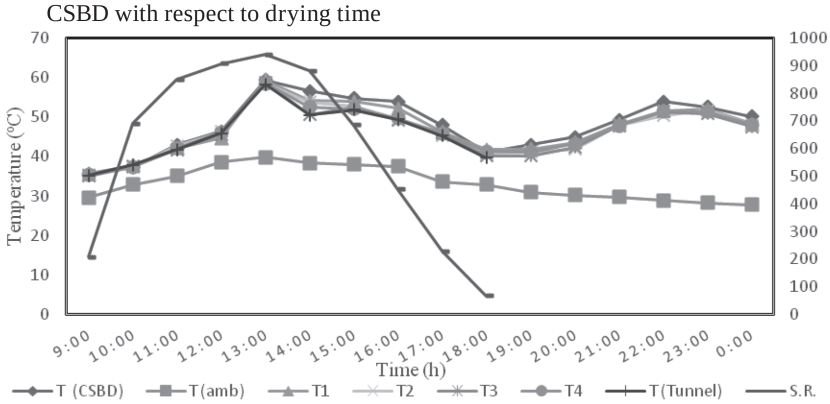

Results and Discussion

3.1. Capacity and Drying Times

A single layer of specified length and thickness, 15 kg of ginger slices (2 kg on each of the tray) were used for study. Moisture present in the product with drying period of the trials of the full load drier is shown in **Fig. 3**. It is clearly shown that drying time for drying ginger in CSBD was 16 h whereas in open sun drying it was 29 h for drying of the same product from moisture content of 415.46 to 6.18 percent (d.b.) during that trial (Doharey, 2009).

3.2. Drying Parameters

The significant variations were measured in drying parameters at different tray levels during day and night. During the day, slices on the top tray dried faster while slices on the bottom tray dried slower. Experiments showed that moisture remained in the slices in continuous solar biomass dryer was 306.70% after the first 4 h of drying compared to 379.38% in open sun drying, respectively. The maximum temperature of the product measured at continuous solar biomass dryer was 59.3 °C during first day and temperatures of the product of open sun drying were 39.8 °C, respectively (**Fig. 4**) (Alakali and Satimehin, 2004). During the night when the gasifier was in operation, the slices on the bottom tray dried faster compared to those upper trays in drying chamber. The maximum temperature of product measured at the night was 52.5 °C. The final moisture content of ginger slices after 16 h of drying were 6.18% with corresponding relative humidity of

13 percent in continuous solar biomass drying system.

Average moisture content (d.b.) of ginger reduced from 415.46 to 6.18 percent (d.b.) in 16 h in continuous solar biomass drying system, from 415.46 to 12.37 percent (d.b.) in 18 h solar tunnel dryer and from 415.46 to 6.18 percent (d.b.) in 29 h in open sun drying (**Fig. 3**).

3.3. Quality Evaluation

Nutritional value and physical appearance in relation to surface color and nutritional value was recorded. Powder colour was determined using Hunter Lab, which includes lightness and chroma saturation (**Table 1**). L is the lightness coordinate ranging from no reflection for black (L = 0) to perfect diffuse reflection for white (L = 100). a is the 'redness' coordinate ranging from negative values for green to positive values for red. b is the 'yellowness' coordinate ranging from negative values for blue to positive values for yellow. Open sundried slices showed their quality got deteriorated. The dried samples (100 g) obtained from batches were powdered and were analysed for total gingerols (mg/g) extraction. For CSBD it was 24.4% and in open sun drying it was 19.9% (**Table 2**) Produce dried in open sun was having less Total gingerols (mg/g) than CSBD dried product and it showed the inferior quality of dried ginger slices were obtained in CSBD (Famurewa et. al., 2011).

3.4. Drier Efficiency

Overall thermal efficiency has been evaluated for the drier. The thermal efficiency over an entire drying trial (g) is the ratio of the energy used to evaporate the moisture from the product to the energy supplied to the drier. In this drier, both solar radiation and biomass supplied the energy. The overall thermal efficiency of the drier is therefore defined as

$$\eta \% = \{(M \times \lambda) / [(S \times A) + (C \times m)] \times 100\}$$

Where, M is the mass of water evaporated (kg); k is the latent heat of vaporization (MJ/kg); S is the total solar radiation on the dryer (MJ/m^2); A is the solar collection area (m^2); C is the calorific value of wood (MJ/kg); m is the mass of used biomass (kg). Overall drying efficiency of system for drying ginger was found to be 34.54%. The total drying time and moisture evaporated of ginger samples were found to be 16-hour and 22.5 kg, respectively. The efficiency was lower which may be due to full capacity of drier has not been utilized. It should be noted that the type of product and its final moisture content level influences the thermal efficiency. The final moisture in a product generally requires more energy to extract than the initial moisture, and the preparation of the product prior to drying such as slicing affects the thermal efficiency.

Conclusions

The developed continuous solar biomass drying system is capable of producing the air temperature between 55 and 65 °C, that was optimum for dehydration of ginger slices. Drying time for ginger had been drastically reduced compared to open sun drying. The efficiency of the whole unit observed was 34.54%. The volatile oil in CSBD system was 24.4% but in open sun drying it was only 19.9%. The quality of product remained maintained in this drier whereas in open sun drying it gets deteriorated. Study concluded that continuous solar biomass drying system is better option for preserving quality of the dried product and slicing improves drying rates.

REFERENCES

Alakali, J. S. and A. A. Satimehin. 2004. Drying kinetics of ginger, Nigerian Food Journal, Vol 22(1): 105-111.

Doharey, D. S., N. K. Jain and S. Kumar. 2009. Fluidized and convective drying kinetics of ginger slices, Journal of Agricultural Engineering, Vol 46(3): 14-18

Famurewa, A. V., P. O. Emuekele and K. F. Jaiyeoba. 2011. Effect of drying and size reduction on the chemical and volatile oil contents of ginger (*Zingiber officinale*), Journal of Medicinal Plants Research, Vol 5(14): 2941-2944.

Ismail, R. K. and Jagan Mohan Rao Lingamallu. 2012. Microwave drying of ginger (*Zingiber officinale*) and its effects on polyphenolic content and antioxidant activity, International Journal of Food Science & Technology, Vol 47(11): 2311-2317.

Kalbande S. R., P. Jadhav, V. P. Khambalkar and S. Deshmukh 2017. Design of solar Dryer Assisted with Reflector for Drying of Medicinal Crop. International Journal Current Microbiology and

(Continued on page31)

Table 1 Colour value testing for ginger powder

Sample	L	a	b
$S1_{(CSBD)}$	65.01	3.44	20.11
$S2_{(STD)}$	62.81	3.45	19.54
$S3_{(OSD)}$	53.89	3.99	18.31

Table 2 Nutritional analysis of ginger powder

Sr. No.	Particular	CSBD	STD	OSD
1	Total gingerols (mg/g)	24.4	22.1	19.9
2	Carbohydrate (g/100g)	86.8	69.9	55.61
3	Dietary fiber (g/100g)	11.91	10.23	10.11
4	Protein (g/100g)	5.32	5.02	8.5
5	Oleoresin content (g/100g)	1.32	1.16	1.05

Development and Evaluation of Power Tiller Operated Harvester for Small Onion

by
N. Nisha
Teaching Assistant
Dept. of Farm Machinery and Power Engg.,
Agricultural Engg. College & Research Institute,
TNAU, Coimbatore-641 003, Tamil Nadu, INDIA
nisha34agri@gmail.com

B. Shridar
Dean (Agricultural Engineering)
Agricultural Engg. College & Research Institute,
TNAU, Coimbatore-641 003, Tamil Nadu, INDIA
tnaushridar@gmail.com

Abstract

Harvesting of small onion crop is an important operation in cultivation of small onion, which has to be carried out at optimum crop maturity to minimize field losses. The small onion harvesters available in India cause more bulb damage and they are not suitable for small scale farmers. A power tiller operated small onion harvester was developed with a digging tool, conveyor and a leveler. The machine and operational parameters influencing the performance of onion harvester include rake angle, forward speed and moisture content of soil. The parameters were analyzed for their effects on harvesting efficiency and the optimized parameters were used to carry out field performance evaluation. Force analysis was carried out for the developed digging tool. The results of the testing of developed small onion harvester indicated maximum harvesting efficiency, bulb damage of , actual field capacity, theoretical field capacity and field efficiency of 97.4%, 1.6%, 0.068 ha h^{-1}, 0.062 ha h^{-1} and 85.2%, respectively. The cost of harvesting of small onion with the developed harvester was Rs. 918/ha.

Introduction

Small onion is a vegetable crop grown commercially in many parts of the world. India ranks first in terms of area in the world with 0.83 million ha (Kaveri et al., 2015). In India harvesting of small onion is done manually. Manual harvesting of small onion is done by using shovel and it requires 21.4 percent of the total energy consumed in small onion cultivation (Ashwini et al., 2014). In manual harvesting, considerable amount of small onion bulbs are lost due to insufficient soil moisture and also manual harvesting is time consuming and labour intensive.

In developed countries onion harvesters are used successfully for harvesting small onion. In India the onion harvesters developed leads to more bulb damage. The onion digger windrower developed by earlier researchers resulted in escaping of bulbs from the windrowing unit. As bulbs fall in soil with too many clods of size bigger than the size of the onion bulbs it becomes difficult to collect the fallen small onion bulbs. The digging efficiency of the onion digger windrower developed was 89.66 percent (Jadhav et al., 1995). This was less than the local practice of onion harvesting using sickle. The percentage of bulb damage was negligible in both methods of onion digging. The machine, however, caused slightly more bulb damage 2.63-3.45 percent than the local method.

Kamaraj (2002) designed and developed a self-propelled onion digger. He tested the performance of the onion digger in field for digging Pusa white round and Agri found red varieties. The effective field capacity was 0.13 to 0.14 ha h^{-1}. The digging efficiency was 96.34 to 97.72 percent and the damage was 7.31 to 9.09 percent. The saving in cost and time were 65.12 and 93.7 percent respectively as compared to conventional method of manual harvesting.

Tapan et al. (2011) designed and developed a tractor-drawn onion harvester. They found the optimal design values of variables like length, speed ratio and slope of the elevator were as 1.2 m, 1.25:1 and 15°, respectively. The digging efficiency 97.7 percent, separation index 79.1 percent, bulb damage 3.5 percent, fuel consumption 4.1 l ha^{-1} and draft 10.78 kN are measured. The saving in cost of onion digging/ha with the use of the developed digger in comparison to manual was found to be Rs. 1,170/ha.

Massah Jafaret al. (2011) studied the comparison between capacitive and photo sensors in depth control of onion harvester. A four-bar mechanism was used in order to move the blade of the machine and to control the operation depth while a DC electrical motor provided the movement of the blade. They have concluded that photo sensor responded better than the capacitive sensor for all obstacle shapes.

Ashwini Talokar et al. (2014) designed and evaluated an onion harvester for the low power capacity tractors range in 15 to 20 hp. In their study the working width and depth of operation of harvester is fixed as 60 cm and 10 cm. The soil mass load on the harvester was found as 1.35 N cm^{-2}. The total capacity of the harvester in respect of the working in the soil is determined as 104 tones/h.

Tamil Nadu records about 13.7 percent of power tillers available in India according to the survey of Government of India. The usage of power tiller is limited as matching equipments are not available for various farm operations. If suitable matching attachments are developed, power tiller available in farmers hand will be used in all the versatile farm operations from tillage to harvesting. Hence, developing a small onion harvester as a power tiller attachment is considered essential and timely.

Keeping in view about the above facts and figures, the present research was carried out with an objective to develop a power tiller operated small onion harvester.

Material and Methods

Machine Description

The power tiller operated small onion consisted mainly of a mainframe, a rotary gear box, a digging tool, conveyor assembly and a levelling roller. The components of the harvester are depicted in **Fig. 1**.

Main Frame

The main frame carries the gears, digging tool and the conveyor assembly. The distance between the conveyor and the digging tool was made adjustable. The side flanges were attached to the main frame. Holes were provided on the side flange to adjust the rake angle of the digging tool at different levels.

Speed Reduction Rotary Gear Box

The rotary gear box was used to transmit the power from the power tiller to the harvester. During operation the rotary gear box of the harvester was connected to the power tiller. Through this gear box two rotational speeds of 0.79 and 1.05 ms^{-1} were obtained. So while operating the speed which is equal to the walking speed of the operator can be selected. The rotary gear box was provided with an output shaft with splined end on which driving pulley was fixed.

Fig. 1 Conceptual drawing of developed small onion harvester depicting its components

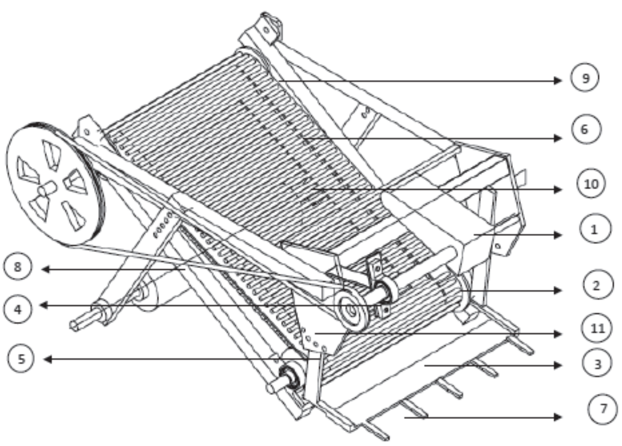

1. Rotary gear box, 2. Tool mounting frame, 3. Tool, 4. V-belt and pulley mechanism, 5. Conveying roller, 6. Conveyor belt, 7. Digging bar, 8. Levelling roller, 9. Conveyor mounting frame, 10. Conveyor bars, 11. Side flange

Digging Tool

A flat digging tool made of mild steel was developed for digging the small onion. The digging tool was fixed on the tool mounting frame. The cutting edge of the digging tool was beveled to an angle of 150. The tool consists of five flat digging bars for initial opening of the soil and for minimizing damage while digging small onion.

Conveyor Assembly

The conveyor assembly consists of a conveyor, conveyor mounting frame and conveyor driving mechanism.

Conveyor

A conveyor was developed to convey the dug out small onion crop to the rear end of power tiller. The conveyor belt was made of canvas material. Conveyor rods were riveted to the conveyor belt at a spacing of 15 mm based on the average bulb diameter of small onion crop. The conveyor mechanism consisted of two hollow conveyor rollers on which the conveyor moves during operation. The conveyor rollers were driven using the power taken through belt pulley mechanism from the rotary gear box. The angle of conveyor was given based on the angle of repose of small onion which is 28.11 to 37.410 (Pandiselvam et al., 2013).

Conveyor Mounting Frame

Conveyor mounting frame carries the components of the conveyor. It was attached to the side flanges of the main frame in order to adjust the position of conveyor.

Belt Pulley Transmission System

The power of conveyor mechanism was provided through belt pulley transmission mechanism. Two B-type pulleys were used of which, the driver pulley was fixed on the splined end of the shaft of the rotary gear box of power tiller, which has the facility of varying speed. The driven pulley was fixed on the shaft of conveying mechanism.

Levelling Roller

A levelling roller was provided for levelling field continuously after harvesting for easy collection of harvested small onion. The levelling roller was attached to the main frame. The roller helps in easy transport of harvester outside the field. It was also used for controlling the depth of operation in the levelled surface only, the harvested small onion falls in the levelled surface. The leveler was used to level the field continuously after harvesting.

Experimental Design to Determine the Effect of Operational Parameters on the Harvesting Efficiency of the Developed Small Onion Harvester

The harvesting was carried out by the developed digging tool. According to the bed width of small onion crop cultivated, the length of digging tool was provided. The harvester was run at 100 mm penetration depth by adjusting the levelling roller. The digging tool was fixed at 10 deg rake angle by adjusting the slot provided on side flanges. The gear position and throttle lever in the power tiller was set to have 1.0 km/h forward speed. Then the small onion harvester in towed position was run for 10 m for ensuring proper working of harvesting unit. All necessary readings were recorded and the average values of readings were calculated. The harvesting efficiency was determined. The above procedure was replicated thrice for optimizing the parameters.

The above experiment was repeated for rake angles set at 12 and 15 deg and the forward speeds at 1.5 and 2.0 km/h. Similarly for the remaining selected soil moisture levels the above procedure was repeated and the observations were recorded and tabulated.

An experiment with Factorial Randomized Block Design (FRBD) was laid out. The factors considered and their levels are furnished in **Table 1**. Analysis of data was carried out by "AGRES" package to analyze the data in order to obtain the necessary analysis of variance and to study the effect of variables. The treatment, which give the maximum harvesting efficiency was selected as the best.

Field Performance Evaluation

For evaluating the performance of prototype, the power tiller operated small onion harvester was tested for harvesting CO (On) 5 variety at Agricultural Machinery Research Centre, Coimbatore. The engine speed of the power tiller was adjusted for 1.0, 1.5 and 2.0 km/h forward speed by selecting the appropriate transmission ratios and by adjusting the engine throttle lever. The observations were made for three replications for different levels of forward speed, rake angle and moisture level. The performance of the conveying mechanism was evaluated in terms of conveying efficiency, soil separation efficiency, bulb damage, theoretical field capacity, actual field capacity. The draft required to pull the power tiller with harvesting attachment was measured using a recording type load cell dynamometer.

Structural Analysis of Small Onion Harvester

The structural analysis of the digging tool was carried out in 'SolidWorks' software. Force analysis was carried out on the digging tool with the optimized level of rake angle under the under the draft force required to pull the harvester. The stress distribution, strain distribution and deformation of digging tool were determined.

Harvesting Efficiency

For determining harvesting efficiency the field was divided into plots of 1 m^2 area. The small onion bulbs collected from the leveled surface and the left out small onion bulbs in the field were collected. The harvesting efficiency was calculated by the below expression (Ibrahim et al., 2008)

$$\eta_h = [W_p / (W_s + W_p)] \times 100$$

Where,

η_h = Harvesting efficiency, percent

W_p = Weight of small onion bulbs collected from the harvested crops in one square meter area, kg

W_s = Weight of left out small onion bulbs collected from the soil in one square meter area, kg

Conveying Efficiency

For calculating the conveying efficiency of the conveyor, the unit was run for 5 meters and the small onion crop conveyed by the conveyor and the crops not conveyed were collected. The conveying efficiency was calculated by the following formula (Tapan et al., 2007).

$$\eta_{pc} = [(W_1 + W_2) / (W_1 + W_2 + W_3)] \times 100$$

Where,

Table 1 Levels of variables selected for performance of weeder

Independent variables	Levels
Rake angle (R), degree	Three (10, 12, 15)
Forward speed (S), km/h	Three (1, 1.5, 2)
Average soil moisture (M), percent	Three (8.2, 9.5, 11.8)
Affected response variable	
Harvesting efficiency, %	

η_{pc} = Conveying efficiency, percent

W_1 = Weight of crops delivered by the conveyor in five meters run, kg

W_2 = Weight of crops remaining on the conveyor in five meters run, kg

W_3 = Weight of unpicked crops by the conveyor in five meters run, kg

Soil Separation Efficiency

The harvested plants from the field were immediately taken to the laboratory and the tests were conducted without loss of moisture. The observations were taken for determining the soil separation efficiency. The soil separation efficiency was calculated as follows (Jadhav et al., 1995).

$$\eta_{ss} = [(W_1 - W_2) / (W_1 - W_2 + W_3)] \times 100$$

Where,

η_{ss} = Soil separation efficiency, percent

W_1 = Weight of crops fed at the picking end, kg

W_2 = Weight of crops collected at the delivery end, kg

W_3 = Weight of soil collected at the delivery end by manually removing the soil particles from all the crops, kg

Bulb Damage

The percentage of bulb damage was calculated from the following equation.

$$C = Q/P \times 100$$

Where,

C = Bulb damage, percent

Q= Number of bulbs collected at the delivery end in a 2 m row length

P = Number of bulbs damaged in a 2 m row length

Theoretical Field Capacity

On the basis of width of the digging blade and speed, theoretical field capacity was calculated by the following formula

Theoretical field capacity (ha/h) = ws/10

Where,

w = Width of the blade, m

s = Speed of travel, km/h

Actual Field Capacity

Actual field capacity of the small onion harvester includes the time consumed for turning in headland and for repair. Actual field capacity was calculated by the following formula

Actual field capacity (ha/h) = A/T

Where,

A = Actual area covered, ha

T = Total time taken to cover the area, h

Field Efficiency

Field efficiency was calculated by using the following formula.

Field efficiency, % = (Effective field capacity, ha/h) / (Theoretical field capacity, ha/h)

Cost Economics of the Developed Small Onion Harvester

The total cost of power tiller operated small onion harvester was calculated. The fixed and variable costs of the unit per hour were calculated as per the procedure enumerated in IS: 9164-1979. From the field capacity of the unit, the cost of operation per ha was calculated. The performance was compared with conventional method of harvesting, in terms of saving in cost and improvement in harvesting efficiency. The break-even point (BEP) of the power tiller operated small onion harvester was also worked out.

Results and Discussion

A 12 hp power tiller was used as a prime mover for the developed small onion harvester. The harvester with a flat digging tool of 530 mm length having 5 equally spaced digging bars was fabricated (**Fig. 2**). A leveling roller of 115 mm diameter and 470 mm length was fabricated. The conveying assembly was fabricated with a conveyor mounting frame made of mild steel and a conveyor with 10 mm diameter conveyor bars and 460 mm width (**Fig. 3**). The gear box consisted of two sets of spur gears having teeth of 40 and 36. The belt pulley transmission was fabricated with two pulleys. The driver pulley was mounted on

Fig. 2 Overall dimensions of digging tool

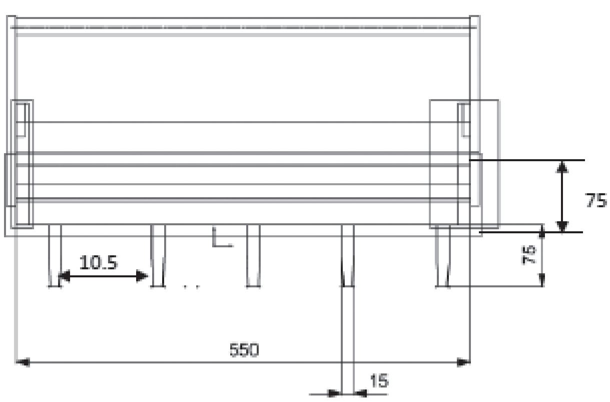

Fig. 3 Overall dimensions of conveying assembly

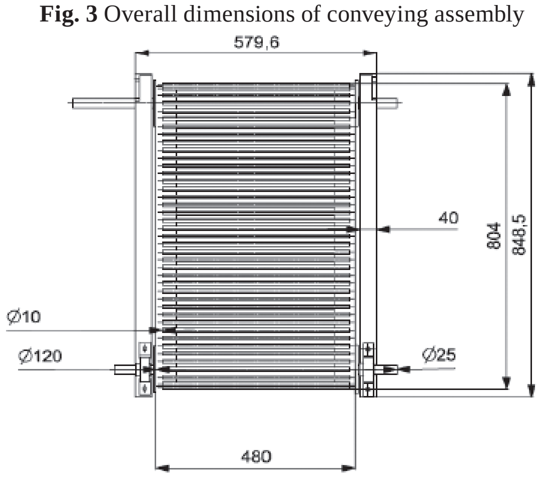

the shaft of the gear box of power tiller. The diameter of the driver pulley was kept as 100 mm and that of the driven pulley as 300 mm (**Fig. 4**). The overall specification of the prototype small onion harvester was given in **Table 2**.

The data measured were analyzed to assess the effect of the variables viz., rake angle (R), forward speed (S) and moisture content (M) on harvesting efficiency. The analysis of variance for harvesting efficiency for operation of harvested is furnished in **Table 3**.

The main effects of each factor (S, R, M) were significant indicating the influence of each factor on harvesting efficiency. The interaction effects of S × R and R × M were significant at 1 percent level, whereas the interaction effect of S × M and S × R × M were significant at 5 percent level.

Table 2 Specifications of developed power tiller operated small onion harvester

1	Name	Small onion harvester
2	Source of power	Power tiller
3	Overall dimensions (L × B × H), mm	1120 × 740 × 560
4	Width of operation, mm	530
5	Depth of operation, mm	100
6	Digging tool dimensions (L × B × H), mm	530 × 150 × 7
8	Length of conveyor, mm	725
9	Width of conveyor, mm	480
10	Diameter of conveyor bars, mm	100
11	Conveyor angle, degrees	28
12	Spacing between conveyor bars, mm	100
13	Number of conveyor bars, mm	72
14	Weight of small onion harvester, kg	95 kg
15	Conveyor speed, m/s	1.3
16	Cost of the unit, Rs.	5,750

Effect of Operational Parameters on Harvesting Efficiency of Developed Small Onion Harvester

The harvesting efficiency of the harvester was measured at selected levels of rake angle (R), forward speed (S) and moisture content (M)

Effect of Rake Angle (R) and Forward Speed (S) on Harvesting Efficiency

The interaction effect of rake angle on harvesting efficiency at different levels of forward speed is depicted in **Fig. 5**.

From the figure, it was observed that the effect of S × R factor means on harvesting efficiency indicated higher percent harvesting efficiency of 92.03 percent at 15 deg rake angle and 1.5 km/h forward speed. The minimum of 77.72 percent harvesting efficiency was obtained at rake angle of 10 deg and forward speed of 2 km/h. This is due to the variation in the penetration depth of the digging

Fig. 4 Belt pulley transmission system

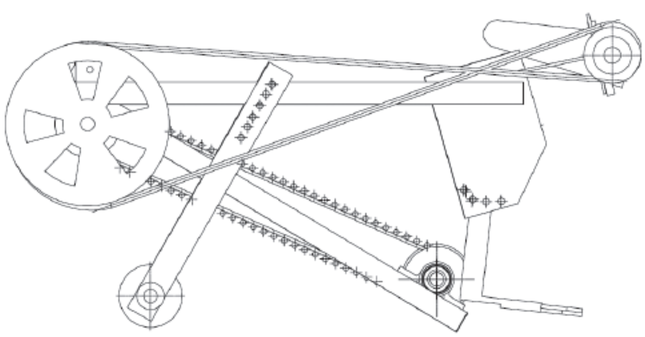

Fig. 5 Effect of rake angle and forward speed on harvesting efficiency

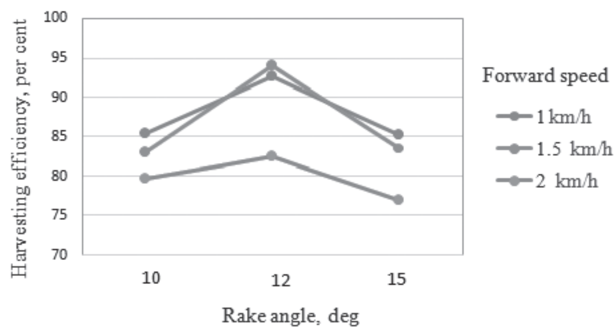

Fig. 6 Effect of rake angle and soil moisture on harvesting efficiency

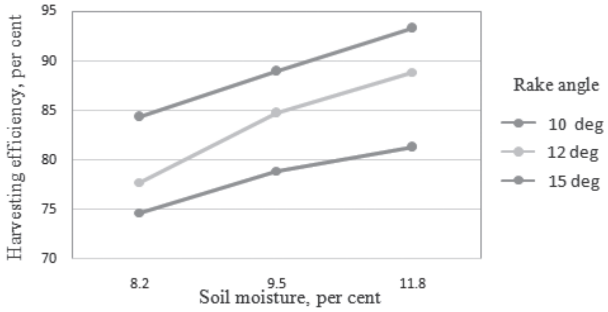

Fig. 7 Effect of soil moisture and forward speed on harvesting efficiency

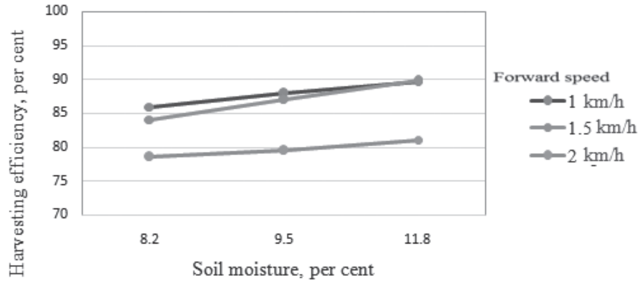

Table 3 Analysis of variance for harvesting efficiency

SV	DF	SS	MS	F
Treatmentment	26	3,252.086667	125.080256	57.6672**
Speed (S)	2	392.965185	196.482593	90.5866**
Rake Angle (R)	2	1,520.886667	760.443333	350.5958**
Soil Moisture (M)	2	1,078.186667	539.093333	248.5443**
S × R	4	139.737037	34.934259	16.1061**
R × M	4	50.906667	12.726667	5.8675**
S × M	4	24.625926	6.156481	2.8384*
S × R × M	8	44.778519	5.597315	2.5806*
Error	52	112.788148	2.169003	
Total	80	3,367.680000	42.096000	

C.V = 1.76 %, ** = Significant at 1 % level, * = Significant at 5 % level

tool at higher rake angle. At higher forward speed due to increased vibration in the digging tool the harvesting efficiency is decreased.

Effect of Soil Moisture (M) and Rake Angle (R) on Harvesting Efficiency

The interaction effect of soil moisture on harvesting efficiency at different levels of rake angles is presented in **Fig. 6**.

From figure it is seen that the effect of R × M factor means on harvesting efficiency indicated higher percent harvesting efficiency of 93.33 at 15 deg rake angle and 11.8 percent soil moisture. The minimum of 74.67 percent harvesting efficiency was obtained at rake angle of 10 deg and soil moisture of 8.2 percent. This might be due less resistance offered by soil in the penetration of the tool at higher moisture content.

Effect of Forward Speed (S) and Soil Moisture (M) on Harvesting Efficiency

The interaction effect of forward speed on harvesting efficiencies at different levels of soil moisture contents is shown in **Fig. 7**.

From figure it is seen that the effect of S × M factor means on harvesting efficiency indicated higher percent harvesting efficiency of 89.81 at 1.5 km/h forward speed and 11.8 percent soil moisture. The minimum of 74.89 percent harvesting efficiency was obtained at forward speed of 2 km/h and soil moisture of 8.2 percent.

The test results were statistically analyzed for harvesting efficiency. The analysis of factor means revealed that maximum harvesting efficiency occurred in the combination of 1.5 km/h forward speed, 15 degree rake angle and 11.8 percent soil moisture. after comparing all possible combination of interactions of the factors considered.

The combination resulting in maximum harvesting efficiency was taken into consideration as the objective of the study is to develop a small onion harvester suitable for all soil and moisture conditions having maximum efficiency. Owing this reason, the factor combination 1.5 km/h forward speed, 15 degree rake angle and 11.8 percent soil moisture was selected as the best combination of factors which has been used for deciding the final prototype of the small onion harvester.

Field Performance Evaluation

The small onion harvester developed as an attachment to power tiller was tested in farmers field for harvesting Co (On) 5 variety small onion crop. The entire developed harvester unit was accommodated in the space between the rotary gearbox and the handle of the power tiller. The operator feels comfort in operating the unit. The harvester was attached to a 12 hp power tiller through its rotary hitch arrangement.

The maximum harvesting efficiency of 97.8 percent was achieved at the optimized combination of 15 deg rake angle, 1.5 km/h forward speed and 11.8 percent soil moisture level for the digging tool with the draft requirement of 85 kg.

In the structural analysis it was found that at 15 deg rake angle the maximum stress and strain of 2,581 N m^{-2} and 8.128e^{-007} were obtained (**Figs. 8** & **9**). The minimum and maximum values of displacement of the digging tool under the action of the applied force obtained were 0 mm and 0.000867159 mm. The obtained values were found to have very less effect on the digging tool.

The field capacity of the developed harvester was found as 0.08 ha/h. The cost of harvesting with the small onion harvester was Rs. 918/- per hectare. As compared to

Fig. 8 Stress and strain distribution over digging tool at 15 deg rake angle

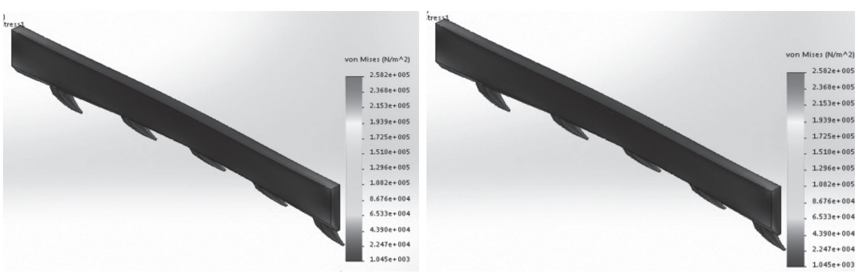

Fig. 9 Displacement of digging tool for the applied force

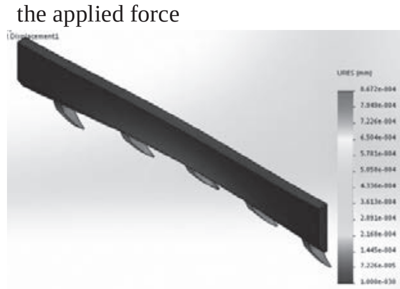

conventional method of manual harvesting the saving in cost and time were found as 59.2 and 93.75 percent respectively. The break-even point (BEP) of the small onion harvester costing Rs. 9,000 was found as 60.13 h of operation per annum. The results of field performance evaluation are tabulated in **Table 4**. The operational view of small onion harvester is shown in **Fig. 10**.

Conclusions

Mechanical harvesting of small onion crop decreased the bulb damage and also saved labour and time. Small onion harvester as a power tiller attachment has found suitable for both small and marginal farms. Hence the study was aimed at developing a power tiller operated harvester for small onion. Analysis of harvesting efficiency was carried out with three parameters viz., rake angle, forward speed and moisture content. From analysis, it was found that at 15 degree rake angle, 1.5 km/h forward speed and 11.8 percent average soil moisture as optimum conditions for harvesting small onion using the developed harvester. The performance parameters such as field efficiency, bulb damage, soil separation efficiency were determined for optimized conditions. As the cost of operation of developed harvester is Rs. 918/- per hectare, it was found suitable for both small and marginal farmers.

REFERENCES

Ashwini T., V. P. Khambalkar and K. Wankhade. 2014. Design of onion harvester. International Journal & Magazine of Engineering, Technology, Management and Research (IJMETMR), 1(3): 11-16.

IS: 9164-1979, BIS test code. Guide for Estimating Cost of Farm Machinery Operation. Indian Standards Institution, New Delhi.

Ibrahim, M. M., E. Amin and A.Farag. 2008. Developing a multi-purpose digger for harvesting root crops. Misr. Journal of Agricultural Engineering.25(4): 1225-1239.

Jadhav, R. V., P. A. Turbatmath and L. V. Gharte. 1995. Design, development and performance evaluation of onion digger windrower. AMA, 26(3): 35-38.

Khambe, V. K., D. De and P. K. Sahoo. 2013. Design and Development of a Tractor Operated Garlic Harvester. Journal of Agricultural Engineering, 50(1).

Kaveri, G. and V. Thirupathi. 2015. Study on geometrical and physical properties of Co 4 onion bulb. International Journal of Recent Scientific Research. 6(3):2897-2902.

Massah, J., A. Lotfi and A. Arabhosseini. 2011. Comparison between capacitive and photo sensors in depth control of onion harvester. Journal of Engineering Studies and Research, 17(4): 64-72.

Omer, A. G. and D. Ahmad. 2001. Comparative study on different peanut digging blades. AMA, 32(3): 43-45.

Pandiselvam, R., R. Kaliappan and D. Smith. 2013. Frictional, Mechanical and Aerodynamic Properties of Onion Seeds. International Journal of Engineering Research and Technology, 2 (10): 2647-2657.

Shridar, B., P. K. Padmanathan and R. Manian. 2006. Utilization Pattern of Power Tillers? in Tamil Nadu. AMA, 37(1): 85-89.

Suryawanshi, S. H., Shridar, B. and Kathirvel, K. 2008. Development of power tiller operated groundnut harvester. AMA, 39 (3):29-32.

Suryawanshi, S. H., B. Shridar and K. Kathirvel. 2009. Comparative evaluation of three types of groundnut digging blades. AMA, 40(1): 9-11

Tapan, K. K., I. Mani and A.P. Srivastava. 2011. Design and development of tractor-drawn onion (Allium cepa) harvester. Indian Journal of Agricultural Sciences, 81(6): 528-532.

■■

Table 4 Field performance of small onion harvester

Harvesting efficiency, %	97.4
Conveying efficiency, %	86.9
Soil separation efficiency, %	84
Conveyor loss, %	2
Theoretical field capacity, ha/h	0.068
Effective field capacity, ha/h	0.062
Field efficiency, %	85.2
Fuel consumption, l h^{-1}	1.2

Fig. 10 Field operational view of small onion harvester

Stability Analysis of Tractor Mounted Hydraulic Operated Ladder Using FEM

by
R. Thiyagarajan
Assistant Professor (Farm Machinery)
Dept. of Farm Machinery & Power Engineering,
Agricultural Engineering College &
Research Institute,
Tamil Nadu Agricultural University,
Coimbatore - 641 003, Tamil Nadu, INDIA
drrthiyagarajan@gmail.com

A. Tajuddin
Professor (Retired)
Dept. of Farm Machinery & Power Engineering,
Agricultural Engineering College &
Research Institute,
Tamil Nadu Agricultural University,
Coimbatore - 641 003, Tamil Nadu, INDIA

B. Suthakar
Dept. of Farm Machinery & Power Engineering,
Agricultural Engineering College &
Research Institute,
Tamil Nadu Agricultural University,
Coimbatore - 641 003, Tamil Nadu, INDIA

A. P. Mohankumar
Dept. of Farm Machinery & Power Engineering,
Agricultural Engineering College &
Research Institute,
Tamil Nadu Agricultural University,
Coimbatore - 641 003, Tamil Nadu, INDIA

Abstract

A tractor-mounted hydraulic-operated ladder was designed to reduce the harvesting /pruning cost, to increase the harvesting/pruning efficiency and to enhance the overall productivity of mango orchards. The design and drawing of the hydraulic ladder was made based on theoretical analysis of the tractor-mounted hydraulic-operated ladder, using the finite element method (FEM) SolidWorks software was used for the stress and stability analyses of the hydraulic ladder under static loading for the ladder. Slight variations were observed in the resultant forces at different heights (6, 8 10 m), different angles of rotation from (0-180° at an interval of 45°) and different varying loads (75, 150, 225 and 300 kg). It is considered to be in a state of stability when no sign of overturning is evident with the hydraulic ladder in operation. The maximum stress observed in the hydraulic ladder for, 8 m and 10 m heights, at different loads and different angle of rotation is 96.64 N/mm^2 which is less than the yielding stress (220.59 N/mm^2).

Keywords: Hydraulic ladder, Design, stability, tractor mounted, stress, stabilizing system,

Introduction

Harvesting of fruits is a labour-intensive operation worldwide, which accounts in many cases for about 50% of total production costs. In India, fruit harvesting is commonly done by experienced tree climbers. Fruit harvesting is a tedious, stoop type job, which is needed to be performed on a seasonal basis during a relatively short time. Besides, issues of safety and quality of plucked fruits during manual plucking are the matters of concern. The declining labour availability and increasing labour costs in the developing countries, combined with more awareness to health and safety issues, make it mandatory to mechanize the fruit harvesting operation. Fruit growers in the developing countries are facing two significant problems that could determine the future of their business. The availability of fruit harvesting labour dwindling every year and the supply of hand fruit pickers continues to shrink. In addition, there are fewer workers available to harvest fruits because of continuous outflow of workers from agriculture to better paying jobs in construction and industry (Blank, 1998). Since the cost of manual labour is constantly rising, at important way to maintain or reduce the labour cost is to increase the productivity of lab markets (Holt, 1999).

With steadily increasing labour charges and migration of the rural people to urban areas, it has become mandatory to manage all horticultural operations mechanically. Therefore, development of machines is a timely step to reduce the drudgery and to increase the yield potential of horticultural crops (Tajuddin et al., 2002). Mechanized harvesting can facilitate the harvesting and packing work, labour-saving machines (mass-harvesting systems) that improve productivity and reduce harvest and packing labour needs and robotic harvesting or automation. Several works have been carried out to develop suitable labour-aids, primarily for fresh-market fruit. Different models of various mechanical picking aids have been developed in many places in the world over a period of more than 50 years. They cover the whole spectrum of labour aids from improvements in clipping devices, ladders, picking bags and working methods to a variety of picker positioning equipment from simple multi-man platforms to a real sophisticated single-man, self-propelled positioning system (Coppock et al., 1959; Perry, 1965; Molitorisz and Perry, 1966; Seamount, 1969; Berlage et al., 1972; Sarig and Coppock, 1986; Sarig, 1993)

Shanab and Sepehri (2005) describes the development of a simulation model for studying the tip-over stability of a typical heavy-duty hydraulic log-loader machine. The results demonstrates that the effects of the manipulator movements, the flexibility of the contact between the base and the ground, the hydraulic compliance, and the friction properties between the wheels and the ground, on the stability of the machine. Particularly, it is shown that the flexibility of the contact between the base and the ground reduces the machine stability, whereas the flexibility at the manipulator joints due the hydraulic compliance improves the machine stability.

Kolhe et al. (2011) model analysed model for the whole assembly of tractor-mounted hydraulic elevator by using ANSYS software. The better stability results with the controlled vibrations and frequency of the lifting platform and welded joints were recorded by keeping constrained boundary conditions. The tractor mounted hydraulic elevator is suitable, safe, less hazardous and economical as compared to manual climbing for coconut harvesting. Hence it is recommended to use tractor-mounted hydraulic elevator for harvesting, cleaning and breeding of coconut orchards up to 14 m height.

Abhinay and Rao (2014) modelled an aerial scissor lift by using ANSYS software which is one of the software used for modelling components in most of the design-based industries. While the modelling of the components the material selection is carried out simultaneously based on the design considerations related to loads, etc. Later the stress and strain concentration, deformation on the aerial scissor lift have been found by applying certain load on the lift's platform, using the Finite Element Analysis (FEA) by using ANSYS software that provides best output within few seconds.

Jaydeep and Pandya (2013) described the design as well as analysis of a simple aerial scissor lift. Conventionally a scissor lift or jack is used for lifting a vehicle to change a tire, to gain access to go to the underside of the vehicle, to lift the body to appreciable height, and many other applications also such lifts can be used for various purposes like maintenance and many material handling operations. It can be of mechanical, pneumatic or hydraulic type. The design described in the paper is developed keeping in mind that the lift can be operated by mechanical means so that the overall cost of the scissor lift is reduced. Also such design can make the lift more compact and much suitable for medium scale work. Finally the analysis is also carried out in order to check the compatibility of the design values.

Henry et al. (2012) carried out the topology, size and shape optimization methods on a long-range aerial lift truck. The first phase involves the determination of the optimum cross-section dimension, overlaps and wall thickness of the telescopic boom segments. The optimization problem is formulated as mass minimization under various structural performance constraints and solved using the metamodel-based optimization method. Optimal-space filling design, Kriging algorithm, and screening methods are used for the design of experiment (DOE) sampling, response surface generation and optimization steps, respectively. The second phase consists of 2 steps that deal with the search for optimum frame reinforcement layout using topology optimization in the first step and frame plate thickness optimization in the second step. The

Fig. 1 Angle of rotation from 0-180° at an interval of 45°

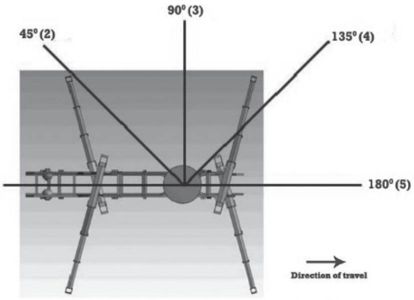

Fig. 2 Schematic view of the hydraulic ladder

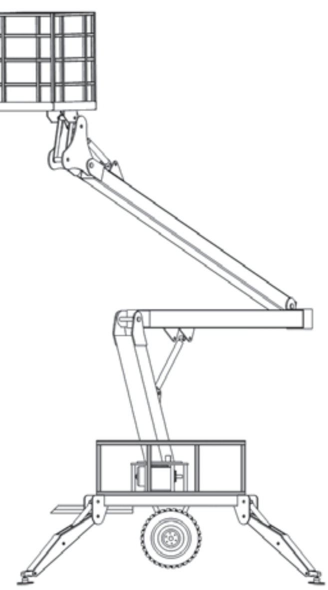

ultimate goal of design optimization in the second phase is to obtain a lightweight frame that is structurally stiff and with improved torsional natural frequency. The design optimization is done using ANSYS Workbench in the first phase while Hyper Works in the second phase. Optimized boom is about 250 kg (2.2%) lighter with significantly lower stresses than the reference design. The stiffness and torsional natural frequency of the frame increase by 33% and 59%, respectively with the weight reduce by 35 kg.

Kusma et al. (2015) designed and fabricated a prototype telescopic raising platform for harvesting oil palm fresh fruit bunches. They have designed telescopic lifting mechanism, sliding mechanism and rope drive mechanisms to lift and take the platform near fresh fruit bunches at crown of the tree. The diameter and speeds of the first, second and third cylinders were 12.065 cm, 9.525 cm, 7.000 cm and 0.0779 m/s, 0.0421 m/s, 0.02624 m/s respectively. The minimum deflection of the sliding mechanism was 2.81 cm and rope drive needs 0.08 hp to operate, which is less than the power availability.

In addition to providing means for reducing the drudgery of harvest labour the harvest machinery improves the farmers' ability to perform operations in time. Mechanization also reduces the risks associated with the need for large amount of seasonal manual labour for short periods of time and lessens the social problems caused due to excessive influx of low-wages. Keeping in view of above facts, the aim of this research work was to analyse the stability of tractor-mounted hydraulic-operated ladder which should provide a safe working environment, in addition to presenting some important tools to help the worker performing the needed practice in a more efficient fashion.

Material and Methods

The design and drawing were made through SolidWorks software and theoretical analysis of the tractor-mounted hydraulic-operated ladder was carried out by finite element method, also using the SolidWorks software for analysis of stress and stability of the hydraulic ladder.

Testing the Stability of the Hydraulic Ladder

Testing the stability of the hydraulic ladder was done by simulation for finding the resultant forces acting on the four stabilizers L1, L2 & R1, R2. The simulation was done for the height of hydraulic ladder (two fold) from ground surface

Table 1 Resultant forces acting on the stabilizers

S. No	Load, kg	Height m	Ø = 0°				Ø = 45°				Ø = 90°			
			L1	L2	R1	R2	L1	L2	R1	R2	L1	L2	R1	R2
1	75	6.0	4,220	4,330	4,180	4,340	4,290	4,360	4,560	4,590	4,380	4,170	4,750	4,500
	150	6.0	4,310	4,450	4,270	4,410	4,330	4,540	4,740	4,910	4,620	4,570	4,730	4,670
	225	6.0	4,320	4,470	4,290	4,420	4,380	4,730	4,920	5,230	4,730	4,680	4,870	4,810
	300	6.0	4,480	4,990	4,660	4,720	4,420	4,910	5,100	5,550	4,970	4,840	4,980	4,940
2	75	8.0	4,460	4,570	4,520	4,670	4,470	4,540	4,680	4,710	4,670	4,760	4,830	4,990
	150	8.0	4,710	4,980	4,630	4,810	4,510	4,620	4,760	4,860	4,790	4,940	4,990	5,090
	225	8.0	4,890	5,170	4,940	5,020	4,720	4,810	4,840	4,940	4,930	5,080	5,110	5,230
	300	8.0	4,990	5,350	5,010	5,130	4,870	4,950	5,030	5,120	5,090	5,170	5,230	5,310
3	75	10.0	4,510	4,620	4,830	4,910	4,750	4,530	4,680	4,230	4,760	4,930	4,820	5,060
	150	10.0	4,730	4,890	4,990	5,090	4,910	4,620	4,830	4,370	4,890	5,170	4,970	5,310
	225	10.0	4,860	4,980	5,110	5,220	5,160	4,790	4,970	4,470	4,940	5,210	5,120	5,480
	300	10.0	5,120	5,170	5,270	5,380	5,370	4,890	5,120	4,590	5,060	5,420	5,230	5,670

S. No	Load, kg	Height m	Ø = 135°				Ø = 180°			
			L1	L2	R1	R2	L1	L2	R1	R2
1	75	6.0	4,260	4,210	4,450	4,340	4,440	4,370	4,390	4,360
	150	6.0	4,530	4,420	4,620	4,470	4,520	4,410	4,490	4,410
	225	6.0	4,610	4,530	4,690	4,580	4,590	4,480	4,570	4,510
	300	6.0	4,810	4,690	4,790	4,690	4,790	4,710	4,810	4,680
2	75	8.0	4,920	4,380	4,960	4,510	4,530	4,420	4,480	4,410
	150	8.0	5,030	4,480	5,120	4,680	4,770	4,690	4,560	4,490
	225	8.0	5,090	4,560	5,230	4,770	4,890	4,780	4,780	4,610
	300	8.0	5,110	4,670	5,340	4,870	5,130	5,010	4,980	4,840
3	75	10.0	4,530	4,770	4,760	4,860	4,760	4,690	4,760	4,610
	150	10.0	4,710	4,810	4,830	4,970	4,960	4,890	4,990	4,840
	225	10.0	4,850	5,170	4,910	5,320	5,110	5,070	5,160	4,980
	300	10.0	4,980	5,350	4,990	5,420	5,190	5,120	5,290	5,170

was kept constant at 6 m. The load inside the bucket was kept 75 kg, for set of this condition different reaction forces on the stabilizer (L1, L2 and R1, R2) were taken by changing angle of rotation from 0-180° at an interval of 45° shown in **Fig. 1**. For this set the load was varied from 75, 150, 225 and 300 kg respectively. The same way for the other different heights, different loads and different angle of rotation was carried out by using the simulation module in the solid works software.

Von Mises Stress Under Static Load for the Hydraulic Ladder

The strength of machine members is based upon the mechanical properties of the materials used. Since these properties are usually determined from simple tension or compression tests. For ductile materials, the limiting strength is the stress at yield point as determined from simple tension test and it is, assumed to be equal in tension or compression. the failure or yielding occurs at a point in a member when the distortion strain energy (also called shear strain energy) per unit volume in a bi-axial stress system reaches the limiting distortion energy (i.e. distortion energy at yield point) per unit volume as determined from a simple tension test.

Construction of Tractor-mounted Hydraulically-operated Ladder

Proper design of functional components would greatly influence performance of hydraulically-operated ladder. The design of functional components is made to achieve optimum performance of the tractor-mounted hydraulically-operated ladder. The arrangements are made in such a way that all the operations like stabilizing, lifting and rotation can be done by the operator at the time of operation in the bucket itself. The schematic view of the tractor-mounted hydraulic-operated ladder is depicted in **Fig. 2**.

Results and Discussion

Testing the stability of the hydraulic ladder was done by simulation method for finding the resultant forces acting on the four stabilizers L1, L2 & R1, R2. The simulation was done for the height of hydraulic ladder (two fold) from ground surface was kept constant at 6m. The values of the resultant forces for the different heights, different loads and different angle of rotation were are presented in the **Table 1** and sample pictures are depicted in **Fig. 3**.

From the **Table 1** it is observed that Resultant force for 0 degree angle of rotation acting on the stabiliz-

Fig. 2 Resultant forces for different heights at different angle of rotation and different loads

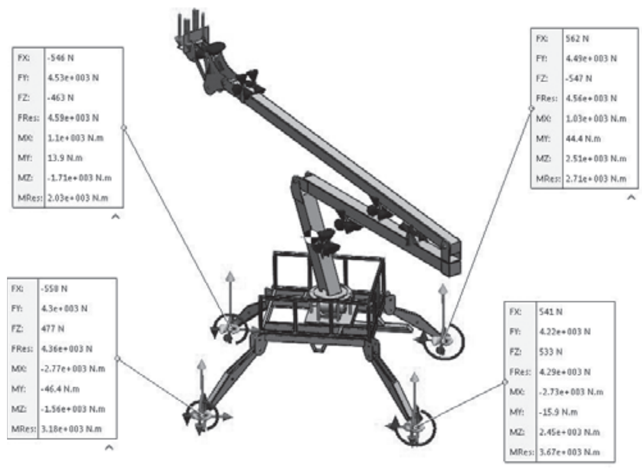

Resultant force for 6 m height at 45 degree for 75 kg load

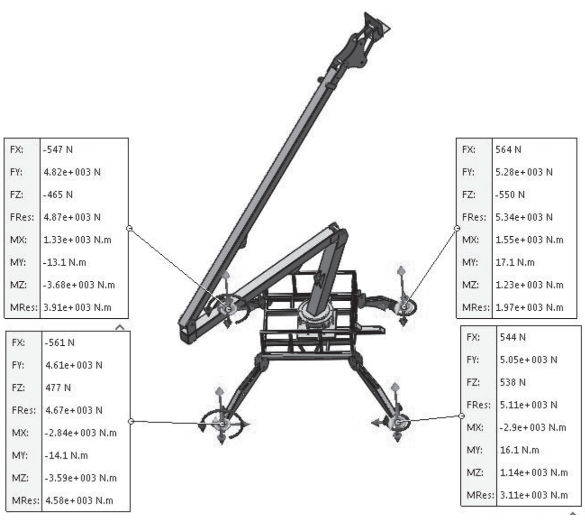

Resultant force for 8 m height at 135 degree for 300 kg load

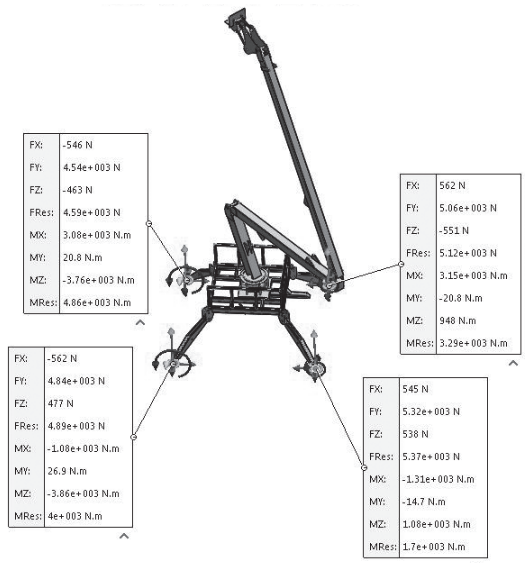

Resultant force for 10 m height at 45 degree for 300 kg load ers L1, L2 and R1, R2 are increasing from 4,180 to 5,380 N for 6 m, 8 m and 10 m height as load increases from 75 kg to 300 kg. For 45 degree angle of rotation the resultant force acting on the stabilizers L1, L2 and R1, R2 are increasing from 4,290 to 5,550 N for 6 m and 8 m height whereas for the 10 m height the resultant forces are decreasing from 5,370 to 4,530 N as load increases from 75 kg to 300 kg. Resultant force for 90 degree angle of rotation acting on the stabilizers L1, L2 and R1, R2 are decreasing from 4,170 to 4,970 N for 6 m height whereas for the 8 and 10 m height the resultant forces are increasing from 4,670 to 5,670 N as load increases from 75 to 300 kg.

Resultant force for 135 degrees angle of rotation acting on the stabilizers L1, L2 and R1, R2 are decreasing from 4,810 to 4,210 N for 6 m height whereas for the 8 and 10 m height the resultant forces are increasing from 4,380 to 5,420 N when the load increases from 75 kg to 300 kg. For 180 degrees angle of rotation resultant force acting on the stabilizers L1, L2 and R1, R2 are decreasing from 5,290 to 4,360 N for 6, 8 and 10 m height as load increases from 75 kg to 300 kg with an interval of 75 kg. From the table it is found that the variations in the resultant forces are minimum for different heights, different angle of rotation and different varying loads. It is considered to be in a state of stability when no sign of overturning is evident with the hydraulic ladder in operation.

The Static Load for the hydraulic ladder is calculated from the solid works software through simulation module for different heights (8 & 10 m), rotation angles at 135 degrees at 300 kg are depicted in **Fig. 4**.

It is observed from the **Fig. 4** that the limiting strength for yield stress is 220.59 N/mm^2. Whereas the maximum stress occurred is 96.64 N/mm^2 for the 8 m height and 96.63 N/mm^2 for the 10 m height at 135 degrees for 300 kg load for refined hydraulic ladder. The maximum stress occurred in the 8 m and 10 m is less than the yielding stress. Similar types of experiments were repeated for different heights (8 and 10 m) by lifting the platform, different angle of rotation (45, 90, 135 and 180 degrees) and different loads (75, 150, 225 and 300 kg) and the maximum stress was noted. The stress noted in the above said variables for the hydraulic ladder is less than the yielding stress.

Mechanical Performance of the Hydraulic Ladder

(a) Factor of Safety

The factor of safety of any mechanical device is the ratio of maximum load bearing capacity to the theoretical or design load bearing capacity. The value of factor of safety must be greater than or equal to 2.

Factor of Safety = [Maximum load on main beam (S + V)] / (Theorrtical Load) [1]

Where,

S = Static load (load of bucket and main beam load)

V = Variable load (operator's loads, fruit load)

The equipment has been designed in such a way that the main beam could able to bear the variable weight of around 100 to 150 kg which is to be considered as the weight of the person on bucket. But this has been demonstrated pragmatically that the equipment is capable of lifting effectively 300 kg i.e. the weight of two persons and fruits. This is therefore clear (Eq. 1) that the factor of safety of the equipment greater than 2.

(b) Height vs. Angle

The height of the platform excluding the height of the person can be plotted X-Y plane with the angle displaced by the main beam from the horizontal. This can easily be realized that a circular path is followed by the platform while it moves up or down. The cage is kept at the height of 3,250 mm from the ground level. At the same time the angle made by the main beam is 10° from the horizontal.

The instantaneous relationship in between height and angle for a particular time can be given by the formula

$H_R = L \sin\Theta$ [i]

where,

H_R = height of the platform from its reference minimum height H_0

L = length of the upper arm i.e. 6,000 mm

Θ = included angle by the beam from horizontal

The reference height of the platform i.e. H_0 is equal to 3,250 mm

Fig. 4 Von Mises stress for different height at 45 degree for 300 kg

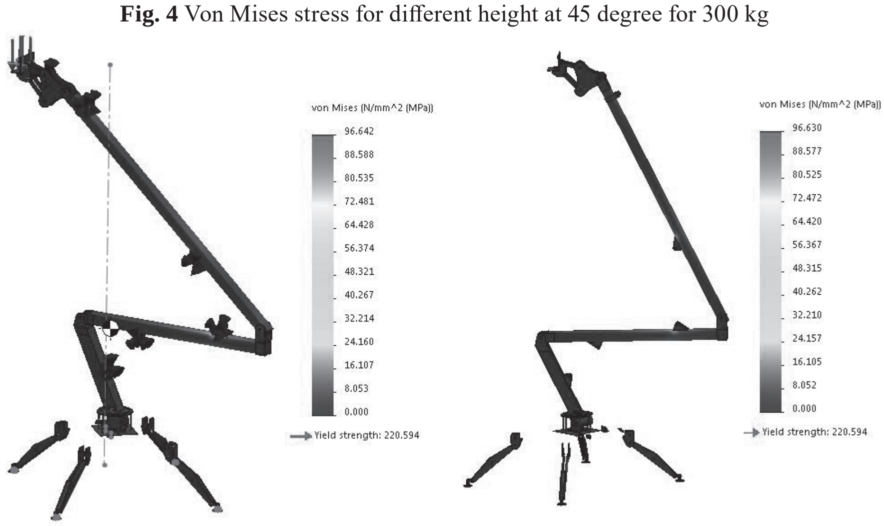

which can be calculated by adding the vertical heights of the ladder and sine of 10° of the beam length.

Therefore,

H_0 = 3,250 mm (approx.)

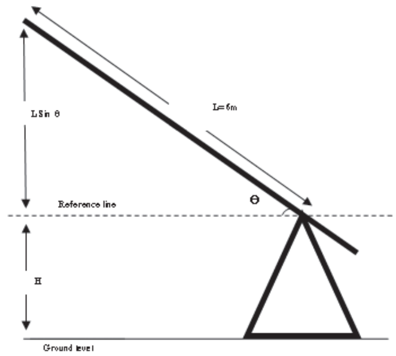

Table 2 shows the height increased from the reference height H_0 in each 5° variation of included angle by the beam from the horizontal.

The estimated maximum height of the platform from the ground level is 8,682 mm (28.9 feet) which can be achieved at the angle of 65° in the upper radial arm. Since this machine contains two arms (lower and upper arm) where one arm (lower) is used for lowering the bucket for the operators stepping in and stepping out and this lower arm also increases the height by 1 m so as to increase the vertical height for the upper arm. By adding this 1m height, the total maximum height can be achieved by this machine is 9,692 mm (32.3 ft.) makes an angle of 65° with reference line. No further height could be achieved beyond an angle of 65°, and hence the angle of elevation is restricted to 65°.

Table 2 Variation of height with angle (Θ)

S. No	Included angle by the beam (Θ), deg	Height of the bucket (H_R), mm $H_R = L \sin \Theta$	Height of bucket from the ground level (H), mm $H = H_0 + H_R$
1	15	1,552	4,802
2	20	2,052	5,302
3	25	2,535	5,785
4	30	3,000	6,250
5	35	3,442	6,692
6	40	3,857	7,107
7	45	4,243	7,493
8	50	4,596	7,846
9	55	4,915	8,165
10	60	5,196	8,446
11	65	5,432	8,682

Conclusions

From the results, it is found that variations in the resultant forces are minimum for different heights (6, 8, 10 m), different angle of rotation from 0-180° at an interval of 45 and different varying loads 75, 150, 225 and 300 kg respectively. It is considered to be in a state of stability when no sign of overturning is evident with the hydraulic ladder in operation. The maximum stress observed in the hydraulic ladder for, 8m and 10 m height with different loads and different angle of rotation is 96.64 N/mm2 which is less than the yielding stress which is 220.59 N/mm^2. It is observed that the equipment has been designed in such a way that the main beam could able to bear the variable weight of around 100 to 150 kg which is to be considered as the weight of the person on bucket and the factor of safety of the equipment greater than 2. The estimated maximum height of the platform from the ground level is 9,682 mm (32.3 feet) which can be achieved at the angle of 650 in the upper radial arm.

REFERENCES

Abhinay, M. and P. S. Rao. 2014. Design and Analysis of an Aerial Scissor Lift, International Journal of Mechanical Engineering, 1(5): 20

Berlage, A. G., R. D. Langmo and G. E. Yost. 1972. Limitations of single and multi-man platform harvesting aids. Agricultural Experiment Station Bulletin, 609, Oregon State University.

Blank, S. C. 1998. The End of Agriculture in the American Portfolio Quorum Books, Westport, CT.; 232.

Coppock, G. E. and P. J. Jutras. 1959. Improved equipment's and methods for harvesting citrus. Transactions of the Citrus Engineering Conference, Florida section. ASME; 5: 1-5.

Henry, P., G. A. In and T. J. Chung. 2012. Multi-phase design optimization of a Long Range Aerial Lift Boom Structure, Proceedings of the World Congress on engineering, 3.

Holt, J. S. 1999. Implications of reduced availability of seasonal agricultural workers on the labor intensive sector of U.S agriculture. A Paper presented at the ASAE/CSAE Annual International Meeting, Toronto, Ontario.

Jaydeep, M. B. and M. J. Pandya. 2013. Design and analysis of an aerial scissor lift, Journal of information, Knowledge and Research in Mechanical Engineering, 2(2): 452

Kolhe, K. P., A. G. Powar, A. D. Dhakane and H. M. Sham. 2011. Stability and Ergonomic Design Features of Tractor Mounted Hydraulic Elevator for Coconut Harvesting. American Journal of Engineering and Applied Sciences, 4 (3): 380-389.

Kusuma, G., K. Sahitya, V. Nagakomali, B. RajKiran and V. V. Satyanarayana. 2015. Design and Fabrication of Prototype Telescopic Raising Platform for Harvest-

ing Oil Palm Fresh Fruit Bunches. Indian Journal of Science and Technology, 8(17): 1-5
Molitorisz, J. and R. L. Perry. 1966. Citrus harvest Mechanization. California Agr., 3: 8-9.
Perry, R. L. 1965. Harvesting aids and the outlook for mechanical harvesting. California Citrograph, 51: 61-70.
Sarig, Y. and G. E. Coppock. 1986. Harvesting techniques. In: Fresh Citrus Fruit (Wardowski, Nagy and Grierson, Eds). AVI Publ. Westport, CT.
Sarig, Y. 1993. Robotics of fruit harvesting: a state-of-the-art review. Journal of Agricultural Engineering Research, Res. 54: 265-280
Seamount, D. T. 1969. Consistency of picker picking rates in oranges as a factor in influencing performance on man positioning devices. Transactions of the ASAE, 14: 911-913
Shanab, R. F. and N. Sepehri. 2005. Tipover stability of manipulator-like mobile hydraulic machines. ASME journal of dynamic systems measurement and control, 127(2): 295-301.
Tajuddin, A., R. Murugesan and V. V. Sreenarayanam. 2002. Farm machines for cultivation of horticultural crops. Food and Agricultural organization of united nations.

■■

ABSTRACTS

The ABSTRACTS pages is to introduce the abstracts of the article which cannot be published in whole contents owing to the limited publication space and so many contributions to AMA. The readers who wish to know the contents of the article more in detail are kindly requested to contact the authors.

2225

The History of the Foundation of the Scientific and Technical Base of Research and Development for Agricultural Machinery in the Russian Far East: Iurii Vaitekhovich, Yakov Osipov, Hideo Hasegawa

The article deals with the Far Eastern region of Russia with a description of the territorial location, topography, and soil types. Plants producing agricultural machinery and implements in the Russian Far East are considered. The history of formation and development of specialized organizations, the purpose of which is research in the field of agriculture, namely the creation of machines and implements, is considered. The article also presents the general methodology of planning and carrying out tests of machines and implements. The purpose of the study is to study the formation and development of specialized organizations in agriculture. Different soil and climatic conditions of Russia in agriculture, have adjustments made in the study and development of agricultural machinery and implements. The specialists of the industry face important tasks to develop new more versatile machines and implements for farming in different soil and climatic conditions. Widely imported foreign equipment pushes domestic producers to improve machinery and implements for agriculture, which contributes to strengthening the technical condition of agricultural machinery. Thus, specialists in the industry face important tasks to create more versatile and productive machines and equipment.

■■

2231

Effects of LEDs on The Physical and Biochemical Properties of *in Vitro* Seedlings of *Nicotiana tabacum* L.: T. Demircia, Ö. Uysal, K. Ekincil, N. Göktürk Baydar

The article deals with the Far Eastern region of Russia with a description of the territorial location, topography, and soil types. Plants producing agricultural machinery and implements in the Russian Far East are considered. The history of formation and development of specialized organizations, the purpose of which is research in the field of agriculture, namely the creation of machines and implements, is considered. The article also presents the general methodology of planning and carrying out tests of machines and implements. The purpose of the study is to study the formation and development of specialized organizations in agriculture. Different soil and climatic conditions of Russia in agriculture, have adjustments made in the study and development of agricultural machinery and implements. The specialists of the industry face important tasks to develop new more versatile machines and implements for farming in different soil and climatic conditions. Widely imported foreign equipment pushes domestic producers to improve machinery and implements for agriculture, which contributes to strengthening the technical condition of agricultural machinery. Thus, specialists in the industry face important tasks to create more versatile and productive machines and equipment.

■■

Performance Evaluation of Three Different Tractor Models

by

I. E. Ahaneku
Professor
Dept. of Agricultural and Bioresources Engineering,
Michael Okpara University of Agriculture,
Umudike, Abia State, NIGERIA
drahaneku@yahoo.com

O. A. Oyelade
Ph.D, Assistant Director (Engineering)
Dept. of Farm Power and Machinery,
National Centre for Agricultural Mechanization (NCAM),
Ilorin, Kwara State, NIGERIA
yemibamigbdejdoyelade@gmail.com

Abstract

A comparative study of three different tractor models of similar horsepower capacity namely, YTO-750, YTO-754 and TAK DI-75 was carried out at the experimental field of the National Centre for Agricultural Mechanization (NCAM), Ilorin, Nigeria. The common tillage implements mounted on these tractors during ploughing and harrowing operations were 3-bottom disc plough and 18 blade off-set disc harrow, respectively. The test parameters measured during ploughing and harrowing operations include travel reduction (wheel slippage), draught force, speed of operation, effective field capacity, theoretical field capacity, field efficiency, time of operation, drawbar power, tractive efficiency, soil volume disturbed, soil moisture content, soil bulk density and soil cone index. The experimental field measuring 50 m by 100 m was laid in a randomized complete block design (RCBD) and which was replicated three times. Test results revealed that TAK DI-75 tractor performed best in terms of fuel consumed during ploughing and harrowing operations which gave a total value of 7.20 l/ha. This was immediately followed by YTO-754 tractor which gave a total value of 7.60 l/ha for both tillage operations. Last among them was YTO-750 tractor which gave a total value of 11 l/ha for both tillage operations.

Keywords: tractor, ploughing, harrowing, performance, operation, soil

Introduction

In Nigeria, most farming operations are accomplished through the use of hand hoes and cutlasses which are labour intensive, time consuming, drudgery laden and expensive. This traditional method of farming in Nigeria puts serious limitations on the growth of the nation's agricultural sector thus exacerbating reduced food production leading to increased food importation (Oyelade and Oni, 2013). Agriculture plays a major role in developed nation's economy. Therefore the word, agriculture, as defined by Lasisi (2010) is the production of food and goods through farming.

The world population has been on the increase thereby demanding for the production of more food to feed the ever-increasing world population. One of the approaches being adopted to solve this food demand is by substituting human power with mechanical power in agricultural production. Different terms in different situations have been used to connote this mechanical power substitution. These include Appropriate technology, Tractorization, Selective Mechanization or simply, Mechanization. The major operation carried out in the field with the use of mechanical power is tillage.

According to Ahaneku et al. (2011), agricultural tillage involves soil cutting, soil turning and soil pulverization and thus demands high energy, not just due to the large amount of soil mass that must be moved, but also due to inefficient methods of energy transfer to the soil. The most widely used energy-transfer method is to pull the tillage tool through the soil. This is mainly realized with the use of tractors.

The most common and best known power source in agriculture today is the tractor which comes in a wide range of types, makes, sizes, power ratings and capabilities. With such a wide range of engine power technology systems to choose from, it is relatively easy for the expert to select and match a system that is appropriate to a specific situation. Considering all the relevant factors, engine power technology is considered the most appropriate mechanization package for agricultural intensification programmes in Nigeria (Odigboh, 2000).

Aneke (1994) observed that out of more than 25 million tractors in existence all over the world, 150,000 tractors representing 0.6% are found to account for those in Sub-Saharan Africa. The primary purpose of agricultural tractors, especially those in the middle to high power range, is to provide power to enable attached soil engaging and other agricultural implements to perform their intended functions. The value of a tractor is measured by its power rating and the amount of work accomplished relative to the cost incurred in getting the work done. Drawbar power is that achieved through the drive wheel to move the tractor and or implements through the soil.

The performance of tractor depends on the performance of a combination of traction devices and the performance of the tractor drive train. While the efficiency of a traction device is defined as tractive efficiency, the efficiency of a complete tractor is defined as power delivery (Zoz et al., 2002). The attributes of an efficient operation of farm tractors include maximizing the fuel efficiency of the engine and drive train, maximizing the tractive advantage of the traction devices and selecting an optimum travel speed for a given tractor implement system (Zoz and Grisso, 2003; Grisso et al., 2008).

Table 1 Tractor Specifications

Parameters	Tractor Models		
	YTO-750	YTO-754	TAK DI-75
Effective output (hp)	74	74	75
Tractor type	4 Wheel	4-Wheel-Drive	4 Wheel
Crankshaft rated speed (rpm)	2,400	2,400	2,200
Bore/stroke (mm)	105/125	105/125	100/118
Displacement (cm^3)	4,300	4,300	3,707
No. of cylinders	4	4	4
Engine firing order	1-3-4-2	1-3-4-2	1-3-4-2
Type of cooling system	Water-cooled	Water-cooled	Water-cooled
Type of fuel	Diesel	Diesel	Diesel
Type of injector pump	In-line	In-line	In-line
Fuel tank capacity (l)	135	115	65
Type of steering system	Power steering	Power steering	Mechanical
Lifting capacity (kg)	1,651	1,346	2,500
Size of front tyre	7.50 - 16	11.2 - 24	7.50 - 16
Ply rating	8	8	8
Type of tread	Radial	Bias	Radial
Recommended inflation pressure for field work (kPa)	147-196	147-196	250
Size of rear tyre	14.9-30	16.9-30	16.9-30
Ply rating	10	10	10
Type of tread	Bias	Bias	Bias
Recommended inflation pressure for field work (kPa)	147-196	147-196	110
Wheel base (mm)	2,400	2,314	2,212
Country of origin	China	China	India

Table 2 Implements Specification

Item	Disc plough	Off-set disc harrow
Type of implement	Mounted	Mounted
Number of bottom/blades	3	18
Diameter of disc (mm)	660	-
Diameter of plane blade (mm)	-	570
Diameter of notched blade (mm)	-	560
Spacing of disc (mm)	500	225
Lower hitch point span (mm)	800	750
Overall length (mm)	2,022	1,087
Overall width (mm)	880	1,084
Overall height (mm)	1,016	1,026

Draft force and energy requirements, based on current soil and operations, are considered important parameters for design and manufacture of improved tillage implements. Thus quantification of these parameters with respect to different soil failure patterns necessitates having good knowledge of soil-tool interaction. Tillage tools apply forces to soil resulting to soil failure for enhanced seedling emergence, improved plant rooting, increased infiltration rate, and controlled soil erosion (Lindstrom et al., 1990). The primary interest in tillage operations is the application of mechanical forces by machines to change the soil condition for agricultural production purposes (Schafer and Johnson, 1982). The continuous use of agricultural tractors with its tillage implements remains the only way to tackle food demand of the ever-increasing world population by rapidly bringing more farm land under cultivation.

This study was undertaken to evaluate the performance of three different tractor models in the field in order to ascertain their performance under Nigeria agro-climatic condition so as to guide farmers or tractor owners in selecting suitable tractor for cost-effective operations.

Material and Methods

The performance evaluation of

the three different tractor models were carried out at the experimental field of the National Centre for Agricultural Mechanization (NCAM), Ilorin (370 m above sea level, Longitude 4°30'E, Latitude 8°26'N) in the North Central States of Nigeria under the southern guinea savannah vegetation (Ahaneku and Onwualu, 2007). The experimental design for the field evaluation was randomized complete block design (RCBD) replicated three times. The soil textural classification of the three test sites was sandy loam. A 50 m by 100 m plot size was used for each test trail. The implement used for ploughing operation was a 3-bottom disc plough while that used for harrowing operation was an 18 blade off-set disc harrow. The specification of the three tested tractors are provided in **Table 1**. The specification of the two implements used are provided in **Table 2**. The pictures of the three tested tractors are shown in **Figs. 1** to **3**.

Parameters measured include speed of operation which was measured by determining the average time it took the tractor to cover 20 m placed in-between the 100 m length of the field; fuel consumed for each tillage operation was measured by starting each tillage operation by filling the fuel tank before use and then refilling the same fuel tank after completing the tillage operation; time factors such as actual time, total time and turning time used for each tillage operation were measured with a stop watch; draught force was determined using the trace tractor technique; depth and width of cuts were measured through the use of a measuring tape; soil cone index was recorded using the digital cone penetrometer; soil moisture content was determined through the use of oven dried method; and soil bulk density was determined from the mass per unit volume of soil. The three soil properties, namely, soil cone index, soil moisture content and soil bulk density were all measured at depths 0-7 cm, 7-14 cm and 14-21 cm. The resulting average values of these three soil properties form part of the data collated.

Table 3 Results of field test on the three different tractor models during ploughing operation

Measured parameters*	Ploughing operation		
	YTO-750	YTO-754	TAK DI-75
Horsepower	74	74	75
Depth of cut (cm)	22.40	23.20	24.50
Width of cut (cm)	92.91	123.81	143.67
Draught force (kN)	5.40	5.50	6.12
Effective field capacity (ha/h)	0.59	0.65	0.63
Field efficiency (%)	80.00	75.00	78.77
Tractive efficiency (%)	24.15	21.53	18.84
Travel reduction (%)	17.00	21.00	20
Time of operation (h/ha)	1.69	1.54	1.58
Speed of operation (km/h)	8.00	7.00	5.58
Drawbar power (kW)	12.00	10.69	9.49
Soil volume disturbed (m^3/h)	1,321.60	1508.00	1,543.50
Sound level under working condition (dB)	63.72	65.80	76.88
Fuel consumption (l/ha)	7.00	6.00	6.30

* Parameter values are average of three replicates

All the parameters of the tractor-implement performance were measured and recorded in line with the recommendations of RNAM test codes and proceedings for farm machinery technical series (1983).

2.1 Test Parameters

2.1.1 Travel Reduction (Wheel Slippage)

Travel reduction (wheel slippage) measured in percentage (%) can be expressed mathematically as:

$$A = [(B_2 - B_1) / B_2] \times 100\% \qquad [1]$$

where,

A = travel reduction/wheel slippage (%)

B_2 = distance covered at every 10 revolutions of the wheel at no-load condition (m)

B_1 = distance covered at every 10 revolutions of the wheel at load condition (m)

2.1.2 Drawbar Power

Drawbar power measured in kilowatts (kW) can be expressed mathematically as:

Fig. 1 Pictorial view of YTO-750 tractor

Fig. 2 Pictorial view of YTO-754 tractor

Fig. 3 Pictorial view of TAK DI-75 tractor

Table 4 Results of field test on the three different tractor models during harrowing operation

Measured parameters*	Harrowing operation		
	YTO-750	YTO-754	TAK DI-75
Horsepower	74	74	75
Depth of cut (cm)	23.44	22.00	13.00
Width of cut (cm)	153.55	163.57	196.10
Draught force (kN)	5.90	5.20	3.63
Effective field capacity (ha/h)	1.02	1.12	1.03
Field efficiency (%)	73.00	78.00	75.36
Tractive efficiency (%)	30.02	25.29	13.98
Travel reduction (%)	11.00	13.00	6.79
Time of operation (h/ha)	0.98	0.89	0.97
Speed of operation (km/h)	9.10	8.70	6.98
Drawbar power (kW)	14.91	12.57	13.11
Soil volume disturbed (m^3/h)	2,390.88	2,464.00	1,339.00
Sound level under working condition (dB)	69.27	64.70	67.11
Fuel consumption (l/ha)	4.00	1.60	0.90

* Parameter values are average of three replicates

C = (D × E) / 3.6 (constant) [2]
where,
C = drawbar power (kW)
D = draught force (kN)
E = speed of operation (km h^{-1})

2.1.3 Effective Field capacity

Effective field capacity measured in hectare per hour (ha/h) can be expressed mathematically as:

F = G (3600) / H [3]
where,
F = effective field capacity (ha/h)
G = area of field (ha)
H = total time taken in completing the whole tillage operation (s)

2.1.4 Field Efficiency

Field efficiency measured in percentage (%) can be expressed mathematically as:

I = F (100%) / J [4]
where,
I = field efficiency (%)
F = effective field capacity (ha/h)
J = theoretical field capacity (ha/h)

Theoretical field capacity can further be expressed mathematically as:

K = G (3600) / L [5]
where,
K = theoretical field capacity (ha/h)
G = area of field (ha)
L = actual time taken in doing the main tillage work (s)

2.1.5 Soil Volume Disturbed

Soil volume disturbed measured in meter cube per hour (m^3/h) can be expressed mathematically as:

M = 10000FN [6]
where,
M = soil volume disturbed (m^3/h)
F = effective field capacity (ha/h)
N = depth of cut (m)

2.1.6 Fuel Consumption

Fuel consumption measured in litre per hectare (l/ha) can be expressed mathematically as:

P = Q/G [7]
where,
P = fuel consumption (l/ha)
Q = volume of fuel consumed (l)
G = area of field (ha)

2.1.7 Time of Operation

Time of operation measured in hour per hectare (h/ha) can be expressed mathematically as:

R = 1/F [8]
where,
R = time of operation (h/ha)
F = effective field capacity (ha/h)

2.1.8 Tractive Efficiency

Tractive efficiency measured in percentage (%) can be expressed mathematically according to (Macmillan, 2002) as:

S = C/T × 100% [9]
where,
S = tractive efficiency (%)
C = drawbar power (kW)
T = wheel power (kW)

We assume power losses in the transmission from engine to the wheels of, say 10%, then the expression becomes:

S = C / (0.9 × U) [10]
where,
S = tractive efficiency (%)
C = drawbar power (kW)
T = engine power (kW)

Results and Discussion

3.1 Results

The results of the data collected for the three different tested tractor models during ploughing and harrowing operations are presented in **Tables 3** and **4**, respectively. Likewise the results of the effects of tractor performance on soil physical properties during ploughing and harrowing operations are presented in **Table 5**.

3.2 Discussion

3.2.1 Tractive Efficiency

The tractive efficiency values as calculated for the three different

Table 5 Effect of field operation on soil physical properties during ploughing and harrowing operations

Tractor Model	Ploughing operation			Harrowing operation		
	Average moisture content (%)	Average bulk density (g/cm^3)	Average cone index (N/cm^2)	Average moisture content (%)	Average bulk density (g/cm^3)	Average cone index (N/cm^2)
YTO-750	9.37	1.43	39.05	8.13	1.26	13.55
YTO-754	8.44	1.47	51.68	7.64	1.38	20.66
TAK DI-75	9.07	1.49	65.20	8.92	1.31	17.00

tractor models tested as shown in Tables 3 and 4 showed that tractive efficiency varied from 18.84% to 24.15% for ploughing operation and from 13.98% to 30.02% for harrowing operation. These low values of tractive efficiency recorded in both tillage operations is indicative of the energy potentials of these tractor models for tillage work. This available energy makes these tractors highly useful in places where there is need for heavier agricultural implements.

3.2.2 Travel Reduction

The traction efficiency of any tractive device is affected by travel reduction. As shown in Tables 3 and 4, it was observed that YTO-754 which is a four-wheel-drive (4WD) tractor gave the highest travel reduction values during ploughing and harrowing operations with a record of 21% and 13%, respectively.

3.2.3 Drawbar Power

Results presented in **Tables 3** and **4** showed that for all implements (3-bottom disc plough and 18 blade off-set disc harrow), mounted on the three different tractor models, the drawbar power ranged between 9.49 kW and 12 kW for ploughing operation and between 12.57 kW and 14.91 kW for harrowing operation. In both tillage operations carried out by the three different tractor models, YTO-750 tractor of 74 hp (55.2 kW), exhibited the highest drawbar power value of 12 kW during ploughing operation while TAK DI-75 tractor of 75 hp (55.95 kW) exhibited the least drawbar power value of 9.49 kW during ploughing operation. In the case of harrowing operation, YTO-750 tractor of 74 hp (55.2 kW) exhibited the highest drawbar value of 14.91 kW while YTO-750 tractor of same 74 hp (55.2 kW) exhibited the least drawbar power value of 12.57 kW. This simply shows that YTO-750 tractor recorded the highest drawbar power values for both tillage operations which may be as a result of higher speed of operation obtained in both tillage operations which is in agreement with the findings of Oyelade and Oni (2013).

3.2.4 Sound Level

The lowest and highest sound level recorded under working condition for the three different tractors tested during ploughing operation were 63.72 dB and 76.88 dB, respectively. While during harrowing operation, the lowest and highest sound level recorded under working condition for the three different tested tractors were 64.70 dB and 69.27 dB, respectively. The minimum and maximum sound level values obtained for these three tractors during their performance evaluation showed that they were all within the acceptable human hearing limit and hence considered safe for the tractor operator.

3.2.5 Fuel consumption

Results presented in **Tables 3** and **4** showed that fuel consumption ranged between 6 l/ha and 7 l/ha for ploughing operation and between 0.90 l/ha and 4 l/ha for harrowing operation. In both tillage operations carried out by the three different tractor models, YTO-750 tractor of 74 hp (55.2 kW), exhibited the highest fuel consumption value of 7 l/ha during ploughing operation while YTO-754 tractor of 74 hp (55.2 kW) exhibited the least fuel consumption value of 6 l/ha during ploughing operation. In the case of harrowing operation, YTO-750 tractor of 74 hp (55.2 kW) exhibited the highest fuel consumption value of 4 l/ha while TAK DI-75 tractor of 75 hp (55.95 kW) exhibited the least fuel consumption value of 0.9 l/ha. This simply shows that YTO-750 tractor recorded the highest fuel consumption values for both tillage operations which may be as a result of higher drawbar power recorded for both tillage operations which is in agreement with the findings of Oyelade and Oni (2013).

3.2.6 Soil Volume Disturbed

Soil volume disturbed is a function of effective field capacity and depth of cut. The performance evaluation conducted on the three different tractor models showed that TAK DI-75 tractor of 75 hp (55.95 kW) had the highest soil volume disturbed value during ploughing operation with a calculated value of 1,543.50 m^3/h which may be attributed to higher depth of cut value obtained during field evaluation of the tractor. Likewise YTO-754 tractor of 74 hp (55.2 kW) had the highest soil volume disturbed value during harrowing operation with a calculated value of 2,464 m^3/h which may be as a result of higher effective field capacity value obtained during field evaluation of the tractor.

3.2.7 Soil Measurements

The soil measurements taken for average moisture content, average bulk density and average cone index before the commencement of ploughing operation as shown in **Table 5** for the three tested tractors were found to be higher than the three soil measurements taken before the commencement of harrowing operation.

3.2.8 Best Choice of Tractor

In the present economic situation of the world, an average farmer or tractor owner will consider the total amount of fuel needed to plough and harrow his or her farm plot in determining the choice of tractor to select. As a result of this, TAK DI-75 tractor performed better in terms of economic value by having the lowest fuel consumption value of 7.20 l/ha which accounted for both tillage operations. This was immediately followed by YTO-754 tractor which recorded a total fuel consumption value of 7.60 l/ha for both tillage operations. Finally, YTO-750 tractor came last as the tractor recorded the highest fuel consumption value obtained during both tillage operations which accounted for a total value of 11 l/ha. Going by economic terms, TAK DI-75 tractor of 75 hp (55.95kW) was selected the best among the three sets of tested tractors.

Conclusion

Three different tractors nearly of similar horsepower were tested at the experimental field of the National Centre for Agricultural Mechanization (NCAM), Ilorin, Nigeria. All test parameters measured during ploughing and harrowing operations were found to be of satisfactory performance. However, in the choice of selecting the best performed tractor, TAK DI-75 tractor was selected based on the lowest amount of fuel used to carry out both ploughing and harrowing operations which amounted to 7.20 l/ha. This selected tractor will be of great benefit to the farmer or tractor owner in the area of minimizing the cost of production. Closest to the choice of TAK DI-75 tractor is that of YTO-754 tractor which used a total amount of 7.60 l/ha to carry out both ploughing and harrowing operations. More importantly, it should be noted during this study that no statistical analysis was carried out on the results obtained to establish their confidence level.

REFERENCES

Ahaneku, I. E. and A. P. Onwualu. 2007. Tillage effects on Maize Performance and Physical Properties of a Sandy Soil. Journal of Applied Science, Engineering and Technology, Vol. 7, No. 1: 42-49.

Ahaneku, I. E., O. A. Oyelade and T. Faleye. 2011. Comparative Field Evaluation of Three Models of a Tractor. Proceedings of the 3rd International Soil Tillage Research Organization (ISTRO) - Nigeria Symposium held February 21-24, 2011 at the University Auditorium, University of Ilorin, Ilorin, Kwara State. Pp. 90-99.

Aneke, D. O. 1994. A Survey of Farm Power Problems in Nigeria. Applied Engineering in Agriculture, American Society of Agricultural and Biological Engineers, 10(5): 623-626.

Grisso, R. D., D. H. Vaughan and G. T. Roberson. 2008. Fuel Prediction for Specific Tractor Models. Applied Eng. Agric., 2: 423-428.

Lasisi, F. 2010. Agricultural Engineering and Society- The Challenges and Sustainability. Being a paper presented at the 1st Departmental Lecture organized by the Department of Agricultural and Biosystems Engineering, University of Ilorin, Ilorin, Nigeria on 1st June, 2010.

Lindstrom, M. J., W. W. Nelson, T. E. Schumacher and G. D. Lemme. 1990. Soil movement by tillage as affected by slope. Soil and Tillage Research, 17: 225-264.

Macmillan, R. H. 2002. The Mechanics of Tractor-Implement Performance: Theory and Worked Examples. A Textbook for Students and Engineers.

Odigboh, E. U. 2000. Confronting the Challenges of Agricultural Mechanization in the next Decade: Some Notes, Some Options. Journal of Tropical Agriculture, Food, Environment and Extension, 1(1): 68-79.

Oyelade, O. A. and K. C. Oni. 2013. Field Evaluation of Three Models of TAK* Tractor for Nigeria's Agricultural Transformation. Journal of Agricultural Mechanization in Asia, Africa and Latin America, 44(3): 49-55.

RNAM. 1983. Regional Network for Agricultural Machinery Test codes and Procedures for Farm Machinery. Technical Series No. 12. General Guidelines in the use of Test Codes.

Schafer, R. L. and C. E. Johnson. 1982. Changing soil condition. The soil dynamics of tillage. In: Tillage Effects on Soil Physical Properties and Processes. American Society of Agronomy Special Publication, Number 44, 14-15.

Zoz, F. M., R. L. Turner, and L. R. Shell. 2002. Power Delivery Efficiency: A Valid Measure of Belt and Tire Tractor Performance. Trans. ASAE, 45(3): 509-518.

Zoz, F. M. and R. D. Grisso. 2003. Traction and Tractor Performance, ASAE Distinguished Lecture Series #27, ASAE Publication Number 913C0403. Paper presented at the Agricultural Equipment Technology Conference held at Louisville, Kentucky, USA, February 9 -11.

■■

Development and Field Evaluation of Hydraulic-driven Real Time Sensor-based Integrated System for Measuring Soil Compaction and Electrical Conductivity of Soil

by
Vinay Kumar
Dept. of Farm Machinery and Power Engineering,
Punjab Agricultural University,
Ludhiana, INDIA
vinaykumarmangotra27@gmail.com

Vishal Bector
Dept. of Farm Machinery and Power Engineering,
Punjab Agricultural University,
Ludhiana, INDIA

Manjeet Singh
Dept. of Farm Machinery and Power Engineering,
Punjab Agricultural University,
Ludhiana, INDIA

Anoop Dixit
Dept. of Farm Machinery and Power Engineering,
Punjab Agricultural University,
Ludhiana, INDIA

Manpreet Singh Mavi
Dept. of Soil Science,
Punjab Agricultural University,
Ludhiana, INDIA

Abhishek Patel
Central Institute of Agricultural Engineering,
Bhopal, Madhya Pradesh, INDIA

Rishabh Soni
Mahindra and Mahindra Ltd. Mohali,
Punjab, INDIA

N. Saravanan
Smart Implements and Machinery,
Mahindra Research Valley,
Chennai, INDIA

Abstract

The tractor-mounted and hydraulically operated real-time sensor-based integrated system for measuring soil compaction and electrical conductivity of soil was successfully developed and evaluated in the field. The design parameters of the developed soil sensor were similar to ASAE Standard S313.3 with the incorporation of soil electrical conductivity measuring sensors at the tip of the cone of the cone penetrometer. The major components of the developed cone penetrometer were a frame, hydraulic cylinder, probe, ultrasonic depth sensor, global position system (GPS), control panel, and data acquisition system. The Finite Element Analysis (FEA) of the critical parts as well as the whole assembly with different types of materials was done by using ANSYS software. Structural steel was selected for the construction of the frame of the soil sensor due to easy availability and cost efficiency. The En8 was selected for the fabrication of the probe of the assembly and low carbon-based steel (EN8 BS970 080M40) material was selected for the hydraulic cylinder. The developed soil sensor was evaluated in two different types of soil at two different locations after the harvesting of the wheat crop, where the paddy crop was the previous crop in rice-wheat rotation, and paddy residue was managed as per the treatments. The developed soil sensor showed a mean sensing accuracy of 95.4% for soil compaction measurement in comparison with manual cone-penetrometer and, 73.94% for soil electrical conductivity measurement in comparison with standard laboratory methods in both locations in both types of soil. The overall results of the developed soil sensor concluded that it was feasible to adopt the developed soil sensor to establish a reliable and faster soil compaction monitoring system with EC measurements.

Keywords: Agricultural Machinery, Soil Compaction, Electrical

conductivity, Cone Penetrometer, Stress Analysis, Stress Distribution of Soil Sensor.

Introduction

Soil compaction is the solidification of soil particles into small volumes due to which the available size of pore space for air and water gets reduced. It is a serious and preventable form of soil degradation that may result in decreased crop yield production. Intensive farming of crops has extended all over the world which involves the use of heavier new introduced machinery systems and shorter crop rotations, leading to an increase in soil compaction (Poesse, 1992). Measurement of electrical conductivity of soil is the simplest and least costly method available today which can provide quick and reliable information about soil health in a very short amount of time than the traditional method of grid sampling. It can be easily associated with specific soil properties that affect crop yields, such as topsoil depth, pH, the concentration of salt, and water holding capacity.

It can be frequently used for the assessment of soil quality, soil salinity percentage, pH, moisture content, and topsoil depth which can be correlated with yield variation (Johnson et al., 2001, Larney et al., 1989 and Corwin et al., 2003). Differences in soil properties are often the major reason for yield variability and measurement of soil electrical conductivity has the potential to guesstimate various variations in some soil physical properties in a field. Methods for calculating or calibrating soil salinity from electrical conductivity have been discussed by many researchers and scientists, including, Nielsen (1973), Rhoades (1993) and Herrero et al., 2003. In addition to this, other properties were also recorded with the electrical conductivity measurements using calibrated techniques such as moisture content in soil (Kean et al., 1987; Sheets and Hendrick, 1995; Khakural et al., 1998), clay content of soil (Williams and Hoey, 1987), clay pan depth identification (Doolittle et al., 1994) and fertility status of soil (Carlos et al., 2001 and Wollenhaupt et al., 1994).

With the current advancement in precision agriculture, spatial variation of soil compaction and electrical conductivity of soil has been the center of attention by many researchers in their research (Kumar and Bector, 2022). Sudduth et al. (2004) developed a hydraulically actuated probe having an electrical conductivity sensor at the tip to measure soil compaction and electrical conductivity simultaneously. In recent years, many integrated soil sensor systems have been developed for measuring soil compaction and electrical conductivity for three-dimensional mapping and are mainly based on soil strength sensors, water content sensors, and conductivity sensors. It has been acknowledged that the recommended methods of using a hand penetrometer (with high accuracy) require more time and intense effort for direct measurement of a huge amount of soil compaction in field conditions, which is labour-challenging and uneconomical for field mapping on large scale (Dexter et al., 2007).

Determination of indirect methods of measurement along with their geographical coordinates has therefore become a more pleasing substitute (Gaultney, 1989). Similarly, measurement of electrical conductivity by laboratory process or by an indirect method is also laborious and time-consuming, especially when large samples are to be analysed. Very limited research has been done on such technologies that can establish a reliable, faster, and demonstrate cost-effective soil compaction monitoring system simultaneously with EC measuring systems in geotechnical site investigations (Grisso et al., 2009). However, equipments are available in advanced countries to measure real-time data of the electrical conductivity by grid mapping like Veris 3100 which is bulky and costly but the farmers do not have access to such costly types of equipment. Therefore, the objective of the study was to develop and evaluate the

Fig. 1 Conceptual design and working mechanism of the sensor based integrated system (Patel, 2019)

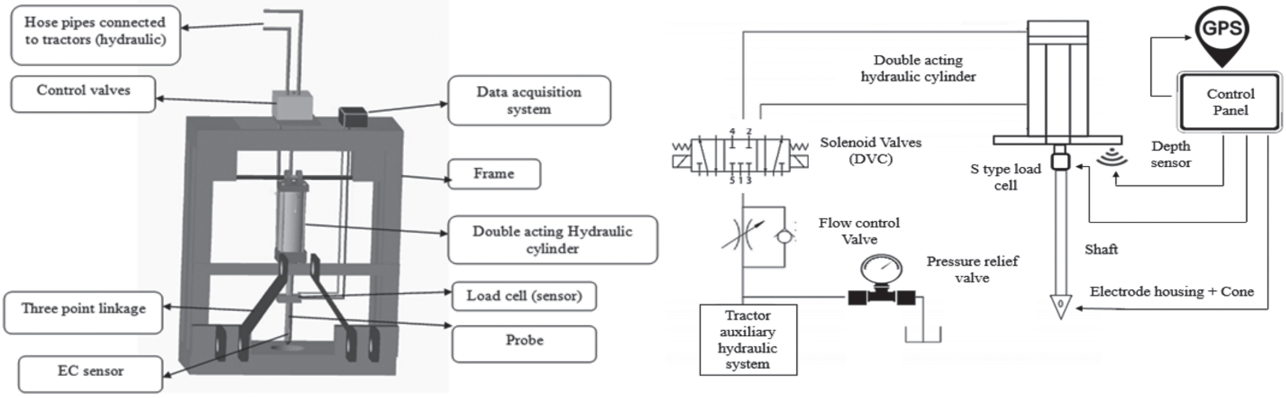

tractor-operated real-time integrated sensor for measurement of soil compaction simultaneously with electrical conductivity to directly acquire the real-time geo-referenced data in the agricultural field to save time, resources and estimate numerous soil-related or associated problems accurately for the farmers in the present era of precision agriculture.

Objective

Measurements of soil compaction and electrical conductivity are commonly done with the help of handheld cone penetrometer and laboratory techniques respectively, which is a time-consuming, tedious, and laborious method. Therefore, we aimed to develop a tractor-operated real-time soil sensor for measuring soil compaction and electrical conductivity of soil simultaneously with GPS-enabled grid sampling and mapping strategy to reveal the soil profile variability within the field for site-specific management.

Material and Methods

2.1 Conceptual Design of the Real-time Sensor-based System

The conceptual design and working mechanism of a sensor-based integrated system for measuring soil compaction and electrical conductivity was developed based on the functional requirements, technical information, and review of the literature (**Fig. 1**). The major components of a sensor-based integrated system for measuring soil compaction were characterised into the mechanical and electronic unit. The mechanical unit comprised of frame, probe, hydraulic cylinder, valve system, and hydraulic hose pipes. The assembly components of the machine were mounted on the metal frame and the frame was attached to tractor through a three-point linkage system.

The designed soil sensor was operated with the help of a tractor hydraulic system having a compensating valve and pressure control relief valve. If the hydraulic fluid pressure was found greater during operation, it could be easily managed by the pressure relief valve. The solenoid valve which acts as a directional control valve was incorporated in the design to provide fluid orientation to the top or bottom of the hydraulic cylinder because the probe attached to the piston rod of the cylinder required the up and down movement to capture data vertically into the soil layers. Therefore, the up and down direction of hydraulic fluid was controlled by an electronically programmed solenoid valve, operated with the help of a 12-volt tractor battery. The S-type load cell unit (500 kg) was connected at the end of the piston rod from the upper inbuilt groves of the load cell and to the probe through lower inbuilt groves for mounting purposes, to measure the quantity of load phased by cone base of the probe during insertion and sends data to the control panel. At the end of the probe a conical attachment, four electrodes were fitted inside the electrode housing for electrical conductivity measurement (Wenner Array method). As the system required depth-wise recording of the soil profile, therefore the ultrasonic type of depth sensor (HC-SR04 sensor module) was selected for the measurement of the insertion depth continuously at particular depth intervals. GPS (NEO-6MV2 GPS module) was also mounted on the soil sensor for recording discrete point sampling locations and making grid size. All the electronic components and sensors were integrated as per the required output through programming logical control (PLC) inside the control unit. The designed model of the whole assembly unit sensor-based integrated system for measuring soil compaction and electrical conductivity of soil based on the conceptual design is shown in **Fig. 2**. The drafting of the machine with engineering details is shown in **Fig. 3**.

Fig. 2 Sensor-based integrated system with various components mounted on the frame

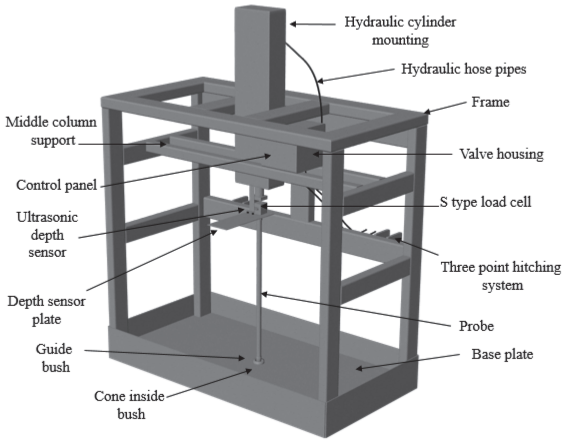

Fig. 3 2D drafting of the sensor based integrated system of tractor operated soil sensor

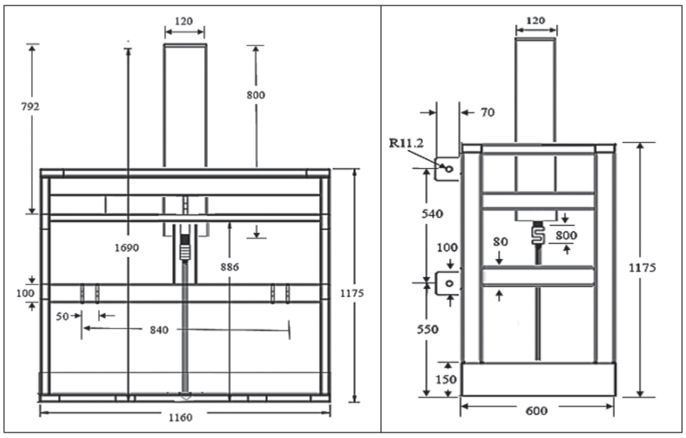

Fig. 4 Stress plot and factor of safety of the three selected materials

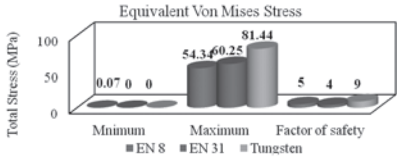

2.2 Design Parameters for the Development of Mechanical Components of the Sensor-based Integrated

2.2.1. Probe

The following factors were taken into account in the design of the probe:

(i) The homogeneity or uniformity of the probe material over the entire length.
(ii) Provision for passage of wires circuitry through hallow space along the center line of probe
(iii) The overall diameter of the soil sensor's probe was kept smaller than the diameter of the upper cone's base to avoid any side thrust on the probe surface.

The probe diameter according to ASABE standards (2006) was 15.8 mm for soft soil and 19.53 mm for hard soil. The later size for hard soil was taken into consideration for probe design. A slight modification due to the incorporation of electrical conductivity sensors and maximum designed pressure (10 MPa) was preferred over the standard dimension as earlier sensors were designed at a maximum pressure of 2 to 5 MPa pressure. Based on the preliminary studies two sizes of probe diameter were selected for analysis (18 and 20 mm) using ANSYS software which confirmed that 20 mm probe shaft diameter was a better option over 18 mm (Patel, 2019). The probe of the soil sensor was analysed in ANSYS software to check its strength against the reactive forces with three materials (EN8, EN31, and Tungsten) on 20 mm diameters. A force of 10 MPa was applied at the top of the probe with fixed support at the bottom of the probe. The EN8 material was finally selected based on the factory of safety and easy availability of the material (**Fig. 4**). The Factor of safety is the ratio of the yield stress of the material and the actual load. The factor of safety greater than 1.5 was considered safe for any industrial machine. The probe was available in the form of solid and hollow bars of EN8 in the market of various sizes and dimensions but the hollow pipe desired dimension was not available in the market. Therefore, a solid bar of EN8 material of 650 mm in length with 20 diameters was procured from the market and drilled throughout the length of the shaft length for the passage of wire from the cone electrical conductivity sensor. The shaft of the probe was threaded from the inside to attach the cone to the bottom of the shaft and outside from the upper part for attachment to the load cell (**Fig. 5**). The shaft was threaded with M20 × 1.5 according to the (IS 2186: 1985).

The cone of 30° angle of EN8 material was selected as per the desired requirements. However, the cone was grinded to achieve the desired dimensions as per ASABE standards (2006). The cone had an external thread according to Indian standards (IS 2186:1985) as M12 × 1.5, where M12 and 1.5 were the nominal and pitch diameters respectively as per the drawing. The provision for electrode fitting was made in the extended part of the cone by drilling holes of 3 mm at an equidistant of 2 mm. The drilling of holes in the cone was very difficult due to less availability of space. The cone was first slightly heated before drilling for easy and accurate drilling. A 3D and 2D view of the cone is shown in **Fig. 6**.

2.2.2. Frame

The frame was the most important component of the hydraulic-operated soil sensor where all the assembly units were mounted on the frame. The frame was hinged to the tractor and the hinge was modified according to the three-point linkage system of the tractor of category II type. The weight of the machine needed to be enough to withstand the upward thrust and any jerk that could lead to the buckling of the probe. The structure needed to be strong enough from welded joints to withstand the opposite thrust and able to distribute the pressure equally over the total frame surface for aimed stability. Therefore, FEA analysis of the frame was required to be carried out to predict the behaviour, strength, and structural failure of the frame. The structural analysis of the frame with different types (Structural steel and chrome-

Fig. 5 2D and 3D model of the probe of the soil sensor (All dimensions are in mm)

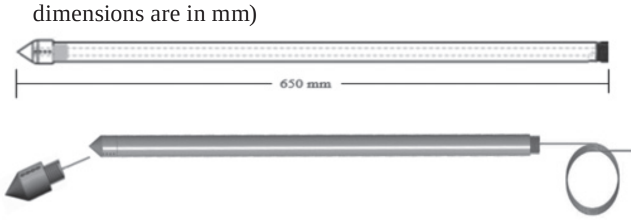

Fig. 6 2D and 3D model of the probe of the soil sensor (All dimensions are in mm)

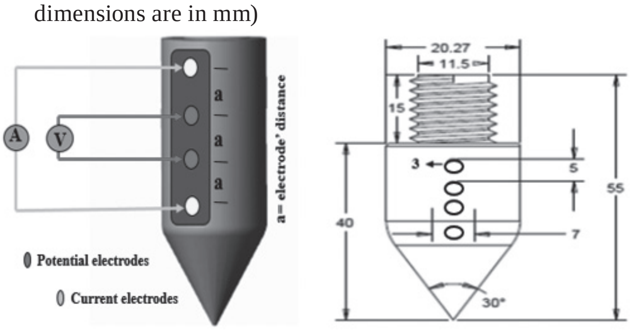

based steel: 4130) of the materials helped in the selection of materials and better understanding of the critical failures of the structural deformation at critical points under critical load and stress. The mechanical properties of the material along with the factor of safety analysed in ANSYS software are shown in **Table 1**.

The frame was fabricated and welded with the help of MIG welding as per the drawing by using structural steel (S275) rectangular cross-sectional vertical and horizontal columns according to Indian Standards (IS 4923:1997). The dimensions of the cross-sectional and horizontal columns were 80 × 40 × 3 mm and 40 × 40 × 3 mm respectively. At the bottom of the frame, a sheet of structural steel (S275) metal with the base plate attached was (1164 × 600 × 4 mm) for the stability of the frame in the soil during operation. It was additionally supported at many locations to increase the strength of the frame. The main support columns of the frame lift the overall weight of the soil sensor machine where three-point linkage was welded and consisted of 100 × 40 × 4 mm. A rectangular box (70 × 120 × 800 mm) of structural steel was welded at the center of the frame for placement of hydraulic cylinder in the re-modified design. The total length, width, and height of the frame were

116.5, 60.0 and 117.5 cm respectively. A control box of structural steel was also attached to the middle support columns for the safety of the electronic circuits and control panel of the soil sensors. Different views of the fabricated frame are shown in **Fig. 7**.

Table 1 Mechanical properties of the material selected for frame analysis

S. No.	Mechanical Property	Material Name	
		Structural steel (S275)	AISI 4130 Alloy Steel
1	Composition (%)	C = 0.23, Mn = 0.7, P = 0.03, Si = 0.3, S ≤ 0.04	C = 0.33, Cr = 1.1, Mn = 0.9, Mo = 0.25, P ≤ 0.035, Si = 0.35, S ≤ 0.04
2	Yield strength (MPa)	275	360
3	Young's modulus (MPa)	200,000	210,000
4	Poisson's ratio	0.3	0.3
5	Density (g/cm^3)	7.85	8.3
6	Cost, Rs./kg (approx.)	65	500
7	Factor of Safety (FOS) recorded due to its self-weight	6.5	19
8	Factor of Safety (FOS) recorded due reaction load by the hydraulic cylinder	5.14	14.8

Table 2 Mechanical properties and analysis results of cylinder tube in ANSYS software

Name	Value	
Material	Medium carbon steel (BS 970 070M20)	
Composition (%)	C = 0.36, Mn = 0.60, P = 0.05, S = 0.005, Si = 0.10	
Density (g/cm^3)	7.9	
Young's modulus (N/m^2)	2×10^{11}	
Poisson's ratio	0.3	
Yield strength (MPa)	280	
Results	Minimum Value	Maximum Value
Total deformation (mm)	0.00	0.93394
Equivalent von mises stress (MPa)	27.631	145
Factor of Safety, FOS = 1.9		

2.2.3. Hydraulic Cylinder

The hydraulic cylinder was the main component of the whole assembly of the soil sensor which acts as a hydraulic fluid that converts the energy of the fluid into useful action. From the literature reviewed, it was observed that the probe during insertion required some force during the withdrawal of the cone from the soil (Patel, 2019). Therefore, a double-acting hydraulic cylinder was selected for the development of the soil sensor as it was more efficient than a single-acting hydraulic cylinder in terms of extracting and retracting positions. The double-acting hydraulic cylinder of the soil sensor was analyzed in ANSYS software to check its strength against the reactive forces inside the cylinder housing and the results are shown in **Table 2**. Finite Element Analysis (FEA) of the cylindrical part was performed to check its strength against the reactive forces inside the cylinder housing. The cut section view of the hydraulic cylinder is shown in **Fig. 8**.

The hydraulic cylinder was

Fig. 7 Side and Front view of the fabricated frame of the soil sensor before placement and fitting of the sensor

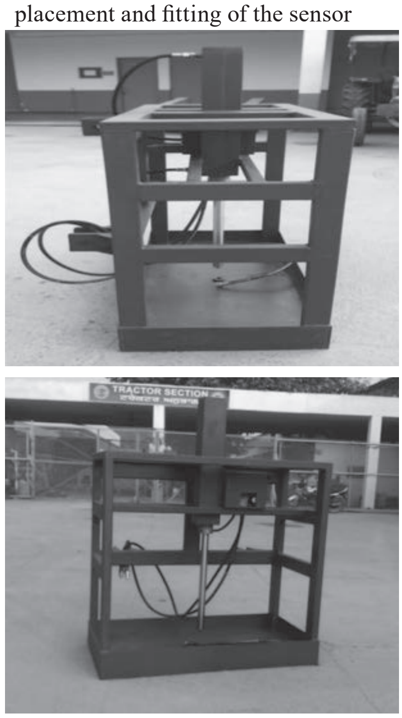

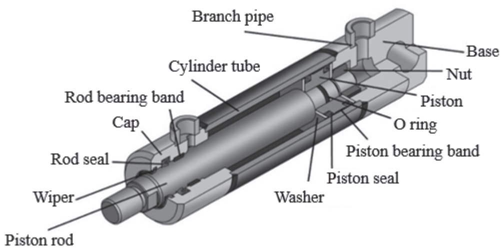

Fig. 8 Cut Section view of hydraulic cylinder used in soil sensor

Fig. 9 Fabrication and fitting of hydraulic cylinder in the hydraulic housing

mounted on the cross-sectional rectangular bars of the frame which pushed the probe into the soil. The upper top end of the hydraulic cylinder was welded and fitted in the rectangular box for the structural stability of the machine during penetration. The rectangular box the welded with the upper base of the frame and middle columns of the frame. The length, breadth, and height of the box were 120, 120 and 800 mm. Two cutouts from the rectangular box were made for the attachment of the hydraulic hose pipe's connections. The black PVC high-pressure hydraulic hose pipe of 1-inch nominal size of the maximum operating pressure of 207 bar was selected for hydraulic circuitry with attachment of quick release coupler connector. The hydraulic valve housing was placed in the rectangular box (250 × 230 × 200 mm) welded with the rectangular box of the hydraulic cylinder and middle columns support of the frame (**Fig. 9**).

2.3. Selection of Sensors/Instruments for the Development of Tractor-operated Integrated Soil Sensors for Measuring Soil Compaction and Electrical Conductivity

The sensors selected for the development of a sensor-based integrated system for measuring soil compaction and electrical conductivity of the soil were an S-type load cell, ultrasonic depth sensor, electrical conductivity measuring sensor based on the Wenner Array method, GPS (Global positioning system), and solenoid valve.

2.3.1 S-type Load Cell

There is a variety of S-type load cells available in the market based on the capacity (10-10,000 kg), depending upon different classes of accuracy such as A, B, C and D. S-type load cells provide precise electrical output under tension and compression load. Therefore, based on the design requirement of the soil sensor the capacity of the load cell was calculated based on the maximum cone index and the base area of the cone.

Maximum force (N) = cone index (MPa) × base area of cone (mm^2) = 10 × 323 = 3230 N = 330 kg (approx.)

Therefore, a load cell of 500 kg capacity of class "A" was selected for the study which was able to record force up to 15 MPa. The signals produced from the load cell when force is applied are very low in the millivolt range which are processed with the help of a signal amplifier consisting of an HX711 chip with analog-to-digital conversion capabilities with 24-bit resolution. The HX711 unit magnifies the output of the low voltage signals of the load cell and sends it to Arduino so that the Arduino can finally calculate the force from the signals into the digital output (**Fig. 10**).

2.3.2 Ultrasonic Depth Sensor

The HC-SR04 ultrasonic depth sensor was used for measuring the depth of insertion of the probe. It works on the principle of sound waves which was integrated with load cell and electrical conductivity data through the control unit. The HC-SR04 sensor module consists of two projectors (eyes) which act as transmitter and receiver. The ultrasonic receiver module transmits an ultrasonic wave that travels in the

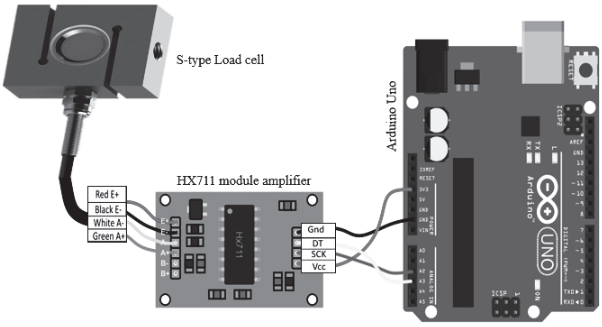

Fig. 10 Interfacing of S-Type Load Cell and HX711 amplifier with Arduino UNO developed in TINKERCAD software

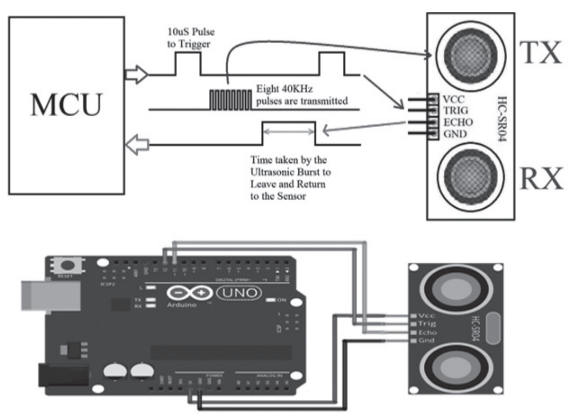

Fig. 11 Pulse generating timing diagram and interfacing of the HC-SR04 ultrasonic depth sensor with Arduino

air and gets reflected when opposed by any project that is received by the receiver module. The built-in circuitry on the module calculates the time taken for the ultrasonic wave to return or come back. The distance was calculated from the speed and time traveled by the wave through the duration measurement function of the Arduino UNO. The Arduino reads the inputs, processes them, and generates digital output (**Fig. 11**). The HC-SR04 can measure the distance from 1 to 400 cm with an accuracy of 0.2 cm and an operating frequency of 40Hz.

2.3.3 Electrical Conductivity Measuring Sensor

Copper electrodes with excellent sensitivity to electrical conductivity (5.96×10^7 s/m) were selected for the development of electrical conductivity sensors as per availability in the market. The four electrodes of 3 mm diameter and 8 mm length at an equidistant of 2 mm were fitted inside the electrode housing of the cone according to the Wenner Array configuration. The electrodes were covered from the outside with epoxy resin tape to insulate the electrodes from the cone. The developed sensor measured the output voltage according to the variable resistance offered inside the soil profile. The external voltage and current were supplied to the two internal and external electrodes due to which potential difference occurred between the two internal electrodes. The sensor system was powered with a 12 V lithium acid battery of the tractor and attached to the potentiometer (LM393 module) to provide voltage output according to the electrical resistance offered by soil to the EC sensing probe. The interfacing of the LM393 module and electrodes with the microcontroller is shown in **Fig. 12**.

2.3.4 GPS (Global Positioning System)

The study required a high-resolution GPS to record instant and real-time data that contains geographical reference sites for soil profile measurements to map spatial changes in the soil. The NEO-6MV2 GPS module Receiver was selected for the developed soil sensor which was integrated with cone index and EC data at each point of penetration. The GPS module has high-performance features even in bad challenging environments with a U-blox six positioning engine which provides its position on earth in longitude and latitude. This module was very flexible and cost-efficient offers several connectivity options in a small compact package. The view of the NEO-6MV2 GPS module is shown in **Fig. 13**.

2.3.5 Data Logger

A data logger was used for recording and saving the data in real-time from all the integrated sensors. The CH376S USB flash module was used as a data logger and was interfaced externally with the microcontroller (**Fig. 14**). The CH376S module is a file manager (control chip) that was interfaced with the Arduino Uno which reads and writes in the USB port flash drive. It sets up the basic USB firmware internally and supports USB-HOST and USB-Device Mode.

2.3.6 Display

The large-size liquid-crystal display module (JHD162A) which has its light-emitting source was used for displaying the sensor's output data in real-time. It could display 80 characters i.e., 20 characters in each 4 rows. It was a very compact type, simpler in design, with lower power consumption and excellent user interference with Arduino. Moreover, the inbuilt quality, safety, and durability of the (JHD162A) module made it an excellent choice over the

Fig. 12 Interfacing of electrical conductivity sensor with LM393 module and Arduino UNO

Fig. 13 Complete view of NEO-6MV2 GPS module and pinout configuration

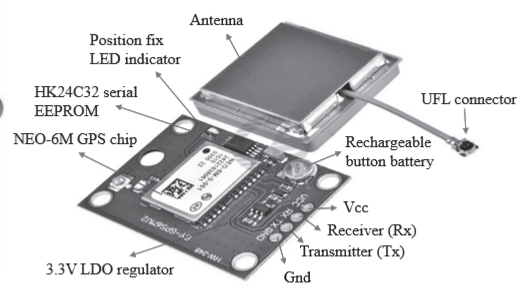

Fig. 14 CH376S USB flash module with pinout layout used for file storage

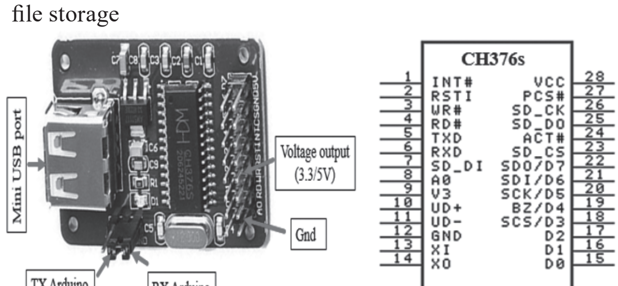

Fig. 15 Liquid-crystal display module (20 × 4) used for displaying data

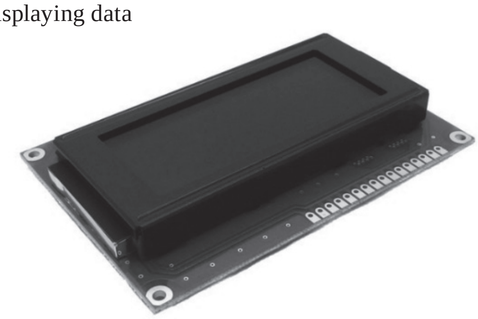

previous graphic display (**Fig. 15**)

2.3.7 Wi-Fi Module

The Wi-Fi module was used for creating an access point and could be connected to a hotspot or Wi-Fi which made it easy to upload and transfer data online by making the Internet of Things (IoT) easily possible. It was used for controlling the operation of the soil sensor and displaying the real-time screen display through mobile phones remotely. The Node-MCU (ESP32) was used in the current study because of its compatibility and easy availability (**Fig. 16**). The Node-MCU was an open-source software platform and its multipurpose IoT controller (SDK) and hardware development environment were built around a low-cost chip system called ESP32 chip having compatibility with Arduino Uno.

2.3.8 Solenoid Valve

For suitable operation of the designed system of the soil sensor, the piston of the cylinder must be extended (lowering), retracted (raising), and stay neutral if there is no need to retract. The solenoid type directional control (5/3) valve was therefore used for raising, lowering, and neutral positions. A 5/3 solenoid valve had 5 ports and 3 positions in which one port was input, the other two output, and the remaining two were exhaust ports. The electromagnetic electrically operated separate 2-channel relay module (HL-52S relay and HW-316 LM2596 power relay) was used for power supply and controlling the high voltage solenoid valve working through the microcontroller. The 5/3 solenoid valve can be stopped at any midpoint so that if data is required up to a certain depth rather than 60 cm can be easily taken or at any troubleshooting in the mechanical system. The view of the solenoid with assembly components is shown in **Fig. 17**.

2.3.9 Arduino

It is a small computer that reads the data from the sensor, embedded with a microcontroller that monitors, performs transformation, and makes decisions on the sensor's input and output signals. It was used to monitor the speed and depth of penetration of the actuator based on the programming language to control the required output. The control panel was designed with the help of an Arduino Uno microcontroller based on ATmega 328P which was equipped with a high-performance AVR technology microcontroller having multiple programming options for a wide variety of different solutions (**Fig. 18**).

Fig. 18 Arduino Uno microprocessor used for control panel mechanism

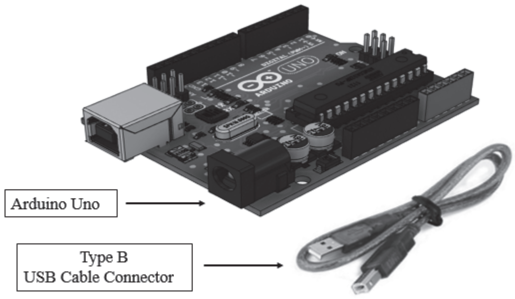

2.3.10 Development of Control Panel and Integration of Sensors

A series of preliminary tests were performed to technically authenticate the functionality of the developed soil sensor in both the hardware and software stages. During these preliminary tests, some improvements in the mechanical as well as in the software system were rectified and made in the final improved designed system. The major improvement was adding safety features to the designed soil sensor system. A visual 360° LED light indicator with a buzzer for sound alert was added in the software system and placed at the top end of the soil sensor to alert the operator. When the load on the soil sensor was found above the pre-defined minimum threshold limit of 8.5 MPa, then it was programmed in the control panel that the soil sensors would produce a sound alert with an indication of red-light signals and warning signals on the screen display. When the soil sensor crosses the minimum threshold limits of 8.5 MPa during penetration, the soil sensor will stop working and the sensing probe will be pushed upward automatically without any user interference. A detailed view of the

Fig. 16 ESP32 module and pinout description (Anon, 2021)

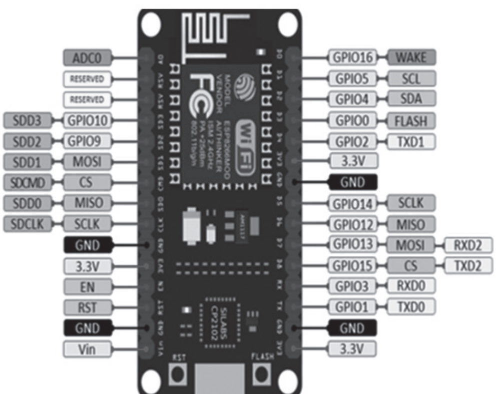

Fig. 17 Solenoid directional control valve (5/3) selected for development of soil sensor

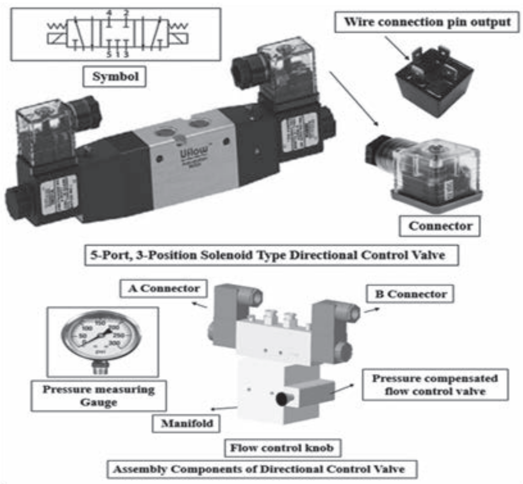

system's components of the control panel is shown in **Fig. 19**.

2.3.11 Control Panel Operation

The programming code for the microprocessor/controller (ESP32) was written in C++ language on Arduino IDE software (Integrated Development Environment) which gives programming editing options at any instant with integrated library support. The compiled program was uploaded to the microprocessor through the computer with USB type B. The ESP32 Arduino was used as the microprocessor controller of the control panel system which was connected to all of the sensors directly and the other peripherals. When the control panel was powered through an external source, it took 2-3 minutes to warm up and start searching the GPS signals. When signals were found, latitude, longitude, and elevation values were displayed on the display. The NEO6M GPS communicates to ESP32 with UART Communication at a 9600 baud rate. The file number for the particular point of data extraction was also displayed on the display screen with an option to create a new folder for distinguishing between a large number of samples. The penetration starts with the down button on the SPDT (Single Pole Dual Throw) type control switch.

When the down button was pressed, the lower relay was ON and when the Up button was pressed, the upper relay was ON. This up and down movement is controlled by these 2-relay modules which were connected to the solenoid valve. This was provided with an additional option for the neutral stage i.e., the movement of the hydraulic cylinder rod could be stopped at any point and continue or discontinue movement. The working mechanism for the sensor system is shown in the flow chart diagram (**Fig. 20**). The digital data from the Load cell through the HX711 signal amplifier, electrical conductivity sensing electrodes, and GPS signals were compiled at each point of penetration. This digital data was then stored in the memory card reader in Microsoft Office Excel format which was easily connected to the laptop or any Android mobile to extract data files and interoperate results.

2.3.12 Mobile Bluetooth App

An Android Bluetooth App was developed for controlling the operation of the developed soil sensor remotely. The Android Bluetooth App shared a live screen display of the soil sensor and the up and down movement of the hydraulic cylinder was also controlled through the Bluetooth App through the sliding type button provided on the App (**Fig. 21**). The Android App structure Android application was written in the Android Studio which communicates with the ESP32 module and collected the measurement data continuously and share live on the App screen. The Bluetooth App was designed in Flutter which was a free open-source framework, software development tool, and powerful language that was used to develop Android applications. Simultaneously, when continuously communicating and receiving data from the ESP32 module of the control panel of the soil sensors, it also sends signals when the operation

Fig. 21 Android App structure developed soil sensor system

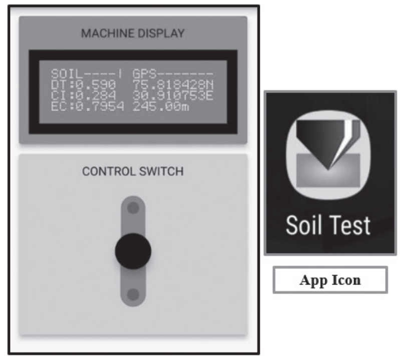

Fig. 19 Control panel with system components of the developed soil sensor fitted inside a detachable box

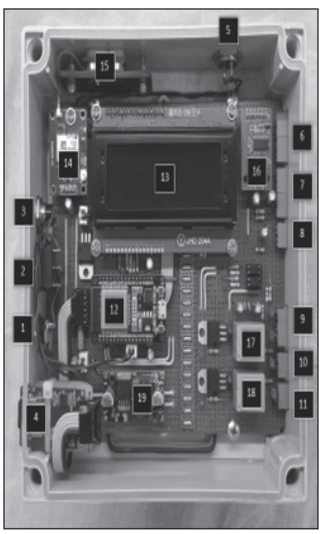

1 - 12V power input jack
2 - Power Switch
3 - New Folder Button
4 - Memory Card Module
5 - External Warning light and Buzzer
6 - External Load cell
7 - External Ultrasonic distance sensor
8 - External Conductivity probes
9 - External control switch (Up, Neutral, Down)
10 - External Solenoid valve (upward motion)
11 - External Solenoid valve (downward motion)
12 - ESP32 Arduino microcontroller
13 - 20x4 character LCD
14 - NEO6M GPS module
15 - GPS Antenna
16 - HX711 Load cell signal amplifier
17 - 12V Relay
18 - 12V Relay
19 - LM2596 Voltage step down

Fig. 20 Flow chart diagram of system components integrated with control panel system

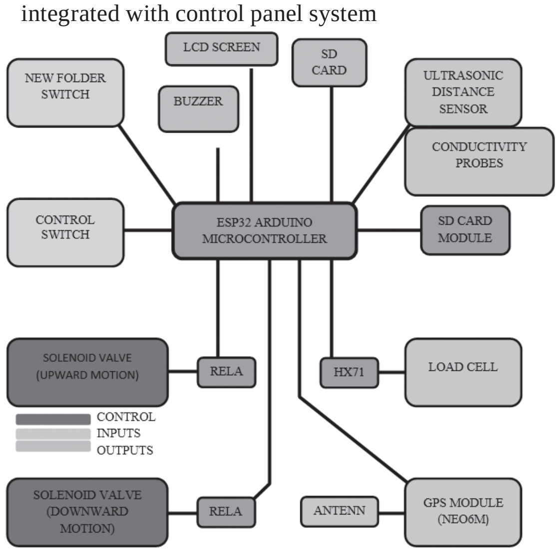

needs to be controlled through the Bluetooth App. ESP32 reads the position of the button on the Android Bluetooth App and communicates with the sensor system in milliseconds.

3.1 Calibration of the Sensor of the Developed Soil Sensor

3.1.1 Calibration of S-type Load Cell

The S-type load cell was calibrated by applying known dead weight (kg) load vertically under a static load experiment set on the top of the load cell in two phases and the output was recorded in millivolt. The relationship between the actual load in kilogram and measured output average mean of loading and unloading in millivolt was found to be highly linear at their respective interval and the linear regression line was fitted to the measured output data with R^2 value of 0.99 as shown in **Fig. 22**.

3.1.2 Calibration of Ultrasonic Depth Sensor

The output reading of the ultrasonic sensor displayed on the screen was manually recorded against the actual reading on the measuring tape by placing a target plate (obstacle) in parallel and gradually moving the targeted plate from 0 to 60 cm at intervals of 2 cm. The experimental results of the depth sensor showed negligible error as compared to the actual distance as shown in **Fig. 23**. Since the error was very small, therefore it was easily corrected in the programming code.

3.1.3 Calibration of Electrical Conductivity Sensor (EC)

The samples were recorded with the help of developed soil sensors from three different types of locations with different soil textures up to 60 cm at an interval of 20 cm and the electrical conductivity of each sample was measured as per the standard laboratory process which served as a reference point for calibrating the developed soil sensor. The relationship was developed between the electrical conductivity (dSm^{-1}) measured by the standard laboratory methods and the developed sensor's voltage (mV) where the linear regression line was fitted in the programming to the measured output data with an R^2 value of 0.83 as shown in **Fig. 24**.

4.1 Field Evaluation and Validation of the Developed Soil Sensor

The developed soil sensor was evaluated in three types of tillage treatments (T1 = residue retained, T2 = residue removed, T3 = residue incorporated) at three different depths (D1 = 20 cm, D2 = 40 cm, D3 = 60cm) in three different sizes of the grid (G1 = 2 × 6 cm^2, G2 = 2 × 12 cm^2, G3 = 2 × 18 cm^2) with a constant speed of penetration with three replications of each at two different locations (L1 = 75°49'06.23'' E, 30°54'39.52'' N and L2 = 75°48'43.71'' E, 30°54'39.52'' N) in two type of soil (S1 = sandy loam and S2 = loamy soil) for field evaluation as shown in **Fig. 25**. The developed soil sensor was operated using 50 hp tractor after the harvest of wheat crop. The penetration recorded with the hand-held cone penetrometer and samples collection for laboratory analysis of the electrical conductivity was near the same point of penetration by the developed soil sensor within the radius of 10-15 cm for attaining more accuracy. The results obtained for soil compactions and electrical conductivity from the developed

Fig. 22 Calibration load cell with loading and unloading known dead weights

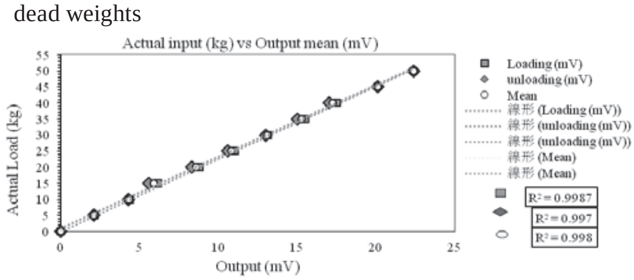

Fig. 23 Calibration graph of the ultrasonic depth sensor

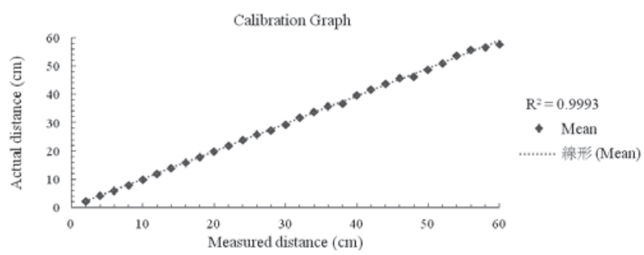

Fig. 24 Calibration graph of EC measurement output of all the three textures of soil

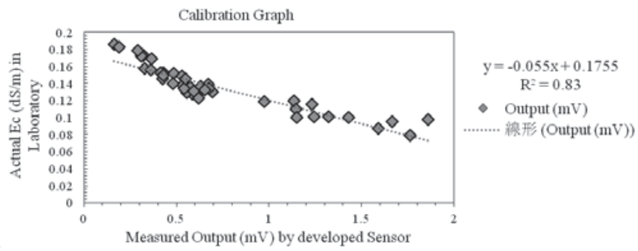

Fig. 25 A map view of two locations selected for field experiment for evaluation of the developed soil sensor

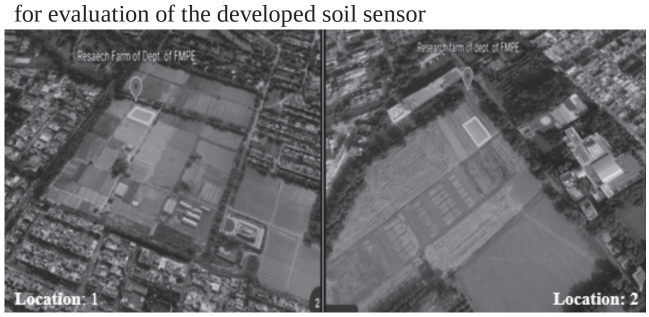

sensor were compared with the results obtained with manual cone penetrometer and laboratory methods respectively (**Fig. 26**). The field experiment trials were laid out in a Randomized Complete Block Design (RCBD) with three replications to determine the variation of the independent parameters measured by the developed soil sensor and the laboratory methods, and interaction between the factor's combinations at 5% level of significance. Statistical analysis software (SAS) was used for the analysis of variance and operation of means.

Results and Discussion

Statistical analysis revealed that there was a non-significant difference between the soil compaction measured by the developed soil sensor (CI-DSS) and the manual cone penetrometer (CI-MCP) in both types of soil at a 5% level of significance. The cone index showed increasing trends with an increase in depth. The depth of penetration and interaction between the three levels of depths also had a significant effect at a 5% level of significance on soil compaction in both types of soil. It was observed that the mean cone index did not vary in all three different types of grid size and was non-significant at a 5% level of significance whereas the interaction between three levels of grid size was also non-significant in both types of soil. The tillage condition had a significant effect on the soil compaction and the interaction between three tillage treatments was also significant on soil compaction at a 5% level of significance. The R^2 value between the developed soil sensor and manual cone penetrometer was 0.99 for all the above three treatments and the mean standard error was 0.021. Therefore, it was concluded from the results that the developed soil sensor had a mean sensing accuracy of 95.4% when compared with the manual cone penetrometer.

The graphs were plotted between the overall mean of the developed soil sensor and hand-held manual cone penetrometer as shown in **Fig. 27**. It was observed from the experiment that the mean cone index showed less variation in the upper layer of the soil up to 200 mm depth, more variation in deeper depth of the soil from 200 to 400 mm and abrupt variation from 400 to 600 mm as more hardpan in the deeper layer of the soil were observed.

Statistical analysis revealed that there was a non-significant difference between the soil electrical conductivity measured by the developed soil sensor (EC DSS) and the laboratory method (EC lab) in both types of soil at a 5% level of significance. The soil electrical conductivity showed increasing trends with an increase in depth. The depth of penetration and interaction between the three levels of depths also had a significant effect at a 5% level of significance on soil electrical conductivity in both types of soil. It was observed that mean soil electrical conductivity did not vary in all three different types of grid size and had non-significant at a 5% level of significance whereas the interaction between three levels of grid size was also non-significant in both types of soil. The tillage condition had a significant effect on the soil's electrical conductivity and the interaction between three tillage treatments was also significant on soil compaction at a 5% level of significance. The R^2 value between the developed soil sensor and the laboratory method (EC lab) was 0.99 for all the above three treatments and the mean standard error was 0.081. Therefore, it was concluded from the results that the developed soil sensor had a mean sensing accuracy of 73.94 % in measuring soil electrical conductivity when compared with the standard laboratory method.

The graphs were plotted between the overall mean of the developed

Fig. 26 Measuring soil compaction with the developed soil sensor and hand-held manual cone penetrometer

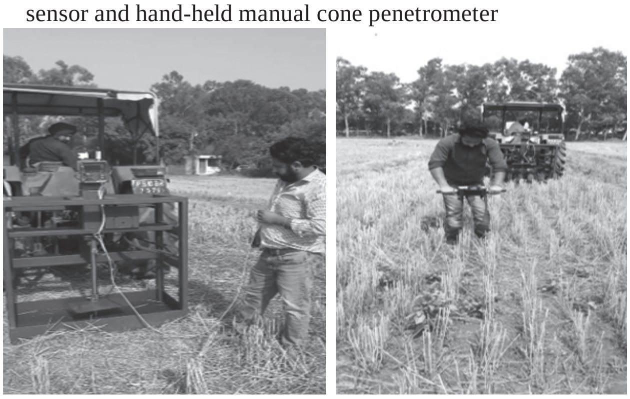

Fig. 27 Measuring soil compaction with the developed soil sensor (CI-DSS) and hand-held manual cone penetrometer (CI-MCP) at both locations

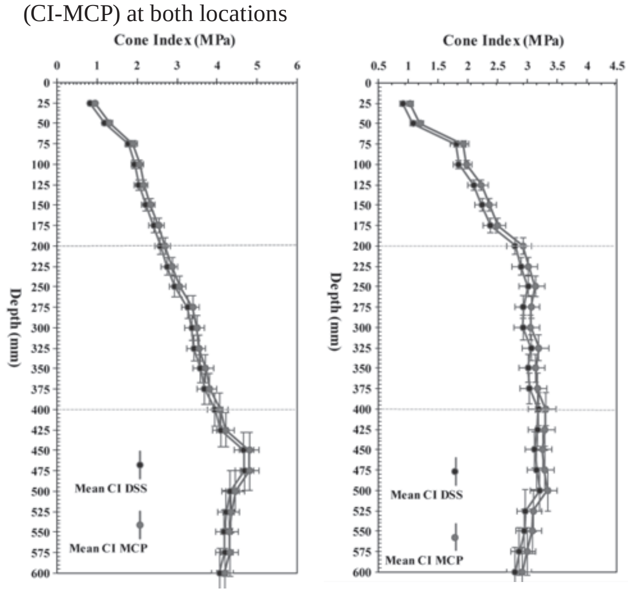

soil sensor and the laboratory method (EC lab) as shown in **Fig. 28**. It was observed from the experiment that the electrical conductivity of soil showed more variations in the upper layer of the soil up to 200 mm depth, less variation in deeper depth of the soil from 0 to 400 mm and vary small variation from 400 to 600 mm. Although the method of measurement of soil electrical conductivity was different the result outputs of the developed soil sensor were quite close to justify the outcomes of the laboratory result outputs.

Conclusion

The results obtained for soil compaction between the developed soil sensor (CI-DSS) and the manual cone penetrometer (CI-MCP) and for soil electrical conductivity in comparison with laboratory methods (EC lab) in terms of accuracy clearly show that the developed soil sensor worked quite excellent in both types of soil. However, it was also observed that the accuracy of the developed soil sensor was slightly more in upper layer but increased slightly during penetration into deep layer of soil when compared with the manual cone penetrometer because constant speed was also disturbed slightly with the manual cone encountered with soft pan in upper layer. As it was mentioned in ASABE standard' test of penetration, that the penetration speed of the probe should be constant which is slightly disturbed either encountered with too soft soil in upper layer or hard layer (> 5 MPa) in deeper layer. Perhaps that's why hydraulic operated soil sensors are coming more into existence by replacing manual hand-held cone penetrometer due to their accuracy of measurement with constant speed of operation. However, it will increase the volume of sampling for a particular area with reduced human error and upgrade the quality of measuring equipments used by scientific community all over the world for measuring soil compaction (CI) and electrical conductivity (EC) of the soil. The tractor operated "on the go and stop" indigenous hydraulic operated dual soil sensor will be accessible for recording or monitoring real time data for soil compaction and electrical conductivity of soil which will play an important role in adoption of precision agricultural technologies.

Fig. 28 Measuring soil electrical conductivity with the developed soil sensor (CI-DSS) and the laboratory method (EC lab) at both locations

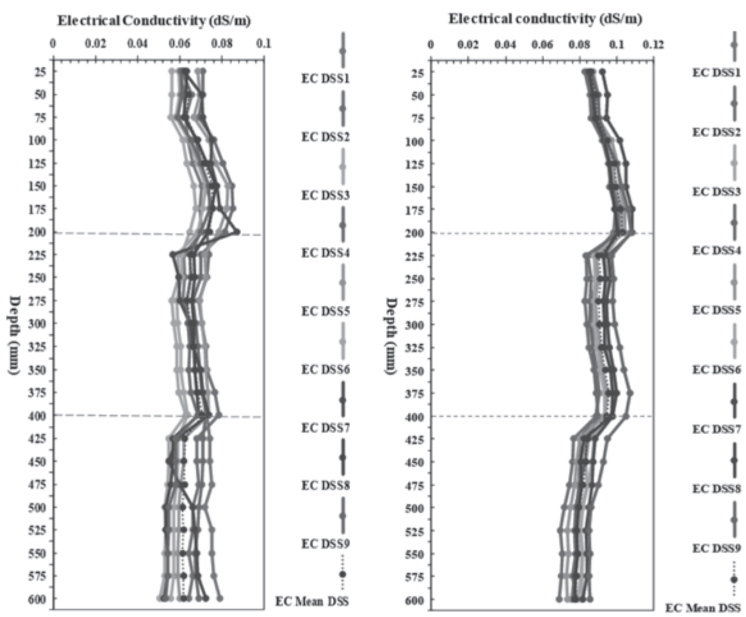

Acknowledgements

The technical guidance provided by department of smart implements and machinery, Mahindra Research Valley, Chennai and Punjab Agricultural University, Ludhiana, India and technical support from NAHEP-CAAST project coordinator team during entire research work is gratefully acknowledged.

REFERENCES

Anonymous. 2021. ESP32 data series. Pp 1-60. Version 3.8 Espressif. https://www.espressif.com/sites/default/files/documentation/esp32_datasheet_en.pdf.

ASABE standards. 2006. Soil Cone Penetrometer. ASABE standards: ASAE S 313.3. FEB04. Pp 902-904. American society of Agricultural Engineer, St. Joseph MI.

Carlos, M. P. V., H. B. Luis and W. H. Jan. 2001. Contribution of water content and bulk density to field soil penetration resistance as measured by a combined cone penetrometer-TDR probe. Soil Till Res 60: 35-42.

Corwin, D. L., S. R. Kaffka, J. W. Hopmans, Y. Mori, S. M. Lesch and J. D. Oster. 2003. Assessment and field-scale mapping of soil quality properties of a saline-sodic soil. Geoderma 114: 231-59.

Dexter, A. R., E. A. Czyz and O. P. Gate. 2007. A method for prediction of soil penetration resistance. Soil Till Res 93: 412-19.

Doolittle, J. A., K. A. Sudduth, N. R. Kitchen and S. J. Indorante. 1994. Estimating depths to claypans using electromagnetic induction methods. J Soil Water Conserv 49: 572-75.

Gaultney, L. D. 1989. Prescription farming based on soil property

sensors. Trans ASAE 48: 1723-30.
Grisso, R. B., W. G. Wysor, D. Holshouses and W. Thomason (ed). 2009. Precision Farming Tools: Soil Electrical Conductivity. Pp 1-7. Virginia Cooperative Extension, Virginia Tech Public University, Virginia.
Herrero, J., A. A. Ba and R. Aragues. 2003. Soil salinity and its distribution determined by soil sampling and electromagnetic techniques. Soil Use Manage 19: 119-26.
Indian Standards. 1985. IS 2186. Pp 1-5. ISO Metric external screw threads for interference fit applications.
Indian Standards. 1997. IS 2186. Pp 1-7. Hollow steel sections for structural use-specification.
Johnson, C. K., J. W. Doran, H. R. Duke, B. J. Weinhold, K. M. Eskridge and J. F. Shanahan. 2001. Field-scale electrical conductivity mapping for delineating soil condition. Soil Sci Soc Am J 65: 1829-83.
Kean, W. F., M. Jennings Walker and H. R. Layson. 1987. Monitoring moisture migration in the vadose zone with resistivity. J Groundw 25: 562-71.
Khakural, B. R., P. C. Robert and D. R. Hugins. 1998. Use of non-contacting electromagnetic inductive method for estimating soil moisture across a landscape. Commun Soil Sci Plant Anal 29: 2055-65.
Kumar, V. and V. Bector. 2022. Recent Trends in Measurement of Soil Penetration Resistance and Electrical Conductivity of Agricultural Soil and Its Management under Precision Agriculture. AMA - Agric Mech Asia Africa & Latin America 53: 12-20. doi: 10.13140/RG.2.2.15977.57447
Larney, F. J., R. L. Huffman, R. T. Schuler, D. R. Taylor, E. J. Kladviko and B. Lowery. 1989. A portable, self-leveling constant-rate cone penetrometer with computer-controlled data acquisition for tillage studies. Soil Till Res 14: 231-39.
Nielsen, D. R., J. W. Biggar and K. T. Erh. 1973. Spatial variability of field-measured soil-water properties. Hilgardia 42: 215-59.
Patel, A. 2019. Computer aided design of tractor operated soil sensor for measuring soil compaction and electrical conductivity. M Tech thesis, Punjab agricultural university, Ludhiana, India.
Poesse, G. J. 1992. Soil compaction and new traffic systems. Pp 79-91. In: G. Pellizzi, L. Bodria, A. H. Bosma, M. Cera, M. A. Baerdemaeker, W. K. Hamza and Anderson (ed) Possibilities Offered by New Mechanization Systems to Reduce Agricultural Production Costs. The Netherlands.
Rhoades, J. D. 1993. Electrical conductivity methods for measuring and mapping soil salinity. In: D. L. Sparks (Ed.), Advances in Agronomy. Pp 201- 51. Academic Press, San Diego, CA, USA.
Sheets, K. R. and J. M. H. Hendrickx. 1995. Non-invasive soil water content measurement using electromagnetic induction. Water Reso Res 31: 2401-09.
Sudduth, K. A., J. W. Hummel and S. T. Drummond. 2004. Comparison of the veris profiler 3000 to an ASAE-standard penetrometer. Appl Engng Agri 20: 535-54.
Sun, Y., D. Ma, L. P. Schulze and M. R. Schmittmann. 2006. On-the-go measurement of soil water content and mechanical resistance by a combined horizontal penetrometer. Soil Till Res 86: 209-17.
Williams, B. G. and D. Hoey. 1987. The use of electromagnetic induction to detect the spatial variability of the salt and clay contents of soils. Aust J Soil Res 25: 21-27.
Wollenhaupt, N. C., R. P. Wolkowski and M. K. Clayton. 1994. Mapping soil test phosphorus and potassium for variable-rate fertilizer application. J Prod Agric 7: 441-48.

■■

(Continued from page77)

Modelling and Optimization of a Solar Powered Groundnut Sheller Performance Using Response Surface Methodology

RSM. Biosystems engineering. 100(4), 591-600.
[37] Tewari, V. K., C. Singh and K. P. Vidhu. 2013. Performance modeling of a groundnut stripper using response surface methodology. International Agricultural Engineering Journal. 22(1), 39-48.
[38] Shukla, B. D., P. K. Srivastava and R. K. Gupta. 1992. Oilseed's processing technology. Central Institute of Agricultural Engineering, Nabi Bagh.
[39] Collins, G. A., L. D. G. Coward and G. S. Pinson. 1977. A feeder to improve the performance of a hand-operated groundnut sheller.
[40] Myers, R. H. 1971. Response Surface Methodology. Boston, MA: Allyn and Bacon: 256.
[41] Ashwini, T., L. Vikas and P. A. Kumar. 2015. Performance evaluation of power-operated sunflower seed decorticator. Environment and Ecology. 33(1), 1-5.
[42] Gitau, A. N., P. Mboya, B. N. K. Njoroge and M. Mburu. 2013. Optimizing the performance of a manually operated groundnut (Arachis hypogaea) decorticator. Open journal of optimization. 2, 26-32.

■■

Modelling and Optimization of a Solar Powered Groundnut Sheller Performance Using Response Surface Methodology

by
Vinod Choudhary
Agricultural and Food Engineering Department,
Indian Institute of Technology Kharagpur,
West Bengal - 721302, INDIA

Rajendra Machavaram
Agricultural and Food Engineering Department,
Indian Institute of Technology Kharagpur,
West Bengal - 721302, INDIA

by
Peeyush Soni
Agricultural and Food Engineering Department,
Indian Institute of Technology Kharagpur,
West Bengal - 721302, INDIA

Abstract

The performance parameter of solar-powered groundnut sheller was analyzed for optimum design parameters, viz., sieve hole size 15 mm, and speed of flywheel 59.86 rpm. The output responses as shelling capacity, shelling efficiency, and broken kernels were obtained to be 135.78 kg/h, 83.23%, and 2.54% against predicted 136.12 kg/h, 83.54%, and 2.66%, respectively with the optimum operational parameters for TAG-24 groundnut variety. The developed quadratic model is extremely statistically significant ($p < 0.0001$) and reasonably explained the shelling capacity, shelling efficiency, and percentage of broken kernels with superior value for the coefficient of determination (R^2) as 0.972, 0.989, and 0.989, respectively. The optimization parameters explained that the sieve hole size and flywheel speed have a major effect on the shelling performance of the solar powered groundnut sheller. The optimized parameters showed that the minimum broken groundnut kernels and highest shelling capacity and efficiency were obtained with the solar-powered groundnut sheller with different groundnut varieties TAG-24, TG-26, and TPG-41. There were no significant differences ($p > 0.05$) between the actual (experimental) and predicted values, pointing to the sufficiency of the equipped models. Hence, the study proves that RSM is an effective tool in predicting superior performance of a solar powered groundnut sheller.

Keywords: Solar powered groundnut sheller; Groundnut; Shelling parameters; CCD; RSM; Optimization

Introduction

Groundnut (*Arachis hypogaea* L.) is the highest cultivated oilseed crop in India about 4.91 million hectares (first rank in the world) with a total production of 9.18 million tons of groundnut pods (stands the second position in the world)[1]. It is the sixth-largest crucial oilseed crop in the world[2]. Globally, the output per year is copious than 10 million tons[3] and the production of groundnut pods in developing countries leads up to 94% with 97% of the area[4].

The groundnut pods are threshed by hand or mechanical thresher from the crop, the pods are dried and shelled to obtain the kernels. It is a cash crop that provides to the nutrition of farm families through consumption of energy and 25-28% protein (essential amino acids necessary for normal body growth and metabolism) rich groundnut kernels (48-50% oil) and supplies nutritious fodder (shells) to livestock in the rural areas. Groundnut kernels after shelling the pods provide 564 kcal from 100 g[5][6]. Worldwide 60% of groundnut pods are shelled for extraction of oil for edible and industrial purposes, while 40% are used in food products and others[7]. Its oil is also used for cooking food due to its high smoking point[8]. Groundnut kernels can be used raw, boiled, roasted, and also consumed to make confections and flour to make baked products. After the shelling of groundnut pods, the shells are utilized for making boards or fuel or filler in fertilizer and feed industries. Its shell part contains 8-15% protein, 1-3% lipids, 9-17% minerals, and 38-45% carbohydrates higher than cereal crops. Its shell also has digestibility around 53% when fed to cattle and heating value up to 2.4 kcal/kg dry basis[9].

Groundnut kernels daily consumption of 43 g/day resulted in a significant reduction of blood cholesterol, blood pressure, and blood triglyceride[10]. Groundnut kernels protein hydrolysates also exhibit different antioxidant properties viz., DPPH free radical scavenging, hydroxyl radical scavenging, and metal chelation and reducing power, and these properties may also contribute to reduce cancer and cardiovascular disease (CVD) among populations frequently consumption of kernels[11][12]. Paramawati et al.[13] explained the contamination of aflatoxin on groundnut cause of liver cancer could be reduced by the quick post-harvest operation. It was also suggested that the processing of groundnut makes it free from contamination of aflatoxin by using the post-harvest machinery viz., shelling of groundnut pods. The damaged groundnut kernels are perceptive to the contamination of aflatoxin; therefore, the minimal damage is admirable[14].

In recent years, many groundnut decorticators have been modified from these existing traditional shelling methods of groundnut. Most of the modified shellers have a major problem regarding the breakage of groundnut kernels and unshelled groundnut pods[15][16]. Abou El-Kheir and shoukr[17] explained the effect of the operational drum speed on the groundnut sheller, a major contribution to shelling capacity and efficiency. It was suggested that the shelling efficiency increased from 80.6 to 92.5% at the drum speed increased from 1.83 to 4.58 m/s. Singh[18] suggested that the wire mesh sieve provided the maximum shelling capacity as 86 kg/h than that of slotted grate 60 kg/h. It was also studied that the shelling efficiency increased from 83 to 89% with the wire mesh sieve than that of the slotted grate from 82 to 84%. They were also explained that the percentage of broken kernels increased from 3.7 to 6.7% and 8.4 to 12.6% with the wire mesh sieve and slotted grate, respectively. It was due to more opening area viz., sieve hole size. The peeling efficiency of the power operated Pongamia Pinnata decorticator was higher than that of the manual operation of groundnut shelling due to the drum preserving a steady and uniform speed[19]. A sufficient speed of pedaling was observed to be 50 to 60 rpm during the shelling of groundnut pods[20][21][22]. The oscillating speed of manually operated shellers was measured to be 48 to 60 strokes per minute[23]. Pinar[24] explained that the grain losses increased from 2.88 to 4.5% with the inappropriate methods of threshing.

It has been reviewed, considering the above-mentioned importance of quick shelling of groundnut pods to remove the fresh (minimum breakage) kernels in post-harvest processing with high shelling capacity and efficiency reduced the fungal growth and contamination of aflatoxin for human health frequently increasing population. Therefore, the operational parameters viz., speed, and sieve hole size were a major effect on the shelling's performance. Apart from the wrong sitting posture and uneven stroke of the manual shelling lever, it has been analyzed that the manual shellers give more damage to groundnut kernels, lesser shelling capacity, and efficiency. These unsatisfactory results may be due to the improper sieve hole size and not uniform stroke length. Hence, the objective of this study was to analyze optimum operational parameters for getting the highest shelling capacity and efficiency with a minimum percentage of broken kernels by using the central composite design (CCD) of response surface method (RSM) which is a quick and cost-effective method with reduced the number of experiments needed to evaluate multiple parameters and their interactions and to help in better understanding and optimizing the response of an experiment[25][26] by basically the putting the software with information which in

Fig. 1 Different parts of solar powered groundnut sheller

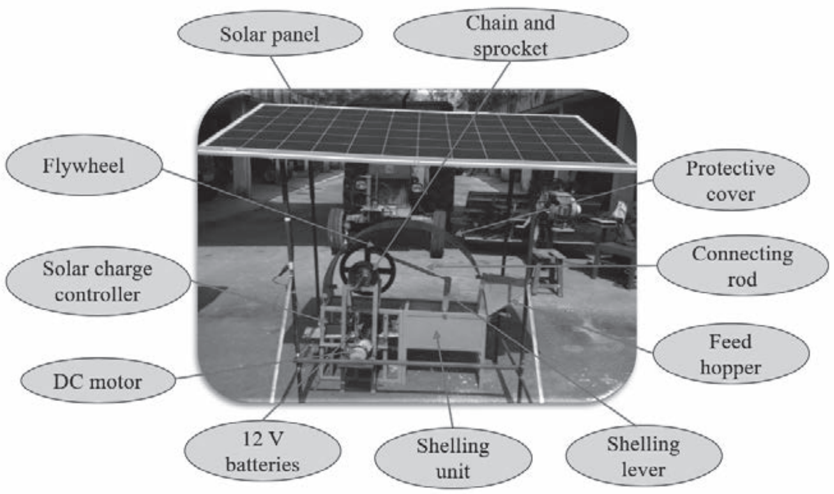

turn provide an accurate prediction of responses and superior graphical presentation. RSM was consciously designed to change experimental response with the predictive one by analyzing the various effects of parameters that will give to optimum response[27]. Therefore, further modification is needed for maximizing shelling output and efficiency with minimum losses of groundnut kernels by changing the sheller parameter through optimization.

Material and Methods

Experimental Setup

Three groundnut varieties viz., TAG-24, TG-26, and TPG-41 were procured from the local farmers of Paschim Medinipur, West Bengal. The solar-powered groundnut sheller (**Fig. 1**, developed in the Department of Agricultural and Food Engineering, IIT Kharagpur, West Bengal, India) with overall dimensions of 1000 × 260 × 1060 mm, weight 80 kg, capacity 131 kg/h, power unit 250 W DC motor, single labour required to load and unload groundnut pods and kernels were used for all the shelling performance studies. It comprises a solar panel, 12V batteries, DC motor, solar charge controller, feed hopper, protective cover, chain, and sprockets, connecting rod, flywheel, shelling unit, and shelling lever. The groundnut pods were crushed between the crushing unit and the perforated sieve. The experiment was carried out at a moisture content of 6.82 % (db) according to procedure described by ASAE[28], which was determined by Choudhary et al.[29]. The drying of groundnut pods in post-harvesting operation is very important, as incapable drying can help stimulate fungal growth and reduce kernel quality for consumption and germination. Therefore, it can be dried to 7-8% moisture content to prevent fungi growth[30].

Experimental Design and Data Analysis

Inscribed Central Composite Design (CCD[31][32][33][34][35][36]) with two independent parameters, viz., sieve hole size (S_{hs}) and speed of flywheel (S_f), was used for optimization the performance of the solar-powered groundnut sheller. Experimental design for optimization consisted of three responses (dependent parameters), viz., shelling capacity (SC), shelling efficiency (SE), and percentage of broken kernels (BK). For this intention, response surface methodology (RSM) using inscribed central composite design (CCD) was used to optimize these parameters for getting the best optimum operational parameters and to set a second-order polynomial quadratic equation for shelling the groundnut pods[37]. The data values of sieve hole size (S_{hs}) varies from 9 to 15 mm, and the speed of flywheel (S_f) varies from 48 to 60 rpm, as shown in **Table 1**. The limiting data values of the sieve hole size were based on the measured physical properties and existing CIAE model of standard manual sheller[29][38][39]. The flywheel's maximum and minimum speed is based on the chain sprocket transmission system and the manually operated sheller's stroke. The transmission ratios were provided between the DC motor and flywheel through chain and sprocket with two ratios as 1:6.25 and 1:5. For the experimental purpose, a 250 W DC motor with 300 rpm was fitted for running the flywheel through chains and sprockets to obtain the flywheel speeds within the range. Five coded levels of independent parameters were taken as +0.5, +1, 0, −1, and −0.5, respectively[31][40]. The details of Inscribed Central composite design (CCD) experimental ranges and level coded are given in **Table 1**.

Table 1 Experimental design for analyzing the test (design: CCDI)

S. N.	Parameters	Coded factors	Coded levels				
			-1	-0.5	0	+0.5	+1
1	Sieve hole size (mm)	S_{hs}	9	10.5	9.5	13.5	15
2	Speed of flywheel (rpm)	S_f	48	51	54	57	60

The size of the sieve with five levels of the hole (**Table 1**) was fabricated in the workshop of the Agricultural and Food Engineering Department, IIT Kharagpur. The second-order quadratic polynomial Equations 1, 2 and 3 were computed to optimize the dependent parameters viz., shelling capacity (SE), shelling efficiency (SE), and broken kernels (BK) for the response as functions of the coded value of the independent parameters[34][36][37][40].

$$SC = \beta_0 + \beta_1 S_{hs} + \beta_2 S_f + \beta_{11} S_{hs}^2 + \beta_{22} S_f^2 + \beta_{12} S_{hs} S_f \quad [1]$$

$$SE = \beta_0 + \beta_1 S_{hs} + \beta_2 S_f + \beta_{11} S_{hs}^2 + \beta_{22} S_f^2 + \beta_{12} S_{hs} S_f \quad [2]$$

$$BK = \beta_0 + \beta_1 S_{hs} + \beta_2 S_f + \beta_{11} S_{hs}^2 + \beta_{22} S_f^2 + \beta_{12} S_{hs} S_f \quad [3]$$

Where,

β_0 = intercept

β_1 and β_2 = linear regression coefficient

β_{11} and β_{22} = quadratic regression coefficients

β_{12} = regression coefficient of the interaction terms

S_{hs} = sieve hole size

S_f = speed of flywheel

The goodness fit of evaluation of the generated non-linear second order regression equations was checked by F-value for lack of fit (F_{lof})[34][36][37][40] and it was calculated by Equation 4.

$$F_{lof} = [\textstyle\sum_{i=1}^{N}(Y_{ei} - Y_{ci})^2 - \sum_{i=1}^{Nc}(Y_{ei} - Y_{av})^2] \,/\, (N - \text{No. of coefficients in regression equation} - n_c + 1) \quad [4]$$

Where,

i = number of independent parameters

Y_{ei} = experimental value of the ith response

Y_{av} = average of actual values of responses

Y_{ci} = calculated value of the ith response

N = total number of experiments;

nc = number of central experiments

The inscribed central composite design (CCD) consisted of 2^2 experiments (experiment number 3, 6, 8, and 11) of factorial design, five replicated center points (experiment number 2, 5, 7, 10, and 12) and four-star points (experiment number 1, 4, 9, and 13) as shown in **Table 2**. The Design-Expert Software (Version 12.0.3.0) was used for the experiments design, regression and graphical analysis of the data were attained from the experiments. The statistical analysis of the model was carried out in terms of analysis of variance (ANOVA). The mathematical model obtained during the response surface methodology (RSM) was checked by obtaining several test points studies. The experimentally received data were compared with the predicted data. The independent parameters were used at five levels in the CCDI experimental design, and a total number of 13 experiments were obtained, as shown in **Table 2**. The desirableness of fit of the computed polynomial Equations 1, 2 and 3 examined by F-value for lack of fit (LoF). The predicted and observed (experimental) values of the responses were compared by the values of the correlation coefficients and residuals. The shelling capacity, shelling efficiency, and percentage of broken kernels were determined as the following Equations given by Ashwini et al.[41]:

Shelling capacity, kg/h = (Weight of the total sample, kg) / (Effective shelling time, h) [5]

Shelling efficiency, % = (Weight of the shelled sample, kg) / (Total weight of sample, kg) [6]

Broken kernels, % = (Weight of broken kernels, kg) / (Total weight of the sample, kg) [7]

Results and Discussion

Optimization of Operational Parameters of Solar Powered Groundnut Sheller

The analysis of shelling of groundnut pods was performed with the coded levels of speed of flywheel and sieve hole size to receive the response against the independent parameters. It was analyzed that the shelling capacity, shelling efficiency, and percentage of broken kernels were normally distributed, therefore it was possible to take a 95% confidence interval for the specimen. Hence, three levels of responses were used as the lower limit, the middle, and the upper limit for every factor addition. **Figs. 2(a-c)** demonstrate the dependent parameters with the blue domain showing the lower limit, the green area showing the central limit, and the red area showing the upper limit. The test results obtained in the laboratory experiment based on the central composite design (CCD) are given in **Table 2**. These output results could be shown as a better collection of the data ranges for the independent parameters and their step value. The mathematical model of the second-order quadratic polynomial was verified for its sufficiency to develop the response parameters (shelling capacity, shelling efficiency, and broken kernels). The numerical and graphical optimization of data (**Table 2**) was analyzed through central composite design (CCD) using response surface methodology (RSM). The details of the response parameters are explained below:

Shelling Capacity (kg/h)

The response surface analysis explained to thirteen experimental plans, and second-order quadratic polynomial Equation 1 computed to the shelling capacity. The regression and statistical (ANOVA) analyses were performed to obtain the model equation and verify the statistical significance of the model. The quadratic model was more influence on the shelling capacity with the coefficient of determination (R^2) value of 0.972 a best one along with adjusted R^2 of 0.952 and predicted R^2 of 0.744 and the developed quadratic model was found to be significant ($p < 0.0001$) as shown in **Table 3**. The lack of fit was found

Fig. 2 Effect of the independent parameters on the performance of solar powered groundnut sheller

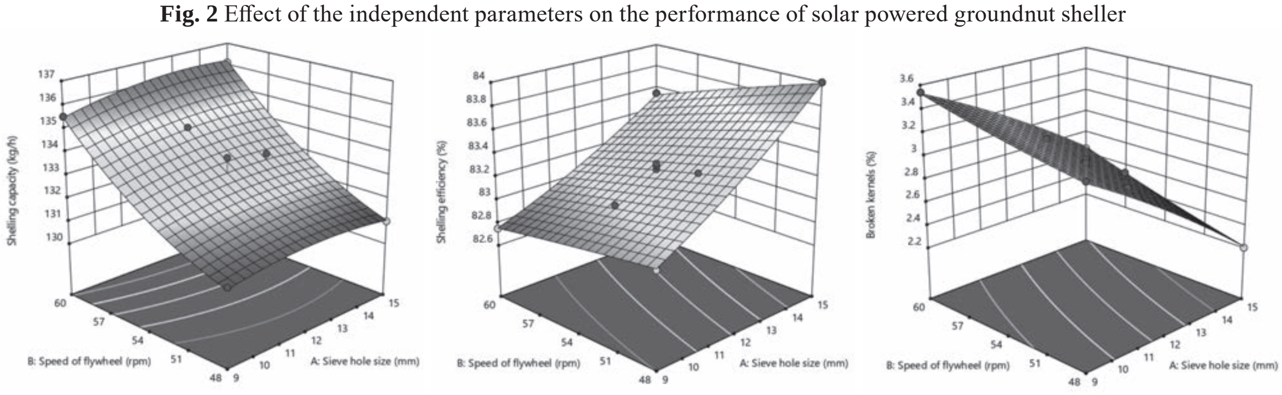

(a) Effect of the independent parameters on the shelling capacity (kg/h) at optimum flywheel speed of (59.86 rpm) and sieve hole size of (15 mm)

(b) Effect of the independent parameters on the shelling efficiency (%) at optimum flywheel speed of (59.86 rpm) and sieve hole size of (15 mm)

(c) Effect of the independent parameters on the broken kernels (%) at optimum flywheel speed of (59.86 rpm) and sieve hole size of (15 mm) insignificant, with an F-value of 0.4016. From **Table 3**, the F-value of the linear term of flywheel speed has copious significance on the shelling capacity than the sieve hole size at a 1% level of significance. The shelling capacity was strongly affected by the speed of the flywheel ($p < 0.0001$) at the linear level, but no influence effect was obtained at the quadratic and interaction levels. The linear term of sieve hole size, quadratic, and interaction terms of all two independent parameters did not provide an influence effect on the shelling capacity even at the 5% and 10% level of significance ($p > 0.05$ and $p > 0.1$). The coefficient of determination (R^2) of the developed model was found to be 0.972, which shows a better fit between the experimental and predicted value. Furthermore, it was also explained that the independent parameters describe 97.2% of the shelling capacity variation. The final second-order mathematical polynomial Equation 8 (in terms of coded factors) with different independent parameters as Shs and Sf were computed to explain the variation in the shelling capacity (SC, kg/h).

$$SC,\ kg/h = 133.12 + 0.2178S_{hs} + 2.43S_f + 0.1500S_{hs}S_f - 0.3353S_{hs}^2 + 0.6247S_f^2 \quad [8]$$

It was observed from Equation 8, the shelling capacity is directly dependent on the independent parameters viz., sieve hole size, and speed of the flywheel, and behalf of the regression coefficient, the flywheel speed was provided the maximum role in the shelling capacity than that of sieve hole size. It was also observed from **Fig. 2a** that, the fixed value of the optimum speed of flywheel (59.86 rpm), the shelling capacity (SE, kg/h) increased with up to sieve hole size 15 mm and obtaining the maximum shelling capacity of 136.12 kg/h. It was due to more sieve hole size opening. Another one at a fixed value of optimum sieve hole size 15 mm, the shelling capacity reduced with a speed of flywheel up to 48 rpm and obtaining minimum shelling capacity 131.01 kg/h, as shown in **Fig. 2a**. The maximum shelling capacity was obtained to be 136.12 kg/h at the optimum speed of flywheel 59.86 rpm and sieve hole size 15 mm. Therefore, the shelling capacity was increased with the increment of the speed of the flywheel from 48 to 60 rpm.

Shelling Efficiency (%)

The response surface analysis was explained to thirteen experimental plans, and second-order quadratic polynomial Equation 2 was computed to the shelling efficiency. The regression and statistical (ANOVA) analyses were performed to obtain the model equation and verify the statistical significance of the model. The quadratic model was more influence on the shelling efficiency with the coefficient of determination (R^2) value of 0.989 a best one along with adjusted R^2 of 0.981 and predicted R^2 of 0.842 and the developed quadratic model was found to be significant ($p < 0.0001$) as shown in **Table 3**. The lack of fit was found insignificant, with an F-value of 1.14. The shelling efficiency was strongly affected by all two independent parameters at a 1% level of significance ($p < 0.0001$) at the linear level, but no influence effect was obtained at the quadratic level and no more influence at the interaction level ($p > 0.01$). The quadratic terms of all two independent parameters did not provide an influence effect on the shelling efficiency even at the 5% and 10% level of significance ($p > 0.05$ and $p > 0.1$). The coefficient of determination (R^2) of the devel-

Table 2 Central composite design (CCD) with coded and un-coded independent parameters and experimental result for the response variables

Exp. N.	Sieve hole size (mm)	Speed of flywheel (rpm)	Responses		
	Coded/un-coded	Coded/un-coded	SC (kg/h)	SE (%)	BK (%)
1	(+0.5) 13.50	(0) 54	133.41	83.45	2.75
2	(0) 12.00	(0) 54	133.78	83.27	2.93
3	(+1) 15.00	(-1) 48	131.00	84.00	2.20
4	(0) 12.00	(+0.5) 57	134.56	83.15	3.05
5	(0) 12.00	(0) 54	132.86	83.32	2.88
6	(+1) 15.00	(+1) 60	136.12	83.55	2.65
7	(0) 12.00	(0) 54	132.83	83.25	2.95
8	(-1) 9.00	(-1) 48	131.00	82.95	3.25
9	(-0.5) 10.50	(0) 54	132.65	83.08	3.12
10	(0) 12.00	(0) 54	133.10	83.30	2.90
11	(-1) 9.00	(+1) 60	135.52	82.75	3.54
12	(0) 12.00	(0) 54	133.05	83.22	2.98
13	(0) 12.00	(-0.5) 51	131.98	83.35	2.85

Table 3 ANOVA for response surface quadratic model (responses: SC, SE and BK)

Source of Variance	df	F-value			p-value			
		SC	SE	BK	SC	SE	BK	
Model	5	49.24	128.22	126.33	<0.0001	<0.0001	<0.0001	Significant
S_{hs}	1	1.94	553.05	542.54	0.2065	<0.0001	<0.0001	
S_f	1	241.04	75.12	84.78	<0.0001	<0.0001	<0.0001	
$S_{hs}S_f$	1	0.8171	9.39	3.36	0.3961	0.0182	0.1052	
S_{hs}^2	1	0.2489	0.4228	0.2322	0.6331	0.5363	0.6446	
S_f^2	1	0.8643	0.0058	0.0429	0.3835	0.9414	0.8418	
Residual	7							
Lack of Fit	3	0.4016	1.14	1.42	0.7603	0.4341	0.3616	Not significant
Pure Error	4							
Cor Total	12							

oped model was found to be 0.989, which shows a better fit between the experimental and predicted value. Furthermore, it was also explained that the independent parameters describe 98.9% of the shelling efficiency variation. The final second-order mathematical polynomial Equation 9 (in terms of coded factors) with different independent parameters as Shs and Sf were computed to explain the variation in the shelling efficiency (SE, %).

$$SE, \% = 81.05 + 0.1950S_{hs} + 0.0327S_f - 0.0034S_{hs}S_f + 0.0059S_{hs}^2 - 0.0001S_f^2 \quad [9]$$

It was observed from Equation 9, the shelling efficiency is directly dependent on the independent parameter viz., sieve hole size, and indirect effect with the speed of flywheel and behalf of the regression coefficient, the sieve hole size was provided the maximum role in the shelling efficiency than that of flywheel speed. The maximum shelling efficiency was obtained to be 83.54 % with an optimum speed of flywheel 59.86 rpm and sieve hole size 15 mm, as shown in **Fig. 2b**. It was also observed from **Fig. 2b** that, the shelling efficiency increased with increasing the speed of the flywheel from 48 to 60 rpm and increased the sieve hole size from 9 to 15 mm, respectively. The shelling efficiency was obtained higher with the high value of the flywheel speed due to the quantity of the unshelled groundnut reduced and energy provided to the groundnut pods high. Hence, it was desired to select an optimum sieve hole size and flywheel speed for a better shelling efficiency.

Broken Kernels (%)

The response surface analysis was explained to thirteen experimental plans, and second-order quadratic polynomial Equation 3 was computed to the response parameter (broken kernels). The regression and statistical (ANOVA) analyses were performed for obtaining the model equation and to verify the statistical significance of the model. The quadratic model was more influence on the broken kernels with the coefficient of determination (R^2) value of 0.989 a best one along with adjusted R^2 of 0.981 and predicted R^2 of 0.810 and the developed quadratic model was found to be significant ($p < 0.0001$) as shown in **Table 3**. The lack of fit was found insignificant, with an F-value of 1.42. The broken kernels were affected by all two independent parameters at a 1% level of significance ($p < 0.0001$) at the linear level, but no influence effect was obtained at the quadratic and interaction levels. The interaction and quadratic terms of all two parameters did not provide an influence effect on the broken kernels even at the 5% and 10% levels of significance ($p > 0.05$ and $p > 0.1$). The coefficient of determination (R^2) of the developed model was found to be 0.989, which shows a better fit between the experimental and predicted value. Furthermore, it was also explained that the independent parameters describe 98.9% of the variation for the broken kernels. The final second-order mathematical polynomial Equation 10 (in terms of coded factors) with different independent parameters as Shs and Sf were computed to explain the variation in the broken kernels (BK, %).

$$BK, \% = 5.37 - 0.1655S_{hs} - 0.0496S_f + 0.0022S_{hs}S_f - 0.0046S_{hs}^2 + 0.0005S_f^2 \quad [10]$$

It was observed from Equation 10 that the broken kernels are directly dependent on the independent parameter viz., speed of the flywheel, and indirect effect with the sieve hole size. It was also observed from **Fig. 2c** that, the fixed value of the optimum speed of flywheel (59.86 rpm), the broken kernels (BK, %) increased with up to sieve hole size 9 mm and obtaining the maximum broken ker-

Table 4 Constraints of design parameters for optimization of output responses

Source of Variance	df	F-value			p-value			
		SC	SE	BK	SC	SE	BK	
Model	5	49.24	128.22	126.33	<0.0001	<0.0001	<0.0001	Significant
S_{hs}	1	1.94	553.05	542.54	0.2065	<0.0001	<0.0001	
S_f	1	241.04	75.12	84.78	<0.0001	<0.0001	<0.0001	
$S_{hs}S_f$	1	0.8171	9.39	3.36	0.3961	0.0182	0.1052	
S_{hs}^2	1	0.2489	0.4228	0.2322	0.6331	0.5363	0.6446	
S_f^2	1	0.8643	0.0058	0.0429	0.3835	0.9414	0.8418	
Residual	7							
Lack of Fit	3	0.4016	1.14	1.42	0.7603	0.4341	0.3616	Not significant
Pure Error	4							
Cor Total	12							

Fig. 3 Optimized output plots of the performance parameters

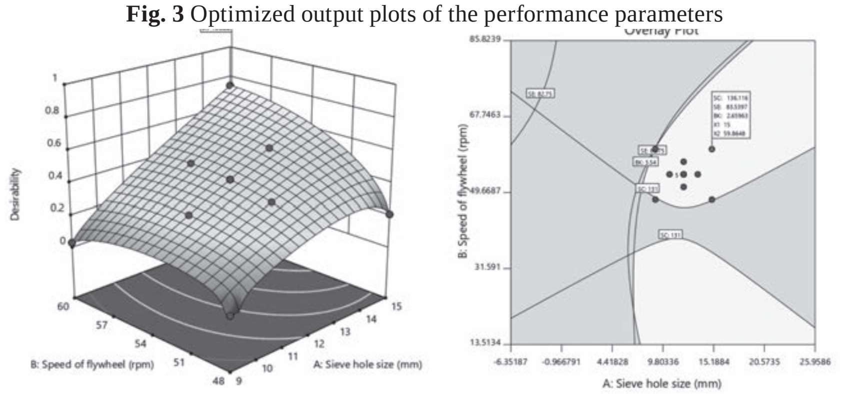

(a) Desirability response surface plot of the performance

(b) Graphical overlay plot for optimizing the shelling capacity, efficiency, and broken kernels

Table 5 Solutions for optimum conditions

S.N.	S_{hs} (mm)	S_f (rpm)	SC (kg/h)	SE (%)	BK (%)	Desirability	
1	**15.00**	**59.865**	**136.120**	**83.539**	**2.660**	**0.746**	**Selected**
2	15.00	59.550	135.922	83.552	2.646	0.744	
3	15.00	58.924	135.539	83.577	2.619	0.739	
4	15.00	58.378	135.217	83.599	2.596	0.733	

nels 3.45 %. Another one at a fixed value of optimum sieve hole size 15 mm, the broken kernels reduced with optimum broken kernels 2.66% at a speed of flywheel 59.86 rpm, as shown in **Fig. 2c**. Therefore, it was analyzed that the percentage of broken kernels was affected more by the combined effect of both the speed of flywheel and sieve hole size while the flywheel speed more dominated over the sieve hole size. From **Fig. 2c**, it was concluded that the percentage of broken kernels increased with the decreased speed of the flywheel and the sieve hole size. Therefore, it was desired to select an optimum sieve hole size for a better shelling efficiency and minimum broken kernels. The obtained performance parameters were a reasonable agreement with the performance of the sheller described by Powar et al.[34], Tewari et al.[37] and Gitau et al.[42].

Desirability of the Optimum Response (Dependent Parameters)

To find the most positive conditions for the machine activity for the best upsides of responses i.e., maximum shelling capacity (SC), least broken kernel percentage (BK), and greatest shelling efficiency (SE) was led utilizing Design-Expert software. First and foremost, in view of model and surface contour plots, the objective of greatest and least constraints of every factor are given as: is in range and their responses are given based on requirements. Then, at that point, by utilizing Design Expert software the limitations of every factor are introduced in **Table 4**. The optimization criteria were found on behalf of the desirability index with a minimum percentage of broken kernels, maximum shelling capacity, and shelling efficiency.

The Design-Expert Software (Version 12.0.3.0) was used for optimization; the software suggests four numbers of optimizing solutions (**Table 5**) in which top first solution was taken for the shelling capacity, shelling efficiency, and broken kernels with better desirability. The desirability value was found to be 0.746 for better optimum operational parameters concerning two independent parameters, as shown in **Fig. 3a**.

Verification of Operational Parameters

The mathematical (numerical) values (**Table 5**) and the graphical optimization (**Fig. 3b**) suggested that the independent design parameters viz., sieve hole size, and speed of flywheel of the machine to attain the maximum shelling capacity and shelling efficiency with the minimum percentage of broken kernels. In graphical optimization, the values shown in the flagged area were grouped together and the optimized values of parameters viz., speed of flywheel 59.86 rpm and sieve hole size 15 mm with a maximum shelling capacity 136.12 kg/h, maximum shelling efficiency 83.53%, and minimum percentage of broken kernels 2.65% were determined as shown in **Fig. 3b**. Therefore, the values obtained by numerical and graphical optimization methods were the same. The experiment was conducted based on the optimum parameters viz., speed of flywheel 59.86 rpm, and sieve hole size 15 mm to verify the legitimacy of the model equations for predicting the optimum response value. The real and the predicted benefits of shelling capacity, broken kernel, and shelling efficiency by the model are displayed in **Fig. 4**. It plainly shows that actual values of data points for shelling capacity, broken kernel, and shelling efficiency got through the trials during the test and the predicted values got to by quadratic model were an almost nearby straight line. This type of model curve shows a

Fig. 4 Comparison of the predicted and experimental (actual) values of the shelling capacity, shelling efficiency and broken kernels

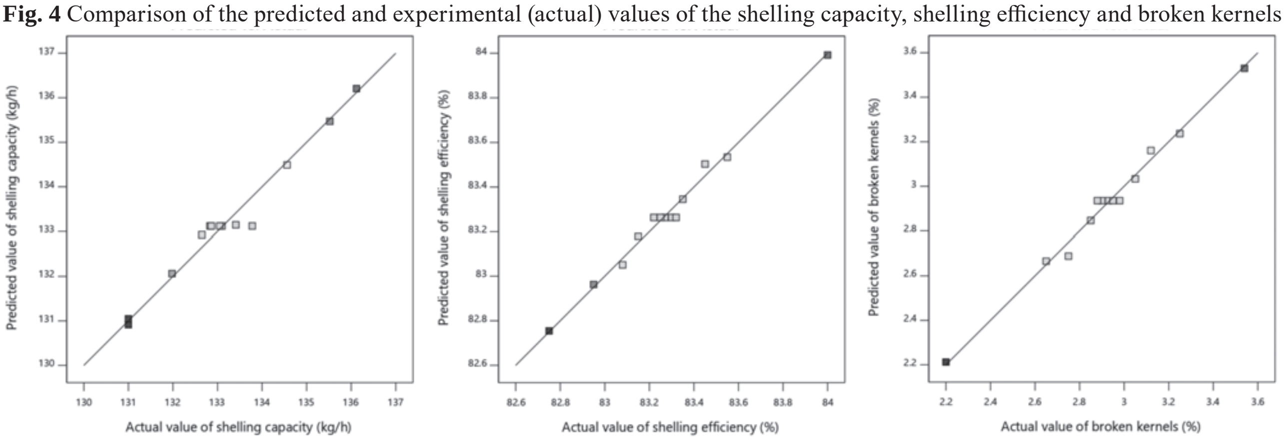

(a) Shelling capacity (b) Shelling efficiency (c) Broken kernels great fit to the model, and the model adequately covers the independent parameters within the experimental range. The experimental (actual) values of the shelling capacity, shelling efficiency, and broken kernels were found to be 135.78 kg/h, 83.23% and 2.54% against the predicted (optimized) values of 136.12 kg/h, 83.54% and 2.66%, respectively with the optimum operational parameters (**Table 6**).

There was no significant difference ($p > 0.05$) between the experimental and predicted values of the responses from optimized parameters, and it was verified that the experimental values consented with the predicted values at a 5% level of significance. The superior correlation between the experimental optimum responses and predicted optimum response values suggested the legality of the provided optimum parameters, and the developed model was perfect and sufficient for predicting the shelling capacity, shelling efficiency, and percentage broken kernels values in the shelling operation. Hence, a solar-powered groundnut sheller was operated with optimized operational parameters viz., sieve hole size 15 mm, and speed of flywheel 59.86 rpm to obtain better output performance.

Conclusions

The inscribed central composite design (CCD) using response surface methodology (RSM) was obtained to be advantageous fixings to enumerate the impact of the operational parameters viz., sieve hole size and speed of flywheel and their quadratic and interaction terms for optimizing the shelling capacity, shelling efficiency and percentage of broken kernels in the operation of shelling of groundnut pods in the post-harvest processing. Analysis of variance (ANOVA) displays that the extremely statistically significant models were produced with a significance level of $p < 0.0001$ for the independent parameters. The developed model revealed sufficient to be equipped to the experimental data values with the coefficient of determination (R^2) > 0.95 and had no significant lack of fit (Lof). Hence, it was concluded that the solar-powered sheller operated at 59.86 rpm speed of flywheel and 15 mm sieve hole size provided superior output results in terms of shelling capacity, shelling efficiency, and minimum percentage of broken kernels. The optimized maximum shelling capacity and shelling efficiency were obtained to be 136.12 kg/h and 83.54%, respectively, with minimum broken kernels as 2.66% for a fixed value of the concave clearance. The predicted values were in a suitable contract with the experimental values with very slight divergence for all dependent parameters. The optimized operational parameters were utilized to construct a machine that was easily handled and powered by a single worker. However, for a better shelling operation with lesser broken kernels, optimum speed of flywheel and sieve hole size must be selected for superior performance results.

Acknowledgements

The facilities provided by the Farm Machinery and Power Workshop and Laboratory, Department of Agricultural and Food Engineering, Indian Institute of Technology Kharagpur, to conduct this experiment are sincerely acknowledged.

REFERENCES

[1] Anonymous. 2018. Ministry of Agriculture & Farmers Welfare, Government of India, New Delhi. Directorate of Economics and Statistics. http://www.agricoop.nic.in.

[2] El Naim, A. M., M. A. Eldoma and A. E Abdalla. 2010. Effect of weeding frequencies and plant density on vegetative growth characteristic of groundnut (*Arachis hypogaea* L.) in North Kordofan of Sudan. International Journal of Applied Biology and Pharmaceutical Technology. 1(3), 1188-1193.

[3] Bano, S. and Y. S. Negi. 2017. Studies on cellulose nanocrystals isolated from groundnut shells. Carbohydrate polymers. 157, 1041-1049.

[4] Anonymous. 2011. Food and Agriculture Organization of the United Nations. http://www.fao.org/home/en/

[5] Jambunathan, R., S. D. Hall, P. Sudhir, V. Rajan and V. Sadhana. 1991. Uses of Tropical Grain Legumes Proceedings of a Consultants Meeting 27-30 March 1989.

[6] Hoffman, J. R. and M. J. Falvo. 2004. "Protein - which is best", Journal of Sports Science and Medicine. 3(3), 118-130.

[7] Birthal, P. S., P. P. Rao, S. N. Nigam, C. S. Bantilan and S. Bhagavatulu. 2010. Groundnut and Soybean Economies in Asia: Facts, Trends and Outlook. Patancheru: International Crops Research Institute for the Semi-Arid Tropics.

[8] Singh, F. and B. Diwakar. 1993. Nutritive value and uses of pigeonpea and groundnut. Manual. Patancheru: International Crops Research Institute for the Semi-Arid Tropics.

[9] Pasupuleti, J., S. N. Nigam, M. K. Pandey, P. Nagesh and R. K. Varshney. 2013. Groundnut improvement: use of genetic and genomic tools. Frontiers in plant

Table 6 Predicted and experimental values for the responses with optimum parameters

Independent parameters		Dependent (responses) parameters					
Shs (mm)	Sf (rpm)	SC (kg/h)		SE (%)		BK (%)	
		Actual	Predicted	Actual	Predicted	Actual	Predicted
15	59.86	135.78	136.12	83.23	83.54	2.54	2.66

science. 4(23), 1-16.
[10] Jones, J. B., M. Provost, L. Keaver, C. Breen, M. J. Ludy and R. D. Mattes. 2014. A randomized trial on the effects of flavorings on the health benefits of daily peanut consumption. The American journal of clinical nutrition. 99(3), 490-496.
[11] Jamdar, S. N., V. Rajalakshmi, M. D. Pednekar, F. Juan, V. Yardi and A. Sharma. 2010. Influence of degree of hydrolysis on functional properties, antioxidant activity and ACE inhibitory activity of peanut protein hydrolysate. Food chemistry. 121(1), 178-184.
[12] Bonku, R. and J. Yu. 2020. Health aspects of peanuts as an outcome of its chemical composition. Food Science and Human Wellness. 9(1), 21-30.
[13] Paramawati, R., P. Widodo, U. Budiharti and H. Handaka. 2016. The role of postharvest machineries and packaging in minimizing aflatoxin contamination in peanut. Indonesian Journal of Agricultural Science. 7(1), 15-19.
[14] Rahmianna, A. A., J. Purnomo and E. Yusnawan. 2015. Assessment of groundnut varietal tolerant to aflatoxin contamination in Indonesia. Procedia Food Science. 3, 330-339.
[15] Chilakpu, K. O. 2018. Development, and evaluation of a serrated disc groundnut decorticator. International Journal of Scientific and Research Publications. 8(6), 435-439.
[16] Helmy, M. A., A. Mitrroi, S. E. Abdallah and M. A. Basiouny. 1993. Modification and evaluation of a Reciprocating machine for shelling peanut. Misr J. Ag. Eng. 24(2), 283-298.
[17] Abou El-kheir, M. M. and A. Z. Shoukr. 1993. Modelling of the action of mechanical shelling of peanut for different materials of beater drum. Misr J. Ag. Eng. 10(1), 123-135.
[18] Singh, G. 1993. Development of a unique groundnut decorticator. Agricultural Mechanization in Asia, Africa and Latin America. 24(1), 55-59.
[19] Manjunath, B. A., K. S. Ahmed and L. K. Sreepathi. 2016. Design and fabrication of pongamia pinnata decorticator. Journal of Mechanical Engineering and Automation. 6(5A), 1-7.
[20] Seabury, J. J., W. C. Adams and M. R. Ramey. 1977. Influence of pedaling rate and power output on energy expenditure during bicycle ergometry. Ergonomics. 20(5), 491-498.
[21] Coast, J. R., R. H. Cox and H. G. Welch. 1986. Optimal pedaling rate in prolonged bouts of cycle ergometry. Medicine and Science in Sports and Exercise. 18(2), 225-230.
[22] Marsh, A. P. and P. E. Martin. 1997. Effect of cycling experience, aerobic power, and power output on preferred and most economical cycling cadences. Medicine & Science in Sports & Exercise. 29(9), 1225-1232.
[23] Hoque, M. A., M. Z. Hossain and M. A. Hossain. 2018. Design, and development of a power groundnut sheller. Bangladesh Journal of Agricultural Research. 43(4), 631-645.
[24] Pinar, Y. 1987. Grain losses at harvesting and threshing of paddy in Turkey. Agricultural Mechanization in Asia, Africa, and Latin America. 18(4), 61-64.
[26] Lee, W. C., S. A. L. M. A. H. Yusof, N. S. A. Hamid and B. S. Baharin. 2006. Optimizing conditions for enzymatic clarification of banana juice using response surface methodology (RSM). Journal of food Engineering. 73(1), 55-63.
[27] Neda, Z., A. Alireza, L. Lye and R. Popescu. 2002. Application of RSM in Numerical Geotechnical Analysis, 55th Canadian Society for Geotechnical Conference, Hamilton, Ontario, Canada.
[28] Anonymous. 1983. ASAE standard S352, moisture measurement-grains and seeds. Agricultural Engineers yearbook. American Society of Agricultural Engineers. St. Joseph, Michigan.
[29] Choudhary, V., R. Machavaram, Vikas and R. S. Singh. 2020. Engineering properties of groundnut pods and kernels: a key role for designing the post-harvest processing equipment. International Journal of Current Microbiology and Applied Sciences. 9(8), 1751-1761.
[30] Jnr, E. Z., A. Muitia, M. I. Amane, R. L. Brandenburg, A. Emmott and A. M. Mondjana. 2018. Effect of Harvesting Time and Drying Methods on Aflatoxin Contamination in Groundnut in Mozambique. In Mycotoxins-Impact and Management Strategies. Intech Open.
[31] Box, G. E. and N. R. Draper. 1987. Empirical model-building, and response surfaces (Vol. 424). New York: Wiley.
[32] Hunter, J. S. 1959. Determination of optimum operating conditions by experimental methods. Indian Quality Control. 15, 6-16.
[25] Fisher, R. A. 1920. Design of Experiment, 8th edition, published by Oliver & Biyd, pg-245.
[33] Mangaraj, S. and K. P. Singh. 2011. Optimization of machine parameters for milling of pigeon pea using RSM. Food and Bioprocess Technology. 4(5), 762-769.
[34] Powar, R. V., V. V. Aware and P. U. Shahare. 2019. Optimizing operational parameters of finger millet threshing drum using RSM. Journal of food science and technology. 56(7), 3481-3491.
[35] Rastogi, N. K., G. Rajesh and T. R. Shamala. 1998. Optimization of enzymatic degradation of coconut residue. Journal of the Science of Food and Agriculture. 76(1), 129-134.
[36] Singh, K. P., I. L. Pardeshi, M. Kumar, K. Srinivas and A. K. Srivastva. 2008. Optimization of machine parameters of a pedal-operated paddy thresher using
(Continued on page68)

Co-operating Editors


B Kayombo


M F Fonteh


S A Ndindeng


S E Abdallah


A A K El Behery


Ahmad Addo

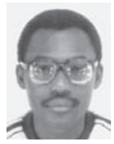
R J Bani


A N GITAU


D K Some


K Houmy


A F Alonge


O A Oy-elade


Umar B Bindir


J C Igbeka


E U-Odigboh


K C Oni


U L Opara


N G Kuyembeh


A H Abdoun


A B Saeed


A I Khatibu


S Tembo


H A Cetrangolo


I de A Nääs


A E Ghaly


E J Hetz


M A L Roudergue


R Aguirre


O Ulloa-Torres


Y M Mesa


P P Rondon

S G C Magaña

H Ortiz-Laurel

A I Luna Maldonado

G C Bora

M R Goyal

A K Mahapatra

Daulat Hussain

M A Mazed

R Ali

Kinga Norbu

M A Basunia

Minzan Li

Xiwen Luo

S M Ilyas

Surya Nath

Indra Mani

C R Mehta

B S Pathak

V M Salokhe

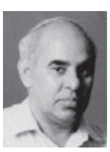
G Singh

P Soni

R Yadav

Kamaruddin Abdullah

M Behroozi-Lar

Saeid Minaei

A Mahdavian

V R Sharabiani

A M Abdul-Munaim

H Hasegawa

E Gasparetto

Y Lobachevsky

M Martinov

J Ortiz-Cañavate

Brian G Sims

Retired Co-operating editors

Name	Nationality	Inaugural year	Retired year
Adrian Moens	Netherlands	1972	1989
Bala Krishna Shrestha	Nepal	1972	1991
A. M. Michael	India	1972	2022
Chul Choo Lee	Korea	1972	2014
Chau Van Khe	Vietnam	1972	1980
Manbahadur Gurung	Bhutan	1972	2006
Merle L. Esmay	U. S. A.	1972	1990
Giuseppe Pellizzi	Italy	1973	2012
Mohamed A. Bedri	Sudan	1973	1987
Shahansha-Uddin Choudhury	Bangladesh	1973	1991
T. B. Muckle	U. K.	1973	1978
Chang Joo Chung	Korea	1975	2014
T. Touggaard Pedersen	Denmark	1975	1990
Bilash Kanti Bala	Bangladesh	1976	1982
George B. Hanna	Egypt	1976	1988
Jun Sakai	Japan	1976	2015
Siswadhi Soepardjo	Indonesia	1976	1985
Tieng-Song Peng Taiwan	Taiwan	1976	2015
Mohammad Ilyas	Pakistan	1977	1981
Amala Prasad Sharma	Fiji	1978	1981
Arumugam Kandiah	Ethiopia	1978	1989
Bherulal T. Devrajani	Pakistan	1978	2004
John Kilgour	U.K.	1978	2014
Satish Chandra	Fiji	1979	1990
Jitendra P. Mittal	Nigeria	1980	1993
Naresh Chandra Saxena	India	1980	1988
Paris Andereou	Lebanon	1980	1984
Wang Wanjun	China	1981	2012
Allah Ditta Chaudhry	Pakistan	1981	2015
Allan L. Phillips	U. S. A.	1981	2004
Julien G. Van Lancker	Brundi	1981	1989
Suppiah Kathirkamathamby	Sri Lanka	1981	1991
Armed Hossain Mirdha	Mexico	1982	1991
A. A. Valenzuela	Chile	1982	2013
David Boakye Ampratwum	Ghana	1982	2011
Kshirode Chandra Roy	Bangladesh	1982	1985
M. H. Abdel Aziz	Saudi Arabia	1982	1991
Krishna Prakash Srivastava	Ethiopia	1983	1989
Muhammad Siddique Chaudhry	U. S. A.	1983	1991
Wimala Tissa Weerakoon	Zambia	1983	1985
Harry D. Henderson	Lebanon	1984	1985
Mohammad Afzal	Pakistan	1984	1994
A. P. Kaloyanov	Bulgaria	1985	2013
Soedjatmiko	Indonesia	1986	2014
Aalbert Anne Wanders	Netherlands	1988	2007
Ali Mahmoud El Hossary	Egypt	1988	2010
Chanchai Rojanasaroj	Thailand	1988	2011
Edward A. Baryeh	Zimbabwe	1988	2014
T. P. Ojha	India	1988	2015
Eltag S. Eldin Mahmoud	Sudan	1990	2011
Henrik Have	Denmark	1990	2009
Graeme Ross Quick	Australia	1995	2015
Rafiq ur Rehman	Pakistan	1995	2015
Abdulsamad Abdulmalik Hazza'a	Yemen	1999	2014
Yunus Pinar	Turkey	1983	2016
William J. Chancellor	U.S.A	1972	2017
Kunihiro Tokida	Japan	2016	2017
Shujun Li	China	2012	2018
S. F. (Sen-Fuh) Chang	Taiwan	1987	2018
Jan Pawlak	Poland	2002	2019
Oleg S. Marchenko	Russia	2003	2019
W. B. Hoogmoed	Netherlands	2007	2019
Sitaram Dagdupant Kulkarni	India	2017	2020
Shah M. Farouk	Bangladesh	1982	2021
S. R. Verma	India	1982	2021
Chetem Wangchen	Bhutan	2006	2022
Israel Kofi Djokoto	Ghana	1987	2022

Back Issues

AGRICULTURAL MECHANIZATION IN ASIA, AFRICA AND LATIN AMERICA

(Vol.53, No.1, Winter, 2022-)

◇ ◇ ◇

Vol.53, No.1, Winter 2022

◇ ◇ ◇

Vol.53, No.2, Sprinter 2022

◇ ◇ ◇

Vol.53, No.3, Summer 2022

◇ ◇ ◇

Vol.53, No.4, Autumn 2022

◇ ◇ ◇

Vol.54, No.1, Winter 2023

◇ ◇ ◇

Vol.54, No.2, Spring 2023

◇ ◇ ◇

Vol.54, No.3, Summer 2023

◇ ◇ ◇

Vol.54, No.4, Autumn 2023

SUBSCRIPTION/ORDER FORM

AGRICULTURAL MECHANIZATION IN ASIA, AFRICA AND LATIN AMERICA (AMA)

Issued Quarterly

AMA has Achieved an IMPACT FACTOR!!

AMA has been read by those involved in agricultural machinery and industry all over the world since the first publishment in 1971. Thanks to many contributions from both the readers and writers, in 2012, we have achieved an Impact Factor, established by Thomson Reuters in U.S.A. AMA is the only Japanese agricultural machinery and industry related magazine which achieved an Impact Factor.

Subscription Rate (includes surface mail postage)

Annual (4 issues).......................... ¥8,000
Single copy...................................... ¥2,500

(Check one)
☐ Please send me/us an invoice
☐ I/We enclose remittance for ¥ __________
☐ Please charge my/our credit card
☐ VISA
☐ MASTER Card. No. ______________________

Exp. date ______________________

Signature ______________________

We deeply appreciate your payment by credit card (NO EXTRA CHARGE NEEDED).
We charge you extra 4,000 JPY when paid by check or wire transfer.

****

Name: ____

Firm: ____

Position: ____

Address: ____

(block letters)

FARM MACHINERY INDUSTRIAL RESEARCH CORP.
1-2-5, Kanda Jimbo-cho, Chiyoda-ku, Tokyo 101-0051, Japan
Tel. +81-3-3291-3674, Fax. +81-3-3291-5717
URL: http://www.shin-norin.co.jp
E-Mail: ama@shin-norin.co.jp